2023

NOVEL STRATEGIES IN HEAD AND NECK TUMOR THERAPY; CONTRIBUTION OF SENESCENCE IN THERAPY RESPONSE, AND RESISTANCE DEVELOPMENT AFTER CISPLATIN TREATMENT

Fereshteh Ahmadinejad

NOVEL STRATEGIES IN HEAD AND NECK TUMOR THERAPY; CONTRIBUTION OF SENESCENCE IN THERAPY RESPONSE, AND RESISTANCE DEVELOPMENT AFTER CISPLATIN TREATMENT

A dissertation submitted in partial fulfillment of the requirements for the degree of Doctor of Philosophy at Virginia Commonwealth University.

By

Fereshteh Ahmadinejad

Virginia Commonwealth University

Advisor: David Gewirtz, PhD

Professor, Department of Pharmacology & Toxicology

School of Medicine

Virginia Commonwealth University

Richmond, Virginia

January 2023

Dedication:

To my mother Mehri and my two younger brothers Ramin and Iman whose love and support have always given me motivation and strength. To the loving memory of my father, Ali who was the biggest inspiration in my life.

Acknowledgments

I would like to express my sincere gratitude to my advisor Dr. David A. Gewirtz. For his guidance and insight during my Ph.D. studies. Dr. Gewirtz's passion and commitment to science have been one of the greatest inspirations in my academic and personal life. I am extremely thankful to have had an advisor who always encouraged and supported me to voice and pursue my hypotheses. I appreciate the trust he always had in me for the responsibilities I had under his supervision. I would also want to thank my committee members: Dr. Jolene Windle, Dr. Hisashi Harada, Dr. Senthil Radhakrishnan, and Dr. Swadesh Das, whose invaluable insight and guidance helped me to develop my studies and be the person I am today. I would also like to thank my previous and current lab mates who made this journey memorable. I thank Ryan Finnegan who started the same journey with me at VCU and always was there for me during hardships and happy moments. I would like to thank Dr. Bin Hu, from the Cancer Mouse Model Core at Massey cancer center for his kind and genuine help and his significant contribution to our studies. Finally, I thank all my family and friends who always supported me even though I was thousands of miles far from them.

Table of Contents

Abbreviations

ATM	Ataxia-Telangiectasia Mutant
ATR	Ataxia Telangiectasia and Rad3 Related
AV	Annexin V
Baf	Bafilomycin A1
Bak	Bcl-2 Homologous Killer
Bax	BCL-2-Associated X Protein
BCL-2	B-Cell Lymphoma 2
BCL-W	BCL-2-Like Protein 2
BCL-X_L	B-Cell Lymphoma-Extra Large
BET	Bromo- and Extra-Terminal Domain
Bid	BH3-Interacting Domain Death Agonist
BRD4	Bromodomain-Containing Protein 4
C/EBP	Ccaat-Enhancer-Binding Proteins
C12FDG	5-Dodecanoylaminofluorescein Di-β-D-Galactopyranoside
cCasp3	Cleaved caspase 3
CDK	Cyclin-dependent Kinase
CDKI	Cyclin-dependent Kinase Inhibitor
Chk1/2	Checkpoint Kinase 1/2
CO2	Carbon Dioxide
CXCL2	C-X-C Motif Chemokine Ligand 2
D+Q	Dasatinib + Quercetin

DAPI	4’-6-Diamidino-2-Phenylindole
DDR	DNA Damage Response
DMEM	Dulbecco’s Modified Eagle Medium
DNA	Deoxyribonucleic acid
EMT	Epithelial-to-mesenchymal transition
FACS	Fluorescence-Activated Cell Sorting
FBS	Fetal Bovine Serum
FVB/N	Friend Virus B/NIH
GAPDH	Glyceraldehyde 3-Phosphate Dehydrogenase
GFP	Green Fluorescent Protein
Gy	Gray
H3K9Me3	Trimethylation of Histone 3 Lysine 9
HDAC	Histone Deacetylase
HP1	Heterochromatin Protein 1
HSP90	Heat Shock Protein 90
IACUC	Institutional Animal Care and Use Committee
IGFBP3	Insulin-like Growth Factor Binding Protein 3
IL1α	Interleukin-1 alpha
IL-1β	Interleukin-1 beta
IL-6	Interleukin 6
IL-8	Interleukin 8
IR	Ionizing Radiation

JAK	Janus Kinase
KD	Knock Down
KRAS	Kirsten rat sarcoma viral oncogene
LC3B	Light Chain Microtubule-Associated Protein
LLC	Lewis Lung Carcinoma
MCL-1	Myeloid Cell Leukemia-1
MDM2	Mouse Double Minute 2 Homolog
MMP	Matrix Metalloprotease
mTOR	Mammalian Target of Rapamycin
NF-κB	Nuclear Factor Kappa-Light-Chain Enhancer of Activated B
NK	Natural Killer
NOTCH1	Notch Homolog 1, Translocation-Associated
NSCLC	Non-Small Cell Lung Cancer
NSG	NOD Scid Gamma
OIS	Oncogene-Induced Senescence
PARP	Poly (ADP-ribose) Polymerase
PBS	Phosphate Buffered Solution
PFA	Paraformaldehyde
PI	Propidium Iodide
PI3K	Phosphoinositide 3-kinase
pRB	Retinoblastoma protein
PROTAC	Proteolysis Targeting Chimera

PTEN	Phosphatase and Tensin Homolog
qRT-PCR	Quantitative Reverse Transcription Polymerase Chain
RNA	Ribonucleic acid
ROS	Reactive Oxygen Species
RPMI	Roswell Park Memorial Institute
RIS	Replicative Induced Senescence
SA-β-Gal	Senescence-Associated-β-Galactosidase
SAHF	Senescence-Associated Heterochromatic Foci
SASP	Senescence-Associated Secretory Phenotype
SD	Standard Deviation
SEM	Standard Error of the Mean
shRNA	Short Hairpin RNA
STAT3	Signal Transducer and Activator of Transcription 3
TGF-β	Transforming Growth Factor β
TIS	Therapy Induced Senescence
UV	Ultraviolet

Abstract

Therapeutic outcomes achieved in head and neck squamous cell carcinoma (HNSCC) patients by concurrent cisplatin-based chemoradiotherapy initially reflect both tumor regression and tumor stasis. However, local, and distant metastasis and disease relapse as well as cisplatin-induced resistance are common in HNSCC patients. In the current work, we demonstrate that cisplatin treatment induces senescence in both p53 wild- type HN30 and p53 mutant HN12 head and neck cancer models. We also show that tumor cells can escape from senescence both in vitro and in vivo. We further established a cisplatin-resistant cell line from HN30 parental cell line that underwent brief senescence after cisplatin treatment. In this study, we evaluated the effectiveness of ABT-263 (Navitoclax) and ARV-825, in the elimination of senescent tumor cells after cisplatin treatment. Navitoclax increased apoptosis by 3.3-fold ($p \leq 0.05$) at Day 7 compared to monotherapy by cisplatin in HN30 and HN12 cells, however, it did not sensitize HN30R cell line. Additionally, we show that ABT-263 interferes with the interaction between BCL-XL and BAX, anti- and pro-apoptotic proteins, respectively, followed by BAX activation, suggesting that ABT-263 induced apoptotic cell death is mediated through BAX. ARV-825 however, significantly induced apoptosis in both HN30 and HN30R cells. The mechanistic studies show that ARV-825 treatment in combination with cisplatin increased DNA double-strand breaks signals in-vitro and in-vivo. Our in vivo studies also confirm senescence induction in tumor cells by cisplatin, and the promotion of apoptosis coupled with a significant delay of tumor growth after sequential treatment with ABT-263 or ARV-825. Sequential treatment with cisplatin followed by ABT-263 extended the humane

endpoint to ~130 days compared to cisplatin alone, where the mouse survived ~75 days. These results support the premise that secondary agents could be utilized to eliminate residual senescent tumor cells after chemotherapy and thereby potentially delay disease recurrence and resistance in head and neck cancer patients.

Disclosures

Parts of the writing and data presented in this thesis have previously been published in:

Senolytic-Mediated Elimination of Head and Neck Tumor Cells Induced into Senescence by Cisplatin

Chapter 1 : General Introduction

1.1. Senescence nature and characteristics

1.1.1. Cellular Senescence History

The phenomenon of senescence was first discovered/identified in the 1960s by Leonard Hayflick, who described senescence as limited proliferative capacity in an in-vitro model (1). He demonstrated that normal human diploid cells stop dividing after a certain number of passages. This was the first time that the longstanding paradigm of indefinite growth of vertebrate cells in culture was proven false; it took Hayflick years to come to the realization that this observation is a natural phenomenon and not an artifact of technical issues, culture medium preparation, and other possible problems (1). He designed co-culture experiments growing old male fibroblast with young female fibroblast cells. After multiple passages, he confirmed that male fibroblasts stopped dividing and the culture was composed entirely of female fibroblast cells, which proved that their observation was accurate and not an experimental error (2). This discovery was further investigated by other scientists, but it was not explained until James Watson identified the “end replication problem” where DNA polymerases stop replicating the lagging DNA strand, resulting in an accumulation of unreplicated nucleotides at the end of the DNA strand, and DNA strand shortening every time the cell completes one cycle. Later, they discovered that these sequences represent the telomeres that are lost in successive divisions, and that telomeres play a major role in cellular senescence(3).

1.1.2. Senescence is a complex phenomenon

Historically, senescence was considered an irreversible phenotype, where the definition connected old or aging cells to their incapability to divide. However, an accumulating body of evidence has altered the senescence paradigm and shown that senescence can be promoted/induced by a number of external and internal stimuli. Senescence types are categorized based on the initial stimuli and are deemed to be one of the following forms: Replicative induced senescence (RIS), oncogene-induced (OIS), or stress-induced premature senescence (4,5). Replication-induced senescence is the first form of senescence that was described based on the findings by Hayflick. Telomere dynamics are one of the most important components of aging and senescence. Since human cells generally do not maintain telomerase activity, most dividing cells undergo telomere shortening. Upon each division, cells fail at replicating specific regions of telomeres, and after telomeres reach a critical length, DNA damage response (DDR) is activated and replicative senescence is induced (4,5). Oncogene-induced senescence also appears to be triggered by the abnormal proliferative signals of oncogenes causing hyperproliferation and DNA damage response (6,7). It has been shown that activation of oncogenes can stimulate cell proliferation, which is recognized as a tumor-promoting event and a necessary step in tumorigenesis in many cancer types, however, it may also act as a genetic stress and cause of growth arrest in cultured cells and tumor tissues (8,9).

Premature or Accelerated Senescence reflects the prolonged growth arrest that takes place after the cell is exposed to a stress-inducing stimulus. This phenotype is typically associated with a primary response from ATM/ATR kinase proteins that activate cell proliferation regulators such as p53, p21, and $p16^{INK4A}$ (Figure 1-1).

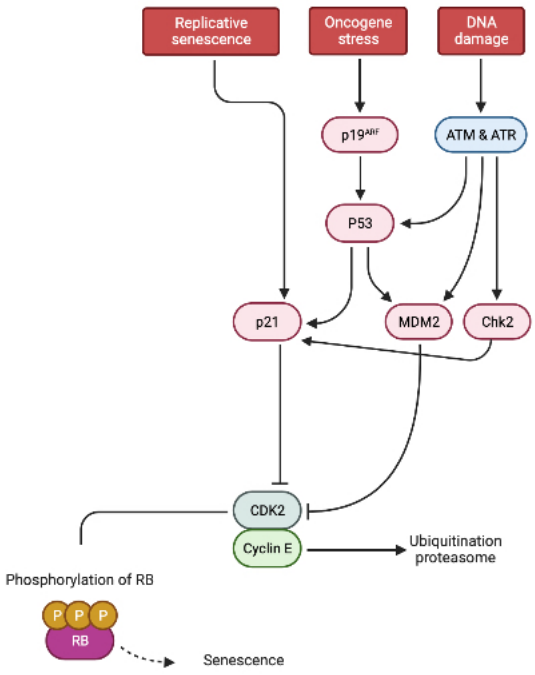

Figure 1-1: Senescence stimulators and main pathways. Persistent DNA damage induced by diverse stimuli and abnormal oncogenic signal lead to senescence mainly by regulating pRb and p53/p21 pathways. This figure was created in Biorender.

This phenotype was further linked to multiple features such as increased β-galactosidase (SA-β-gal) activity, and decreased levels of Ki-67 protein. Other features were also connected to this phenotype such as increased levels of cell cycle regulators such as p53, p21, and p16ink4a, elevated secretion of pro-inflammatory chemokines and

cytokines such as IL-6, IL-8, IL-B, MMP3, Vascular endothelial growth factor (VEGF) which is identified as senescence-associated secretory phenotype (SASP)(10), and condensation of facultative heterochromatin regions due to increased levels of trimethylated histone H3 lysine 9 (H3K9me3) which is termed as senescence-associated heterochromatin foci (SAHF)(11–15).

Senescence can be induced by different extrinsic and intrinsic stimuli. Depending on the origin of the cell and the intensity and nature of the stimulus, cells may activate different molecular pathways resulting in the development of a variety of characteristics However, studies have shown that even a combination of multiple positive markers cannot confirm the senescent phenotype with complete certainty since this phenotype shares some features with other cell cycle arrest modes such as quiescence and delayed cell death (16,17). Further investigations in characterizing the senescence phenotype against quiescence showed that continuous activity of the mTOR pathway in senescent models may be the most critical marker that helps researchers to distinguish this phenotype from quiescence (18–20). Additionally, cellular morphology has been reported unaltered in quiescent cells, however, senescence has been associated with dramatic morphological changes. During senescence, the cells become flattened, enlarged, and multinucleated. Moreover, proliferative recovery takes place shortly after quiescence induction, while senescent cells have been shown to have a longer growth arrest phase (21). However, there are more factors that play an important role in cell fate towards senescence or quiescence, such as pRB dephosphorylation in senescence (22), p27 (CDK inhibitor) activation in quiescence (23), and “TP53-induced glycolysis and apoptosis regulator” (TIGAR) protein activation in senescence (24).

1.1.3. Senescence and quiescence

Senescence has been a controversial topic over the past years. Many studies have been published in efforts to investigate the nature of this phenotype, distinguish it from quiescence, understand its durability when induced by chemotherapy or various stress stimulators, and finally, understand its role in aging and diseases (21). It has been shown that senescence and quiescence can both result from chemotherapy; however, senescence is perceived as a more durable growth arrest with the characteristics described in the previous section, whereas quiescence is associated with a transient growth arrest with much more rapid recovery (25). Unlike senescent cells, quiescent cells have been shown to respond to mitotic stimulation. The metabolic activity also has been shown to increase during senescence, while in quiescence mRNA transcription and protein synthesis are drastically repressed (26).

1.1.4. Senescence, Development, and Aging

It is well established that senescence plays an important role in aging-related diseases and embryonic development (27). Senescence in certain regions of the embryo develops independently of DNA damage and is critical for tissue remodeling. p21 has been shown to be the primary protein inducing growth arrest and senescence in murine embryos and p21 knock-out models were shown to develop abnormal morphologies in mice(28).

Additionally, senescence has been associated with multiple age-related diseases such as Alzheimer’s disease, vascular atherosclerosis, pulmonary fibrosis, kidney disease, obesity, and osteoarthritis. It has been shown that telomere shortening results

in senescent cell accumulation and consequently contributes to age-related diseases (29–33).

1.2. Senescence role in cancer

1.2.1. Therapy-induced senescence or TIS

A number of cancer therapeutics have been shown to induce senescence, at least in cell culture; these include DNA cross linking and alkylating agents such as cisplatin, carboplatin, and cyclophosphamide, topoisomerase II inhibitors such as etoposide and doxorubicin, CDK4/6 inhibitors such as Palbociclib (34), and radiation (35). TIS (therapy-induced senescence) has been considered a desirable outcome in anticancer therapy in patients because it results in prolonged cancer cell growth arrest and tumor stasis (36). It has also been shown that the cytokines and chemokines associated with the SASP (senescence-associated secretory phenotype) contribute to halted tumor cell progression by inducing senescence in neighboring cells via the bystander effect (37–40). However, there is an accumulating body of evidence showing that senescence induction is a double edge sword with the ability to both inhibit or promote tumor progression at different stages of therapy (34,41). Below we will discuss the contribution of senescence to cancer cells survival and tumor progression.

1.2.2. Tumor suppressor effect of senescence phenotype

The therapy-induced senescent phenotype has been considered to have tumor suppressive effects as it theoretically contributes to halting replication and arresting cell cycle progression (42–44). Consistent with this role, cellular senescence has been shown to be controlled by several tumor suppressor genes including p53 and pRB which play

the most crucial roles in tumor-suppressor pathways. Depending on the stimuli, the interaction between tumor suppressor genes will determine the pathways that will be involved in senescence induction. For example, in therapy-induced senescence, DNA damage stress response results in ATM/ATR activation followed by p53 and p21 phosphorylation and finally pRB activation and senescence induction. Moreover, SASP contributes to inflammation and immune cell activation. Consequently, the immune system can eliminate the senescent cells and hinder tumorigenesis in its early stages (45–47). This pathway has been reported as the most common pathway activated in therapy-induced senescence in tumor models, however, alternative pathways and oncogenes such as ras, raf, MEK, Akt, E2F1/3, mos, PTEN, NF1, Stat5, KLF-4, and Runx have also been shown to be involved in senescence induction. Additionally, studies indicated that reversal or escape from senescence contributes to tumor progression (48–51). This mounting evidence of senescence pathways involving both tumor suppressors and oncogenes, and the fact that reemerging cells from senescence state contributes to tumorigenesis introduces senescence as a two-edge sword that can halt or promote tumor progression depending on the context (52).

1.2.3. Therapy induces senescence is not a permanent growth arrest

Due to the senescence phenotype's complex nature, the durability of growth arrest in senescent cells has been a controversial topic without consensus over many years. The scientific community has long debated whether the senescence phenotype is irreversible or transient (45–47). In studies investigating aging mechanisms, the telomere hypothesis suggests that telomere shortening over time induces cellular senescence and

promote a cell cycle arrest with no proliferative recovery (53). However, in cancer research, therapy-induced senescence has been described as a transient phenotype from which cancer cells escape and recover their proliferative capacity (54,55). The duration of growth arrest varies in different cancer types and depends on the therapeutic regimens applied. However, many of the more recent studies investigating cancer cells' response to chemotherapeutics, including those from our own laboratory, have provided compelling evidence that almost all cancer models recover from the proliferative arrest after senescence induction (56–59). For example, Roberson et al. showed that H1299 non-small lung cancer cells escaped senescence after chemotherapy (57). Additionally, it was shown that genotoxic chemotherapeutics or irradiation-exposed tumor cells can escape the growth arrest phase and lose their senescence characteristics such as SASP factors expression, beta-gal enzyme activity, and CDKI downregulation (60). Moreover, studies have shown that the existence of different subpopulations in a tumor or a cultured cell line can result in escape from senescence and the evolution of resistant cells (61–63). While the mechanisms of drug resistance may vary between different cancer types and cell models, escape from senescence mostly contributes to the same outcomes including resistance to the primary chemotherapeutic agent, resistance to secondary compounds with senolytic or synergistic activity, the emergence of cancer stem cells with a more aggressive phenotype, metastasis, and secondary tumors (48,64,65).

The escape mechanism from TIS is still unknown and is likely dependent on the cancer type and the therapeutic approach. A number of different mechanisms have been suggested to contribute to escape from therapy-induced senescence which will be discussed in the section below.

1.2.4. Escape mechanisms

Escape from therapy-induced senescence has been investigated for years, and studies have shown the various pathways and genes that may be involved in this process. Early studies showed that clinically relevant concentrations of doxorubicin induced senescence in $p16^{INK4a}$ null MCF7 breast cancer cells from which a subpopulation of cells overexpressed the cyclin-dependent kinase, cdc2 and was able to escape senescence (57,66). Additionally, Wu et.al. also showed an association between the over-expression of cdc2 and escape from senescence in p53 and $p16^{INK4a}$ deficient lung cancer cell lines. Other reports have identified a role for cdks such as cdk2 in bypassing senescence (57). ROS or reactive oxygen species quenching has also been shown to contribute to escape from senescence. In this pathway, an NFκB subunit, p65, was shown to be localized in the nucleus after glioblastoma cells were treated with ciprofloxacin (67,68). This localization was associated with escape from senescence, and interference with p65 localization resulted in a “permanent” senescent arrest (67,69).

Finally, some potential mechanisms of escape can contribute to resistance development such as acquiring an enhanced ability to repair chemotherapy-induced DNA damage. Other mechanisms such as the development of stem-like characteristics, downregulating of membrane transporters to decrease intracellular concentration of the drug, and over-expression of detoxifying proteins can contribute to senescence escape and resistance (70,71).

1.3. Clinical and laboratory benefits of secondary compounds

1.3.1. Senescence targeting compounds

To overcome the limitations of chemotherapeutic drugs used in the clinic, and to address the harmful effects of recovered senescent cells, development and improvement of secondary compounds and small molecules that might mitigate the deleterious effects of senescence have been of great interest. In this section, we will specifically discuss senescence targeting compounds.

The senescence targeting compounds are mainly categorized as: i) senomorphics and ii)senolytics (72–74). Senomorphic compounds usually target SASP related pathways such as the NFκB signaling pathway. This pathway has been shown to be crucial in inflammation regulation and SASP development (75). Senomorphics interfere with this pathway and reduce the production of SASP factors such as IL-6, IL-8, IL-1B, and MMP3 (72). Intriguingly, these compounds do not interfere with senescence induction, but rather eliminate SASP and inflammation in tumors. Compounds with senomorphic characteristics include metformin (10,76) flavonoids such as apigenin and kaempferol (65), and glucocorticoids (77). An additional pathway targeted by senomorphics is the JAK/STAT3 pathway. Interfering with this pathway using ruxolitinib (125,126), or mTOR inhibitors such rapamycin can also reduce SASP induction and is attributed to the senomorphic abilities of these compounds (78,79).

1.3.2. Senolytics

Senolytics are one of the most interesting groups of senescence-targeting compounds. These agents have generated attention due to their ability to promote cell

death in senescent cells in a “two-hit” approach (74,80). Senolytics were primarily developed as siRNA molecules blocking a specific target after identifying pro-survival and anti-apoptotic pathways activation in senescent cells. PI3K, BCL-XL, PAI-2, and p21Cip1 are among the targets that have been shown to increase after senescence induction as pro-survival mechanisms, and the development of siRNAs against these genes resulted in the elimination of senescence cells and not their proliferating counterparts (81). The exact mechanism of survival mediated by these genes are still under investigation, however, promoting cell cycle arrest and DNA repair mechanism are primary factors contributing to the pro-survival roles (82). Effective siRNAs were developed into small inhibitor or degrader molecules and screened in different models. After screening over 40 compounds, the first effective combination was introduced as D+Q, or Dasatinib in combination with Quercetin(81). This combination resulted in the elimination of senescent cells in-vitro and in-vivo aging-related models as well as Alzheimer's disease (83,84), hepatic steatosis (85), and obesity-induced metabolic dysfunction (32). This approach is currently being tested in clinical trials in patients with chronic kidney problems, and Alzheimer’s disease [NCT02848131, NCT02874989, NCT04210986].

Another intriguing senolytic that has been utilized in preclinical and clinical trials is the BH3 mimetic, Navitoclax or ABT-263 (86). This compound was designed to target the senescent cells that develop a BCL-xL dependent pro-survival phenotype. It thereby mimics BH3 protein's interaction with the pro-survival proteins from BCL-2 family to activate pro-apoptotic proteins such as BAX and BAK. The effectiveness of this compound has been shown in various models such as head and neck cancer (59), lung fibrosis,aging-associated bone loss, lung emphysema (87), uterine leiomyoma (88), tau-

dependent neurodegenerative disease (89), neurodegeneration (90), pulmonary hypertension (91), osteoarthritis (92,93), synthetic implant-mediated fibrosis (94), and DMD or Duchenne muscular dystrophy. Navitoclax promotes apoptosis by binding to pro-survival/anti-apoptotic BCL-2 family proteins and dissociates them from binding to Bax or Bak, pro-apoptotic proteins after senescence induction. Moreover, additional senolytics that are broadly being investigated in pre-clinical and clinical studies include Fisetin (95,96), Curcumin/EF-24 (97,98), Panobinostat (99,100), 17-DMAG (101,102), Metformin(103), and Bromodomain and extra-terminal (BET) family protein inhibitors/degraders (104).

The Bromodomain and extra-terminal (BET) family proteins represent a group of epigenetic readers and erasers that play critical roles in gene transcription, DNA repair, telomere elongation, and cellular proliferation and differentiation (105). BRD4 is one of the most important members of this family and has been shown to be involved in DNA machinery assembly at DNA breakpoints, recruiting the positive elongation factor (P-TEFb) complex along with transcriptional co-activators JMJD6 and CHD4 to assist RNA polymerase II (RNAPII) elongation (106). In particular, BRD4 has been shown to be concentrated at super-enhancer regions upstream of the MYC promoter in oncogenic cells, making it an attractive target in multiple models of cancer (107). BRD4 overexpression also has been reported to be an important factor in worse outcomes in cancer patients (108,109). Various small molecules and PROTAC compounds have been designed and utilized in anti-cancer therapy, including ARV-825 (105). This compound was designed to overcome the limitations of the first-generation BRD4 inhibitor JQ1 and improved the efficiency and effectiveness in BRD4 inhibition (110). ARV-825 has been

shown to specifically target and inhibit BRD4 by a selective intracellular proteolysis mechanism (111). Monotherapy using ARV-825 has shown promising outcomes in neuroblastoma, thyroid cancer, leukemia, breast cancer, lung carcinoma, and myeloma (112–116).

Based on the prior evidence suggesting that the accumulation of senescent cells is detrimental to patient outcomes, we hypothesize that following cisplatin therapy, a population of tumor cells enter and persist in a senescent state. These cells contribute to disease outgrowth and recurrence either through cell-autonomous effects such as escape from the senescent growth arrest or through paracrine effects of the SASP. Therefore, we further hypothesize that the elimination of these cells via senolytic/secondary agents will enhance—and perhaps prolong—response to standard-of-care, senescence-inducing anti-cancer therapies.

1.3.3. Senolysis pathways

Previous studies have shown that senolytics function via different pathways including apoptosis, autophagy, and ferroptosis (104,117,118).

Apoptosis is canonically described as two intrinsic and extrinsic pathways **(Figure 1-2)**. Intracellular stimuli are mostly responsible for intrinsic apoptosis. During this pathway, pro-apoptotic BCL-2 family proteins are activated, which subsequently result in the inhibition of pro-survival BCL-2 members and activate the executioner proteins BAX and BAK (119). After activation, BAX and BAK oligomerize and localize at the mitochondrial outer membrane, and this results in the mitochondrial outer membrane permeabilization. Once permeabilization happens, cytochrome c releases into the

cytoplasm, and from this, a cascade of caspase activation takes place, and apoptosis begins. (120).

On the other hand, during extrinsic apoptosis, ligands bind to death receptors leading to the activation of caspase 8, which consequently activates downstream effector caspases. Caspase 8 can also cleave the BH3-only protein BID into its active form, and in this way, the extrinsic and intrinsic apoptosis can converge (120). Markers of apoptosis include the characteristic “blebbing” to form apoptotic bodies, release of cytochrome c from the mitochondria into the cytoplasm, activation of the caspases, and the externalization of phosphatidylserine in the cellular membrane (121,122).

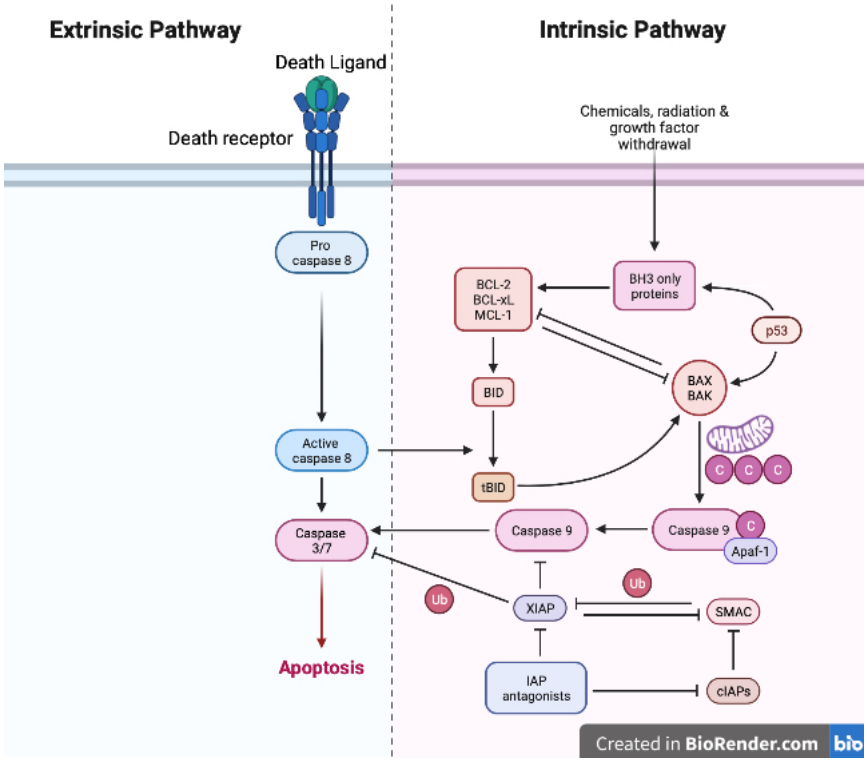

Figure 1-2: Intrinsic and Extrinsic Apoptosis pathways: Apoptosis can be mediated by either the intrinsic (mitochondria-mediated) pathway or extrinsic (death-receptor mediated) pathways. Both pathways converge upon executioner caspases

(Caspase-3 and 7) that induce apoptosis. Figure was modified from a template provided by Biorender.

Autophagy in another pathways that has been reported to be induced by senolytics. For example, the BRD4 degrader ARV-825 has been shown to induce senolysis via inducing autophagy (123). Autophagy is the process of “self-eating” (124,125) **d**uring which a part of the endoplasmic reticulum forms a bilayer vesicle called a phagophore, which then elongates into the autophagosome.. The autophagosome then joins the lysosome, at which point, the cargo contained within the newly formed autolysosome is degraded and recycled. Markers of autophagy include an increase in acidic vesicles, increased lipidation of LC3B, and degradation of the cargo adaptor protein p62 (126,127).

There are many functions attributed to autophagy in cells exposed to therapy, including cytoprotective, cytotoxic, and cytostatic, (124). In the protective form, autophagy maintains the metabolism of the cell in a way that chances of survival increase. In the cytotoxic form, autophagy plays a necessary role to promote drug-induced cell death. In the cytostatic form, autophagy mediates some form of growth arrest. As a senolytic, autophagy can mitigate the function of a senolytic and play a cytoprotective role, or it can mediate the effectiveness of the senolytic and play a cytotoxic role. (125–127)**.**

Chapter 2: Materials and Methods

2.1. Cell Culture and Treatments

Investigations were carried out on two HPV-negative human HNSCC cell lines, HN30 (wild-type p53) and HN12(truncated non-functional p53), which were provided by Dr. Andrew Yeudall (Augusta University). HN30R was established in Dr. Harada's laboratory, and SCC was provided by Dr. Jiong Li from the school of pharmacy at VCU. A549 cell line was purchased from ATCC (Manassas, VA, USA). Cells were cultured in DMEM (Thermo Fisher, 10569010) supplemented with 10% (v/v) fetal bovine serum (Gemini, 26140), 100 U/ml penicillin G sodium and 100 µg/ml streptomycin sulfate (Thermo Fisher, 15140148) at 37º C and 5% CO_2. Cisplatin (Sigma-Aldrich, 15663-27-1, ≥98% (HPLC) was dissolved in PBS, and ARV-825 (MedChem, HY-16954, 99.32%), was dissolved in DMSO and administered in the dark at the desired concentrations. Drugs are stable after preparation in multiple aliquots and were kept at -20ºC in the dark.

2.2. Cell viability and Clonogenic survival assays

Cell viability was determined by monitoring the number of viable cells over time using trypan blue dye exclusion staining before, during, and after drug treatment. Cells were treated with 5 µM cisplatin for 24 hours and were collected by trypsinization at specific time points, and stained with 0.4% trypan blue (Sigma, T8154) and counted using hemocytometer under light microscopy. For clonogenic survival assays, cells were seeded at a low density at 5 x 10^3/10 cm dish or 1,000/6-well plates, then treated 2 µM ABT-263, ABT-199, A-1155463 or vehicle for 24 hours. Colony formation was monitored

overtime, and at the experiment end point (at Day 14, when the vehicle-treated condition formed distinct colonies with more than 50 cells), colonies were fixed with 100% methanol, air-dried, stained with 0.05% crystal violet and counted using a colony counter (COLOCOUNT Discovery Technology Intl).

2.3 SA-β-galactosidase Staining/Enrichment

Histochemical staining of SA-β-gal was performed as previously described (14,128). Images were taken by a bright field inverted microscope (Olympus inverted microscope IX70, 20x objective, Q-Color3™ Camera; Olympus, Tokyo, Japan). The C_{12}FDG flow cytometry was performed using the protocol described by Debacq-Chainiaux et al (128). At the specific time points, cells were collected, washed with PBS, and analyzed by flow cytometry (using BD FACSCanto II and BD FACSDiva software at the Virginia Commonwealth University Flow Cytometry Core Facility). Similarly, for immunofluorescent staining of C_{12}FDG, cells were exposed to 100 nM of bafilomycin A1 (Sigma Aldrich, B1793, >90% HPLC) for one hour, and after increasing the lysosomal PH, cells were exposed to 100 µM C_{12}FDG (Thermo Fisher, D2893) for 2 hours. After washing with PBS, nuclei were stained with Hoechst 33342 (Thermo Fisher, 33342) for 20 minutes in complete media. Images were taken using the Olympus inverted microscope. To enrich the senescent population, cells were seeded at high density for 1-2 x 10^6/150 mm dish and cultured overnight. The next day, cells were treated with cisplatin, and at the indicated time points, they underwent C_{12}FDG staining as described above. Finally, cells were sorted by FACS. All the above experiments were performed at Day 5 after treatment with 5 µM cisplatin for 24 hours.

2.4. Total cell lysates, subcellular fractionation, and Western blotting

Total cell lysates were prepared using the CHAPS buffer [20 mM Tris (pH 7.4), 137 mM NaCl, 1 mM dithiothreitol (DTT), 1% CHAPS (3-[(3-Cholamidopropyl) dimethylammonio] 1-propanesulfonate)]. The mitochondria fraction was prepared with Qproteome Mitochondria Isolation Kit (Qiagen, 37612) according to the manufacture's protocol. Western blotting was performed as described (129). Antibodies used in1:1000 dilution: cleaved PARP (Cell Signaling, 5625), cleaved caspase 3 (Cell Signaling, 9664,), GAPDH (Cell Signaling, 5174), BCL-2 (Sigma, B3170), BCL-X_L (Cell Signaling, 2764), BAX (Cell Signaling, 2772), BAK (Cell Signaling, 12105), p53 (Santa Cruz, 23959), p21 (Cell Signaling, 2947), COX-IV (Cell Signaling, 4850), BRD4 (cell signaling, 13440).

2.5. Co-immunoprecipitation

BCL-X_L (Cell Signaling, 2764) or BAX (Santa Cruz, 23959) primary antibodies (1:100 dilution) were added to equal amounts of total lysates extracted from treated and non-treated cells. After overnight incubation at 4ºC, Protein A/G beads (Thermo Fisher, 53132) were added for 1-hour incubation at 4ºC to precipitate the protein-antibody complexes. Samples were centrifuged, washed, and resuspended in 50/50 CHAPS buffer and 2X SDS-loading buffer. After boiling the samples for 5 mins, they were subjected to SDS-PAGE followed by Western blotting as described above.

2.6. Cell cycle, Annexin-V/PI staining, and γ-H2AX analysis

Cell cycle analysis was performed based on propidium iodide staining (Saleh et al. 2019), and apoptosis quantification was done using AnnexinV-FITC apoptosis detection kit (556547, BD Biosciences, NJ, USA). Cells were seeded at the density of 4 x 10^4 cells per milliliter, treated with 5 µM cisplatin for 24 hours, and harvested at the indicated time points. After washing the samples with PBS, cells were resuspended in 100 µl of 1x Binding Buffer and incubated for 15 min in the dark at RT. Up to 500 µl of extra binding buffer was added to the final suspension and then the samples were analyzed by flow cytometry. Cell cycle analysis was performed at Day 5 after treatment with cisplatin, and apoptosis was assessed at Day 7. For γ-H2AX analysis, cells were seeded at a density of 4 x 10^4 cells per milliliter, treated with 5 µM cisplatin or vehicle for 24 hours. At Day 5, 2 µM ABT-263 was added to the combination conditions for 48 hours and γ-H2AX induction was monitored by flow cytometry at Day 7. Cells were harvested, fixed with 3.7% formaldehyde and permeabilized with cold methanol. After washing the pellets, cells were incubated with 1:250 dilution of γ-H2AX antibody conjugated to FITC (anti-H2AX (pS139), BD Biosciences, Cat. No. 560443) for 30 minutes.

2.7. Live-cell imaging

HN30 cells were plated (5 × 10^5 cells per milliliter) in 6-well plates and incubated overnight. After treatment with 5 µM cisplatin or vehicle for 24 hours, the plates were immediately placed on a CytoSMART digital microscopy system inside a humidified CO_2 incubator at 37 °C. Live time lapse images were taken every 15 min for 48 hours on

Day 5 (growth arrested and control cells, respectively) and Day 10 (cells escaping from senescence and recovering their proliferative capacity).

2.8. qRT-PCR

Apoptosis by Annexin-V/PI (Fisher Scientific) and cell cycle by propidium iodide were performed as previously described (130,131). All flow cytometry quantification was performed on the BD FACSCantoII cytometer, and at least 10,000 events were analyzed per sample.

2.9. Immunofluorescence Microscopy

Cells were fixed in 3.7% paraformaldehyde, permeabilized with 0.1% TritonX-100, and then blocked with 5% BSA in PBS. Primary antibodies were applied at 1:200, overnight at 4ºC, followed by secondary antibody at 1:500 for 2 hours at room temperature. Cells were then counter-stained with DAPI and imaged at 100X (DNA probes) or 10X-20X on an Olympus inverted 132 microscope IX70, with a Q-Color3TM Camera), Primary antibodies: CTR1/SLC31A1 (Novus Biologicals, NB100-402SS), CD44 Monoclonal Antibody (Thermofisher, 14-0441-82), ALDH (Cell signaling 36671), secondary antibodies: AlexaFluor 488- anti-rabbit (Thermo Fisher), and AlexaFluor566-antirabbit (Thermo Fisher)

2.10. Cellular ROS assessment

DCFDA / H2DCFDA - Cellular ROS Assay Kit (ab113851) was used to assess ROS levels in cells before and after treatment. Cells were plated and treated with cisplatin and vehicle

followed by ARV-825 treatment, then incubated with DCFDA for 30 mins in 37^0C. Then trypsinized and analyzed using flowcytometry at 535 nm.

2.11. In-vivo experiments

2.11.1. ABT-263 project

All animal studies were conducted in accordance with Virginia Commonwealth University IACUC guidelines. We first established the mouse oral squamous cell carcinoma (OSCC) cell line, 602, derived from the 4-nitroquinoline-1 oxide (4NQO)-developed tumor on the tongue. Female C57BL/6 mice (5 weeks of age; Envigo) were treated with 50 µg/ml 4NQO-containing water for 16 weeks. Then the drinking water was reverted to regular water until Week 22. When a single lesion on the tongue became ~50 mm^3, a tumor was removed and digested, and cells were isolated to establish a cell line. To establish tumors, 1 x 10^6 of 602 OSCC cells were suspended in 50/50 PBS-Cultrex basement membrane matrix (Cultrex, 3632-005-02) and subcutaneously inoculated into the rear flanks of C57BL/6 female mice (Day 0). When tumor size approached ~100 mm^3, mice were randomized in five groups (Day 13, N=6/group) and treated with cisplatin (5 mg/kg) by intraperitoneal injections at Day 13, 16, 20 and 23, then with ABT-263 (80 mg/kg) by oral gavage daily at Day 27-31 and Day 34-38. The second round of treatments was performed with cisplatin at Day 41, 44 and 48, followed with ABT-263 at Day 55-59 and Day 62-66. Tumor volumes were taken by manual caliper measurements.

2.11.2. ARV-825 project

To establish tumors, 1 x 10^6 of HN30 cells were suspended in 50/50 PBS-Cultrex basement membrane matrix (Cultrex, 3632-005-02) and orthotopically inoculated into the

buccal area of NSG female mice. When tumors were formed, mice were randomized into four groups (N=9/group) and treated with cisplatin (5 mg/kg) by intraperitoneal injections at day 0, and 8, then with ARV-825 (10 mg/kg) at days 15, 17, 20 and days 27, 29, and 31. Tumor volumes were taken by manual caliper measurements.

2.12. Immunohistochemistry

For cleaved caspase-3 (Cell Signaling, 9664) and γ-H2AX (Cell Signaling, 9718), tumors were fixed in 10% formalin phosphate buffer and performed on BOND RX Fully Automated Research Stainer. Slides were stained overnight at 4°C with cleaved caspase-3 (1:500) γ-H2AX (1:400), or BRD4 (1:500) primary antibodies then for 8 min at room temperature with the secondary antibody included in the BOND Polymer Refine Detection kit (Leica, DS9800). Slides were mounted with Dako CoverStainer (Agilent). Images were taken on Vectra Polaris Automated Quantitative Pathology Imaging System (Akoya Biosciences) at 20X at the VCU Cancer Mouse Models Core (CMMC). For X-Gal staining, tumors were frozen into OCT molds and cut into 10-micron sections by the VCU Tissue and Data Acquisition and Analysis Core (TDACC).

2.13. Blood analysis and platelet/neutrophil counts

Mice treated with vehicle, cisplatin, ABT-263, ARV-825 or a combination of cisplatin and ABT-263/ARV-825 were subjected to Complete Blood Count (CBC) analysis at the indicated time points (Figure 6E). Blood samples (~0.2 ml) were collected by facial vein using EDTA coated syringes and immediately analyzed by hematology analyzer Hemavet 950FS (Drew Scientific, Miami Lakes, FL, USA) at the VCU CMMC.

2.14. Statistical Analysis

Unless otherwise indicated, all quantitative data is shown as mean ± SD from at least three independent experiments (biological replicates), all of which were conducted in triplicates or duplicates (technical replicates). GraphPad Prism 6.0 software was used for statistical analysis. All data was analyzed using either a one- or two-way ANOVA, as appropriate, with Tukey or Sidak post hoc, with the exception of cell cycle, C_{12}FDG data, and platelet counts which were analyzed with unpaired, student's t-tests.

Chapter 3: Senolytic-mediated elimination of head and neck tumor cells induced into senescence by cisplatin

3.1. Introduction

3.1.1. Head and Neck Cancer and treatment options

Head and neck cancer is the sixth most common type of malignancy worldwide, with head and neck squamous cell carcinomas (HNSCCs) accounting for >90% of cases. HNSCC incidence largely correlates with tobacco and alcohol usage and is often diagnosed in advanced stages (132). There is also a rapidly increasing incidence of a human papillomavirus-related (HPV+) subtype of HNSCC, which arises in a younger patient demographic that includes many never-smokers (133).

Head and neck cancer is generally treated with a combination of surgery, radiation, and chemotherapy, with cisplatin being a primary therapeutic modality (134,135). Locally advanced head and neck cancer, LA/HNSCC patients might be eligible to receive 5-FU, Carboplatin, or Paclitaxel. Recurrent and metastatic patients on the other hand receive immunotherapy compounds such as Cetuximab a monoclonal EGFR antibody, or Pembrolizumab, a PD-1 inhibitor (136–139).

Despite recent advances in cancer therapeutic approaches, 40% and 20% of patients with HPV-negative HNSCC experience locoregional and distant failure, respectively, after cisplatin-based chemoradiotherapy. While head and neck cancer is

generally responsive to initial therapy, the disease almost invariably recurs, often becoming refractive to further therapy (140,141). An accumulating body of evidence has shown that cancer relapse often occurs after both conventional and advanced therapeutic approaches, where the therapy results in an accumulation of non-proliferative residual cancer cells (142,143). The cross-talk between these tumor cells and their microenvironment can result in escape from the growth-arrested state via recovery of the cellular proliferative capacity, leading to *disease recurrence* (144,145).

3.1.2. Cisplatin and senescence induction

cisplatin was accidentally discovered in 1965 by Dr. Barnett Rosenberg, a biophysics researcher at Michigan State University. Dr. Rosenburg and his colleagues applied electrical currents to a solution containing E. coli and observed morphological changes and growth arrest in bacterial cells. After two years of investigation, they discovered that the electrical current is not affecting the growth of the bacterial cells, but it's the Platinum released into the solution from the electrodes (146). Studies in different cancer models such as leukemia and sarcoma finally resulted in an NCI-funded clinical trial in 1972 to assess Platinum's effectiveness in cancer patients. Primarily, studies were focused on cisplatin toxicity, especially nephrotoxicity and apoptosis mechanisms (147). Cisplatin-induced senescence was first reported in nasopharyngeal carcinoma cell (NPC) models by X Wang et.al in 1998 (148,149). They characterized senescent cells by studying proliferation arrest, enlarged and flattened cellular morphology, multinucleated and vacuolated cellular appearance, and SA-b-gal overexpression (149).

Eventually, Cisplatin-based chemotherapy became the standard treatment for bladder, head and neck, testicular, ovarian, and cervical cancers (150). DNA has been shown to be the major target for cisplatin, however, this compound can bind to a broad range of different cellular components such as RNAs, proteins, thiol-containing peptides, membrane phospholipids, and protein filaments in the cytoplasm (151). Cisplatin uptake in the cells takes place through passive or active diffusion, however many membrane transporters with differential distribution in various tissues have been shown to be involved in cisplatin uptake (152). Platinum agents undergo aquation and they are positively charged once they are in the cell. These reactive forms have the potential to bind to the imidazole ring of the purine's guanosine and adenosine and form intra-and inter-strand crosslinks. Resulted crosslinks alter the DNA structure, followed by DNA damage response activation, apoptosis, and cell cycle arrest (153). Nucleotide excision repair (NER) pathway is the major DNA repair mechanism activated in response to cisplatin-induced DNA-adducts (154). Transcription-coupled repair (TCR) and global repair (GR) are two different NER pathways that remove the induced DNA-adducts from actively transcribed strands (TS) and non-transcribed strands (NTS), respectively (155). Here, in this study, we evaluated the effectiveness of cisplatin in head and neck cancer *in-vitro* and *in-vivo* models and investigated the efficacy of senolytic ABT-263 in eliminating senescent cells.

3.1.3. Objectives

The objectives of this study were to determine i) whether ABT-263 is an effective senolytic in head and neck cancer models after therapy-induced senescent and ii) the ABT-263 mechanism of senolysis.

3.2. Results

3.2.1. Senescence induction in HN30 and HN12 cells after cisplatin treatment

Pharmacokinetic studies have indicated that the highest plasma concentration of cisplatin achieved in patients is 12 μM at 5 minutes after injection, while the plasma concentration decreases to 5.9 μM after 2 hours. Up to 90% of total cisplatin is excreted (depending on the patient's renal function) in 24 hours. Consequently, initial experiments to investigate the cellular response to cisplatin in head and neck cancer cells involved exposure to clinically relevant concentrations of cisplatin (2, 5 and 10 μM) for 24 hours (156–158). As expected, cisplatin induced a temporary growth arrest after 24 hours of treatment in both HN30 (p53 wild-type) and HN12 (p53-null) head and neck cancer cell lines. As we have reported in other tumor cell models (54,117), the cells ultimately escaped and recovered their proliferative capacity (**Figure 3.1.A**). Cell cycle analyses confirmed that both cell lines were arrested primarily at the G0/G1 phase (**Figure 3.1.B**).

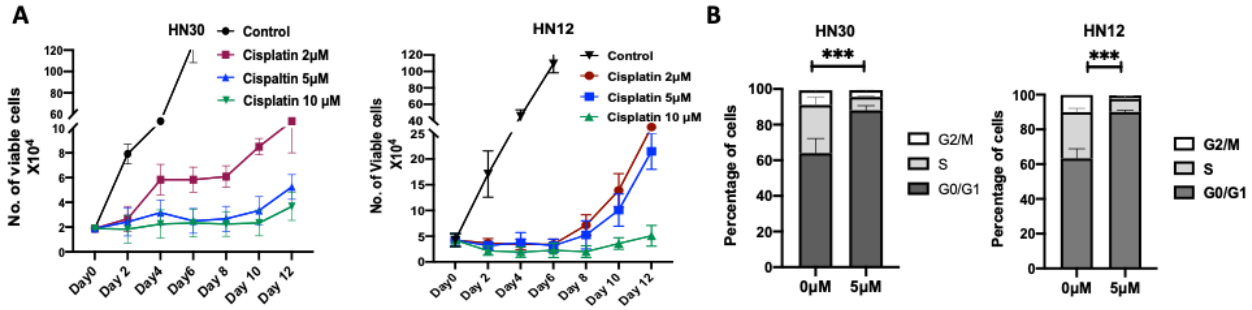

Figure 3.1. **Cisplatin induces a reversible growth arrest in both HN30 and HN12 cell lines. A**) Cell viability was monitored over a period of 12 days by trypan blue exclusion in HN30 and HN12 cells after 24 hours of exposure to 2, 5, and 10 μM cisplatin. **B**) Cell cycle analysis of HN30 and HN12 cells on Day 5 after treatment with 5 μM cisplatin for 24 hours. Cell cycle distribution is shown in the bar graphs. * $p \leq 0.05$, ** $p \leq 0.01$, *** $p \leq 0.001$, **** $p \leq 0.0001$ indicate statistical significance of each condition compared to control as determined using Student's t-test.

The antitumor activity of cisplatin is generally ascribed to the induction of DNA single- and double-strand breaks subsequent to the cross-linking of DNA (159–161). Consistent with the fact that senescence has been suggested to be a primary response of tumor cells to chemotherapeutic agents and cellular stress conditions (162), we confirmed that cisplatin promotes senescence in our experimental models. This determination was based on a number of characteristics such as morphological changes, qualitative and quantitative measurement of SA-β-gal activity using X-gal staining (**Figures 3.2A**) and fluorescence-based labeling with C_{12}FDG (**Figures 3.2.B**), and upregulation of the tumor suppressor p53 and the cyclin-dependent kinase inhibitor p21 (**Figure 3.2C**). Additional senescence markers, specifically heterochromatic foci (H3K9Me3) formation (**Figure 3.2A, lower panels**) and increased expression of

Senescence-Associated Secretory Phenotype (SASP) components such as *IL-6, IL-8, and IL-1β,* (**Figure 3.2D**) further confirmed that cisplatin treatment can promote senescence in HNSCC cells regardless of the *p53* status.

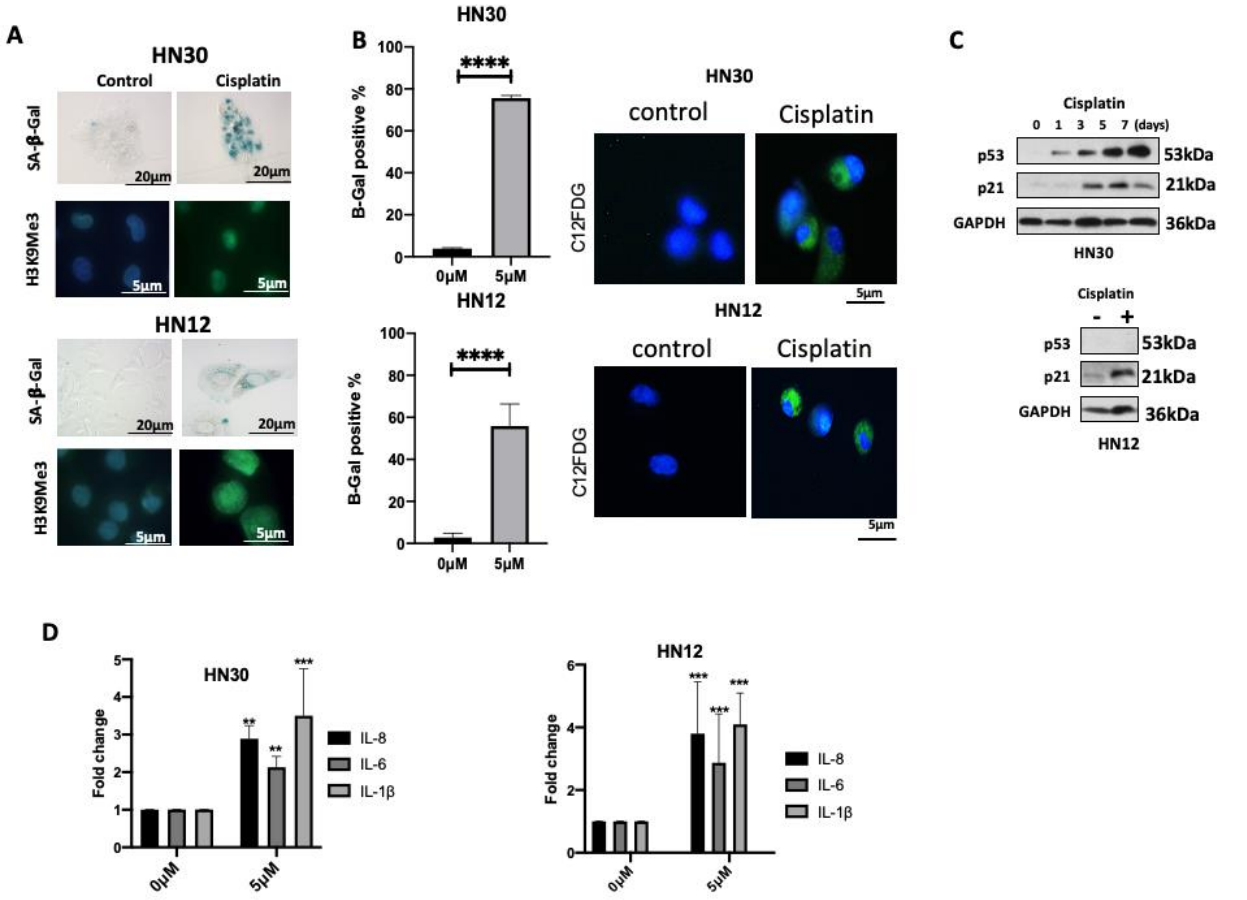

Figure 3.2. Growth-arrested cells show senescence characteristics. **A**) Cells were analyzed for increased expression of SA-β-gal using X-gal (20x objective, scale bar: 20 μm, bright field images) and increased SAHF formation by H3K9ME3 immunofluorescence (100x objective, scale bar: 5 μm, fluorescent images). Blue fluorescence indicates nuclear staining with DAPI, and green fluorescence reflects H3K9Me3 immunostaining. Staining was performed 5 days after treatment with 5 μM cisplatin for 24 hours. **B**) C_{12}FDG flow cytometry (bar graphs) and immunofluorescent images to quantify and confirm senescence. **C)** Western blotting for p53 and p21 in HN30

and HN12 cells at the indicated time points after cisplatin treatment. **D)** qRT-PCR for the SASP mRNAs IL-6, IL-8, and IL-1*β*. RNA was extracted at Day 5 following cisplatin exposure. All images are representative fields or blots from at least three independent experiments, and all quantitative graphs are mean ± SD from at least three independent experiments. * $p \leq 0.05$, ** $p \leq 0.01$, *** $p \leq 0.001$, **** $p \leq 0.0001$ indicate statistical significance of each condition compared to control as determined using two-way ANOVA with Sidak's *post hoc* test. All images are representative fields or blots from three independent experiments ($n = 3$).

3.2.2. Proliferative recovery in cisplatin-treated HNSCC cells is associated with a decline in senescence markers

Despite the long-held paradigm that therapy-induced senescence (TIS) is an irreversible and permanent form of growth arrest, which would be consistent with a favorable therapeutic outcome of senescence induction (163), our previous studies along with rigorous experiments by other investigators have firmly established that at least a subpopulation of cells can and will evade the senescent arrest and re-emerge with self-renewal capacity (57,66,117,164–166). To interrogate whether this is also the case for head and neck cancer cells induced into senescence by cisplatin, we utilized multiple approaches to investigate the capacity for proliferative recovery from senescence in our experimental models. Live-cell imaging microscopy was utilized to monitor proliferative recovery from cisplatin-induced senescent HN30 cells (**Videos S1A, B, and C**). A comparison of the morphologic characteristics of cells at different time points established that the emerging population at Day 11 in **Video S1C** was indeed derived from the senescent population. Further confirmation of the involvement of senescence in recovery

was based on the observation that proliferative recovery in our models is associated with diminution of the senescence markers (**Figure 3.3**). Specifically, SA-β-gal activity showed a significant reduction after the cells recovered their proliferative capacity (**Figure 3.3.A**). Similarly, the decline in additional senescence markers such as components of the senescence-associated secretory phenotype (SASP) (**Figure 3.3.B**), further indicates that the cisplatin-induced senescent-like state *is not sustained.*

It is possible that the recovered population originated from a subclone that was resistant to the primary effects of cisplatin de novo rather than via escape from chemotherapy-induced senescence (44,167). To confirm that cells can and do recover from chemotherapy-induced senescence, cisplatin-induced senescent cells were labeled with the fluorescent substrate of SA-β-gal, C_{12}FDG, and enriched for the highest ~30% of the C_{12}FDG-positive (SA-β-gal-positive) and morphologically enlarged population using fluorescence-activated cell sorting (FACS). This protocol ensures a highly specific and selective purification of senescent population from a heterogeneous mixture of tumor cells after treatment. The highly C_{12}FDG-positive population was then re-plated and monitored for senescence markers such as proliferative arrest, and SA-β-gal activity. As shown in **Figures 3.3.C and 3.3.D**, the sorted population recovered proliferative capacity after 16 days accompanied by the suppression of SA-β-gal activity.

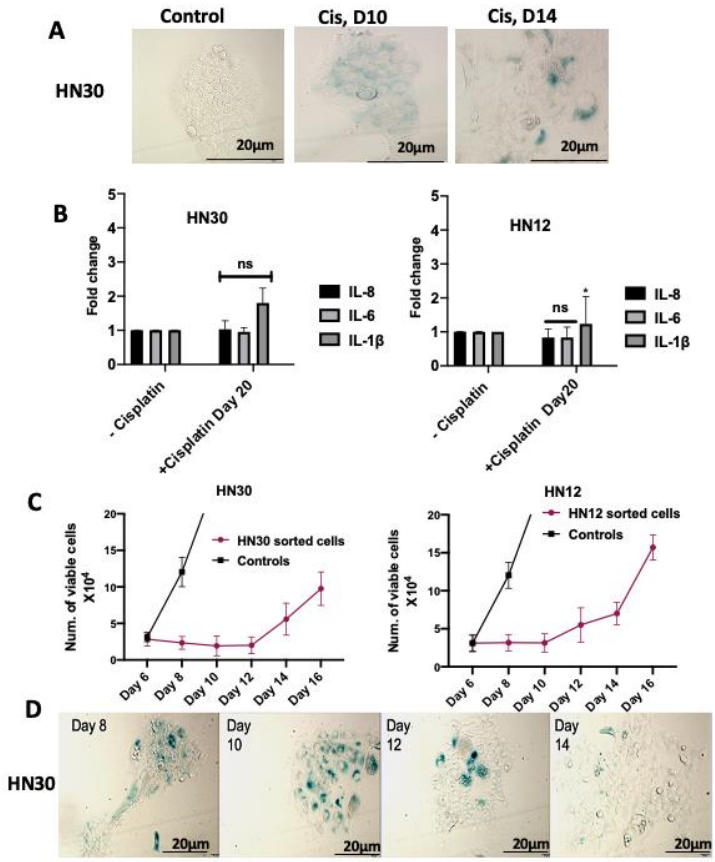

Figure 3.3. Proliferative recovery from cisplatin treatment in HN30 and HN12 cells is associated with the reduction of senescence-associated features. A) Histochemical SA-β-gal staining (20x objective, scale bar: 20 µm, bright field images). Cells were treated with 5uM cisplatin for 24 hours and stained for SA-β-gal activity at days 10 and 14. Note that the enzyme activity declines with cellular proliferative recovery. **B)** qRT-PCR for the SASP mRNAs IL-6, IL-8, and IL-1β. *P ≤ 0.05, **P ≤ 0.01, and ***P ≤ 0.001 indicate statistical significance of each condition compared to control as determined using two-way ANOVA with Sidak's post hoc test.**C)** Growth curve and **D)** SA-β-gal staining for high-C_{12}FDG-positive HN30 and HN12 cells (enriched on Day 5 after cisplatin treatment).

3.2.3. ABT-263 selectively eliminates senescent tumor cells in vitro

The proliferative recovery in tumor cells re-emerging from a therapy-induced senescent population has been shown to contribute not only to recurrence of a more aggressive form of the disease, but also to acquired resistance to chemotherapy or radiation (168,169). Consequently, in an effort to eliminate the cisplatin-induced senescent population, cisplatin-treated HN30 and HN12 cells were exposed to a single dose of ABT-263, an agent that has demonstrated senolytic properties (129,170) for 24-hours. A significant decrease in the number of viable cells (**Figure 3.4.A**) strongly suggests that ABT-263 selectively eliminates cisplatin-treated senescent cells, while showing minimal effects on untreated cells. Clonogenic survival assays using increasing concentrations of ABT-263 on non-treated tumor cells confirmed that ABT-263 alone, even at higher concentrations, was ineffective in perturbing colony formation for non-senescent tumor cells (**Figure 3.4.B**). This result was recapitulated with selective inhibitors of BCL-2 (ABT-199) and BCL-X_L (A-1155463) (**Figures 3.4.B**). In addition, ABT-263 treatment resulted in a significant decrease in the SA-β-gal positive (senescent) population (**Figure 3.4.C**), further confirming the selective activity of ABT-263 for the senescent population. As we have reported previously in models of non-small cell lung cancer and breast cancer (54,60), ABT-263 effectiveness diminishes over time as the treated cells escape senescence and recover their proliferative capacity (**Figure 3.4.D, upper panel**) in marked contrast to the effectiveness of ABT-263 after the second dose of cisplatin (**Figure 3.4.D, lower panel**). This observation reaffirms the selectivity of ABT-263 for a senescent cell population.

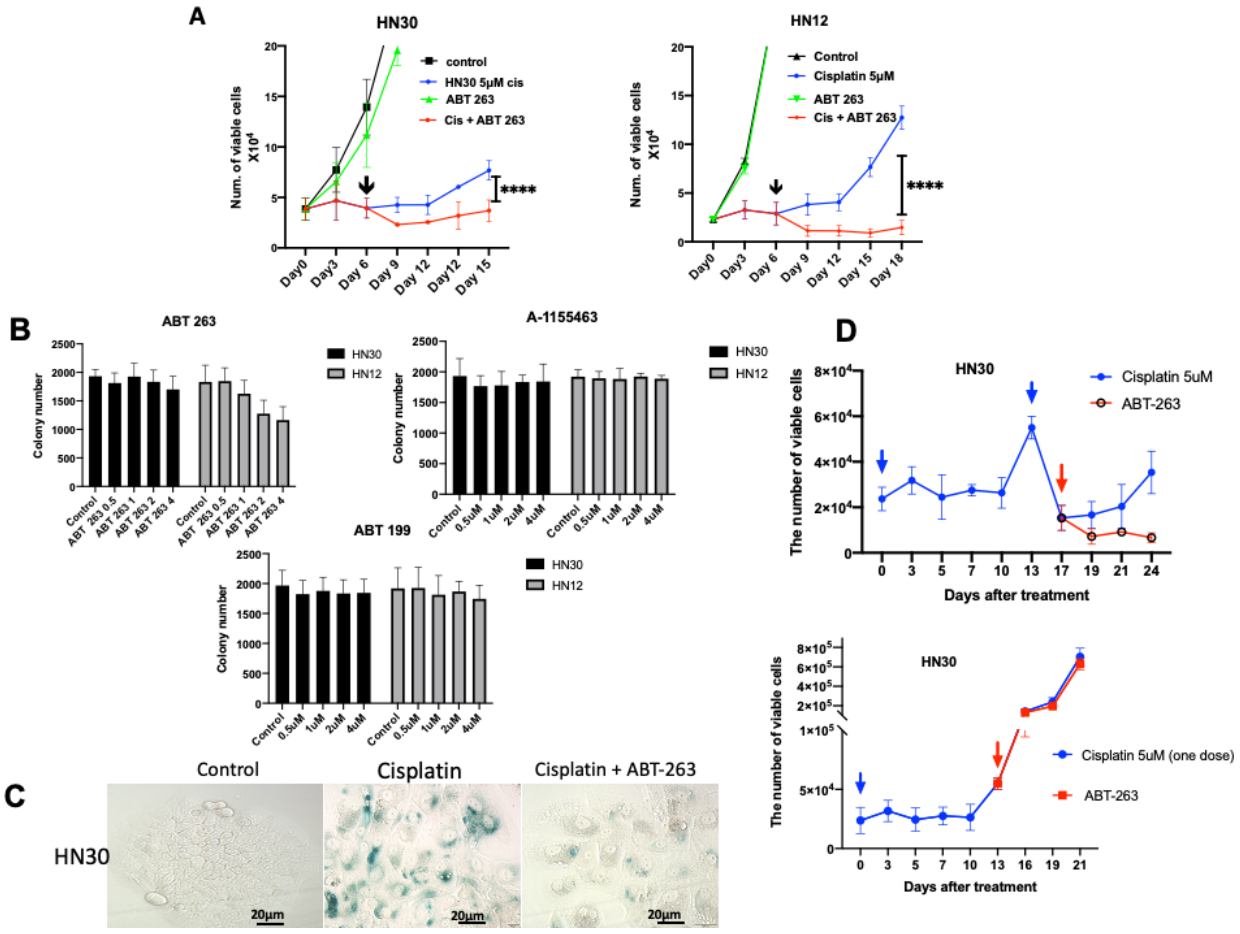

Figure 3.4. ABT-263 has minimal cytotoxicity on non-senescent cells or proliferative recovering cells from senescence. A) Growth curves for cells treated with cisplatin followed by either vehicle or 2 μM ABT-263 for 24 hours. Arrows indicate the time of ABT-263 treatment. **B)** Clonogenic survival assay performed on control cells treated with different concentrations of ABT-263 for 24 hours. The number of colonies were counted and analyzed. **C)** X-gal staining after sequential treatment of HN30 cells with cisplatin and ABT-263; decreased population of SA-β-gal positive cells show that ABT-263 treatment eliminates senescent cells**. D)** ABT-263 effectiveness diminishes over time when HN30 cells recover their proliferative capacity. Blue arrows indicate the cisplatin treatment timepoint. Red arrows are ABT-263 treatment timepoints. Note that HN30 cells undergo cell death only when they are in senescence state (top), but not in

recovery stage (bottom). All quantitative graphs are mean ± SEM from at least three independent experiments.

3.2.4. ABT-263 promotes senolysis by apoptotic cell death

Consistent with previously published studies on ABT-263 as an apoptosis inducing agent (171), there was a significant increase in Annexin-V/PI staining and the apoptosis marker, cleaved-caspase-3, in the combinatorial treatment group (cisplatin followed by ABT-263) compared to cisplatin or ABT-263 alone (**Figures 3.5.A and B**). Taken together, these observations strongly confirm that ABT-263 acts as a selective senolytic *in vitro* by significantly decreasing the number of cisplatin-induced senescent cells.

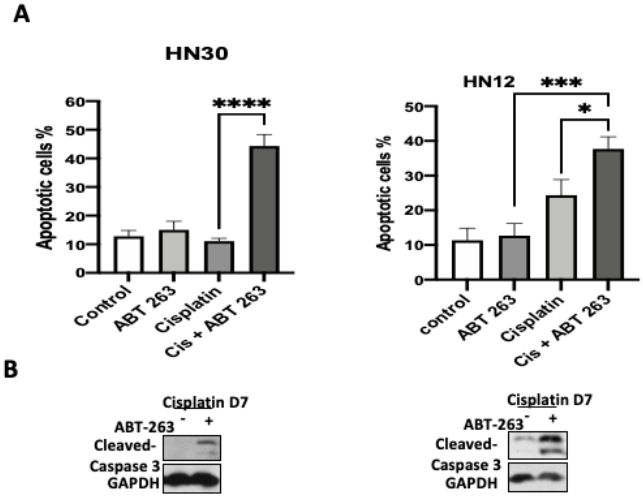

Figure 3.5. ABT-263 induces apoptotic cell death in cisplatin-induced senescent cells. A) Annexin-V/PI quantification of apoptosis induced by 2 μM ABT-263 with overnight exposure 24 hours after drug removal (Day 7) in HN30 and HN12 cells after treatment with cisplatin. **B)** Western blots for cleaved-caspase 3 in HN30 and HN12 cells. Cells were treated with 5uM cisplatin followed by ABT-263 for 24 hours and harvested at day 7. All images are representative fields or blots from at least three independent

experiments, and all quantitative graphs are mean ± SD from at least three independent experiments. * p ≤ 0.05, ** p ≤ 0.01, *** p ≤ 0.001, **** p ≤ 0.0001 indicate statistical significance of each condition compared to control as determined using two-way ANOVA with Sidak's post hoc test.

3.2.5. The BCL-X_L/BAX axis is the primary target for cell death induced by ABT-263 in cisplatin-induced senescent HNSCC cells

ABT-263 is known to specifically inhibit the function of the anti-apoptotic BCL-2 and BCL-X_L proteins to induce apoptotic cell death (171). In order to delineate the specificity of the inhibitory activity in head and neck cancer, we treated cisplatin-induced senescent HN30 cells with a BCL-2 specific inhibitor, ABT-199 and a BCL-X_L specific inhibitor, A-1155463. These agents do not have an effect on non-senescent HN30 cells (**Figures 3.6 A and B**).

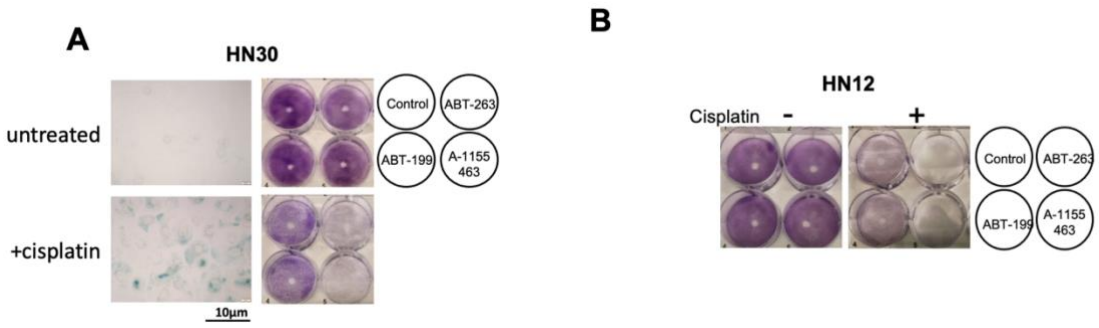

Figure 3.6. BCL-XL is the primary target for ABT-263-induced senolysis. Clonogenic survival assay performed on **A)** HN30 and **B)** HN12 cells treated with vehicle or cisplatin followed by ABT-263, ABT-199, and A-1155463 (1uM for 24 hours).

However, A-1155463, but not ABT-199, eliminated senescent cells, suggesting that BCL-X_L is the primary target in senescent HNSCC cells (**Figures 3.7.A, and 3.6.A**). We further confirmed that ABT-263 and A-1155463-mediated cell death was occurring primarily via apoptosis using Annexin-V staining (**Figure 3.7.C**). Similar specificity to BCL-X_L was also observed in p53-null HN12 cells **(Figure 3.7.B, D, and 3.6.B)** These results strongly suggest that BCL-X_L is the primary target of ABT-263-induced senolytic cell death.

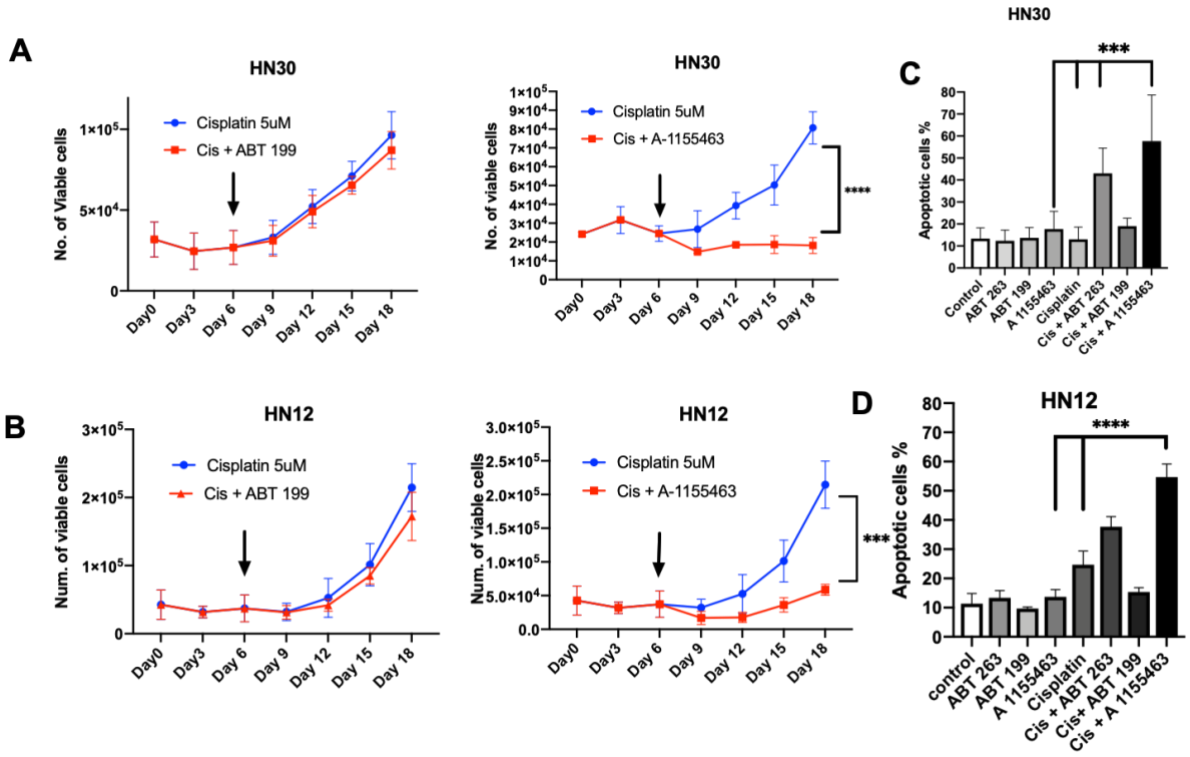

Figure 3.7. BCL-X_L is the primary target for ABT-263-induced senolysis. Growth curves for **A)** HN30 and **B)** HN12 cells treated with 5uM cisplatin followed by either vehicle, 2 µM A-1155463 (Left) or ABT-199 (Right) for 24 hours. Arrows indicate timepoints of A-1155463 or ABT-199 treatment. **C)** and **D)** Apoptotic cell death was determined in HN30 andHN12 cells, respectively, by Annexin-V/PI staining followed by FACS analysis. *** $p \leq 0.001$, **** $p \leq 0.0001$ indicate statistical significance of each

condition compared to indicated condition as determined using two-way ANOVA with Sidak's post hoc test.

In order to further support that the senolytic activity of ABT-263 in head and neck cancer cells was driven by inhibition of BCL-X_L, we next determined the expression of major BCL-2 family proteins in cisplatin-induced senescence HN30 cells. The level of the anti-apoptotic protein, BCL-X_L, gradually increased following cisplatin treatment (**Figure 3.8.A**). Consistently, these increases were also observed in the HN12 cells (**Figure 3.8.B**). Changes of other BCL-2 family proteins were inconsistent (**Figures 3.8 A and B**).

ABT-263 inhibits the interaction of BCL-X_L with BAX/BAK, thereby inducing apoptosis(117). To elucidate the involvement of these executioner pro-apoptotic proteins following ABT-263 treatment, we established stable HN30 cells with shRNA for BAX (shBAX), BAK (shBAK) or scrambled-control (shC) (**Figure 3.8.C**). Although these cell lines undergo similar induction of senescence following exposure to cisplatin (**Figure 3.8.D, bottom**), cisplatin-treated shBAX-expressing cells, but not shBAK expressing cells, failed to undergo cell death following exposure to ABT-263 (**Figure 3.8.D, top**), indicating that BAX is essential to ABT-263-induced senolysis.

The above results prompted us to investigate the subcellular localization of BAX and BCL-X_L, their interaction, and BAX conformational change/activation. The mitochondria-enriched lysates revealed the accumulation of BAX in cisplatin-induced senescent and further in ABT-263-treated HN30 cells (**Figure 3.8.E**). In contrast, the amounts of BCL-X_L and BAK at the mitochondria were only modestly perturbed (**Figure 3.8.E)**. We then investigated the BCL-X_L/BAX interaction by co-immunoprecipitation experiments. When BCL-X_L was immunoprecipitated, BAX was present in both the control and cisplatin

treatment groups. However, when ABT-263 was introduced, the BCL-X_L/BAX interaction was significantly decreased (**Figure 3.8.F**), suggesting that ABT-263 inhibits the BCL-X_L/BAX interaction and releases BAX from the complex. This result indicated that BAX became activated to allow apoptosis to occur.

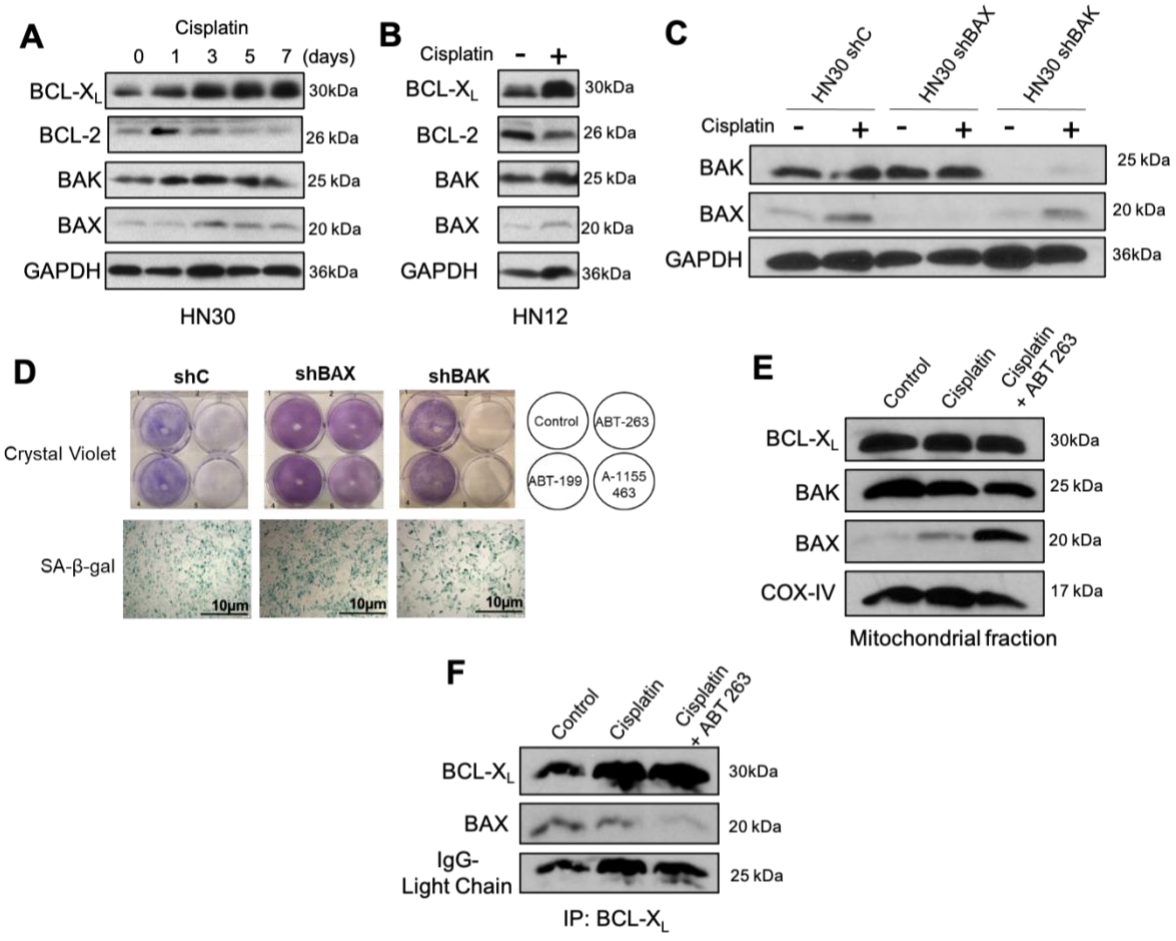

Figure 3.8. ABT-263 induces senolytic activity through modulation of the BAX/ BCL-X_L interaction. A) HN30 cells were treated with cisplatin and harvested at the indicated times**. B)** HN12 cells were treated with 5uM cisplatin and harvested at Day 7. Total cell lysates were subjected to Western blotting with the indicated antibodies. **C)** HN30 shBAX, shBAK and shC (scrambled control) cells were treated with cisplatin (5 μM)

for 5 days. Total cell lysates were subjected to Western blotting with the indicated antibodies. **D)** Senescent cells in (C) were treated with ABT-263, ABT-199, and A-1155463 (1 μM each) for 24 hours and stained with trypan blue and X-gal activity. (10x objective, scale bar: 10 μm, bright field images). **E)** BAX is recruited to the mitochondria membrane upon ABT-263 treatment. HN30 cells were treated with cisplatin (5 μM) for 5 days followed by ABT-263 (1 μM) for 16 hours. The earlier time point allowed us to detect navitoclax effects on apoptosis regulatory proteins before apoptosis completion, which might have resulted in the degradation of select proteins. Mitochondria-enriched (heavy membrane) fractions were subjected to Western blotting with the indicated antibodies. **F)** ABT-263 disrupts the interactions of BCL-X_L and BAX. HN30 cells were treated as in (E), and total cell lysates were immunoprecipitated with anti- BCL-X_L antibodies followed by Western blotting with the indicated antibodies. All images are representative fields or blots from three independent experiments (n = 3), and all quantitative graphs are mean ± SD from three independent experiments (n = 3).

3.2.6. ABT-263 selectively eliminates cisplatin-induced mouse oral squamous cell carcinoma cells in vitro and in vivo

In order to test the senolytic activity of ABT-263 *in vivo*, we first established the mouse oral squamous cell carcinoma (OSCC) cell line (602) derived from the 4-nitroquinoline-1 oxide (4NQO)-developed tumor on the tongue (see Materials and Methods). A crystal violet and senescence associated-β-galactosidase (SA-β-gal) stain revealed that cisplatin induced 602 cells into senescence and sensitized the cells to ABT-263 (**Figure 3.9.A**). We then evaluated senolytic activity of ABT-263 in a syngeneic mouse model. Cisplatin treatment resulted in brief tumor stasis compared to the control and ABT-263 monotherapy (**Figure 3.9.B**). Sequential cisplatin and ABT-263 treatment

resulted in a distinct therapeutic benefit characterized by delayed tumor recurrence and longer survival (**Figure 3.9.B and C**). Furthermore, two rounds of cisplatin followed by ABT-263 treatment (combination B) outperformed all groups, including the single round of cisplatin followed by ABT-263 (combination A), in terms of delayed tumor recurrence and improved animal survival.

We further extracted and analyzed the 602 tumors to evaluate markers of senescence and the senolytic activity of ABT-263. Cisplatin-induced senescence in tumors *in vivo* was clearly detected as X-gal staining with increased SA-β-gal activity, which was then decreased upon ABT-263 treatment (**Figure 3.9.D, left panels**). Cisplatin also induces DNA single- or double strand breaks (DSBs). The phosphorylated form of histone H2AX (γ-H2AX) marks sites of DNA DSB repair. Compared to the control, γ-H2AX was strongly stained in tumors exposed to cisplatin (**Figure 3.9.D, middle panels**). Extensive cleavage of caspase-3 (c-casp3), indicative of apoptosis, was evident in tumors treated with cisplatin followed by ABT-263 (**Figure 3.9.D, right panels**). These results

suggest that the benefit of sequential treatment is a result of apoptosis caused by ABT-263 in cisplatin-induced senescent tumors.

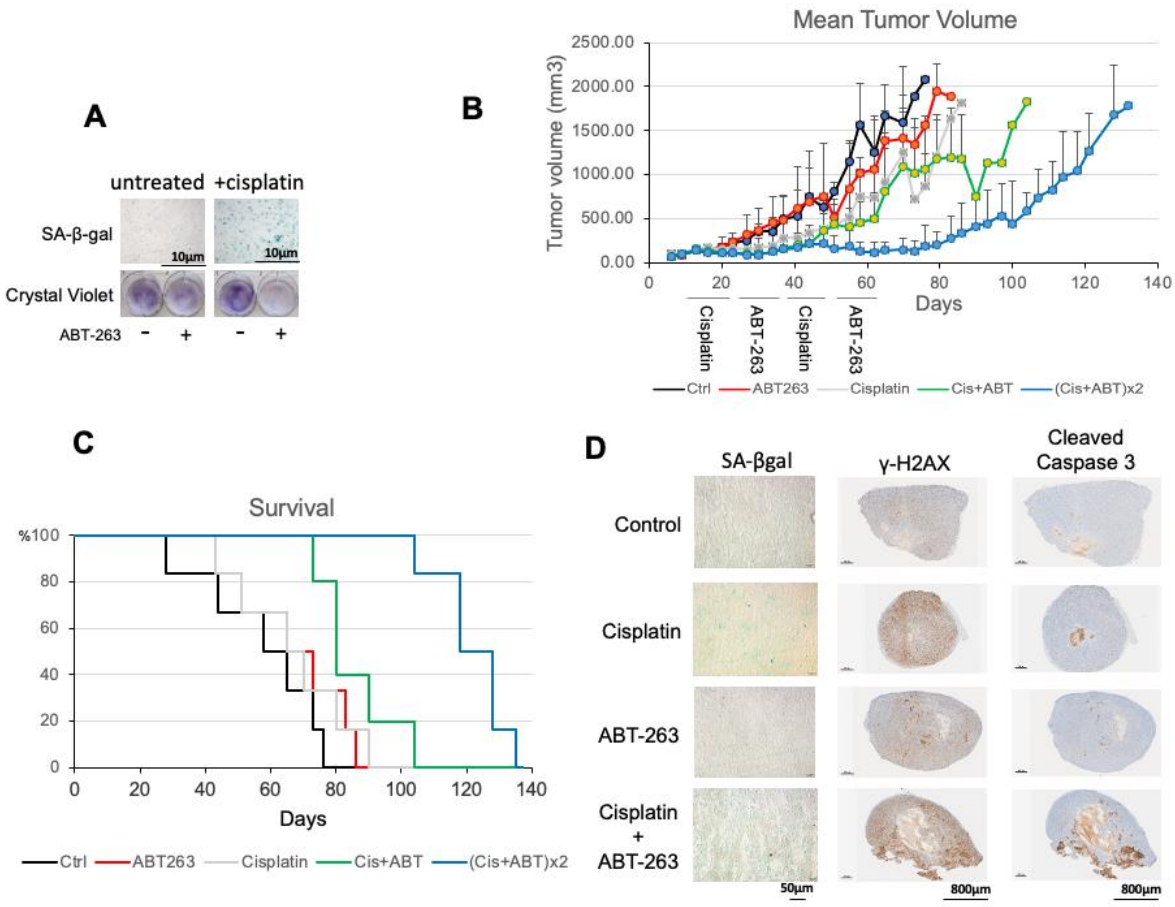

Figure 3.9. Sequential administration of ABT-263 following cisplatin delays tumor recurrence in a syngeneic mouse model of OSCC. A) ABT-263 eliminates cisplatin-induced senescent mouse OSCC cells in vitro. Mouse OSCC 602 cells were treated with cisplatin (2.5 μM) for 5 days followed by exposure to ABT-263 (1 μM) for 24 hours. X-gal staining in SA-β-gal positive cells indicates senescence after cisplatin treatment. (10x objective, scale bar: 10 μm, bright field images). **B)** 602 cells were subcutaneously inoculated in C57BL/6 mice at the flank (Day 0). When tumors achieved a size of ~100 mm3, mice were randomized into five groups (Day 13, N=6/group). Mice were treated with cisplatin (5 mg/kg) at Day 13, 16, 20 and 23, followed by ABT-263 (80 mg/kg) daily

at Day 27-31 and Day 34-38. The second round of treatments was performed with cisplatin at Day 41, 44 and 48, followed with ABT-263 at Day 55-59 and Day 62-66. Tumor volume (B) was determined by caliper measurements and survival **(C)** was monitored by Kaplan-Meier curves. **D)** Tumors were excised after treatment with vehicle (control), cisplatin, ABT-263 or cisplatin followed by ABT-263. SA-β-gal activity was monitored by staining with X-gal, and DNA double-strand breaks repair and apoptosis were monitored by immunohistochemical staining with antibodies against γ-H2AX and cleaved-caspase-3, respectively (Original magnification = 20X). Graphs are represented as mean ± SEM. All tumor images are representative fields from four tumor slices (*n* = 3) taken from three mice per group (*n* = 3).

Based on the previous preclinical data in animal models (172), ABT-263 treatment results in rapid and concentration-dependent thrombocytopenia that resolves after drug cessation (173,174). Here, we evaluated the safety of ABT-263 in our animal model by analyzing Complete Blood Counts (CBC), particularly by focusing on the dynamic of circulating platelets and neutrophils (Figures **3.10, and 3.11)**. The number of circulating platelets and neutrophils in different groups of mice shows that ABT-263 treatment alone

or in combination with cisplatin does not result in thrombocytopenia or neutropenia in our perimental model system.

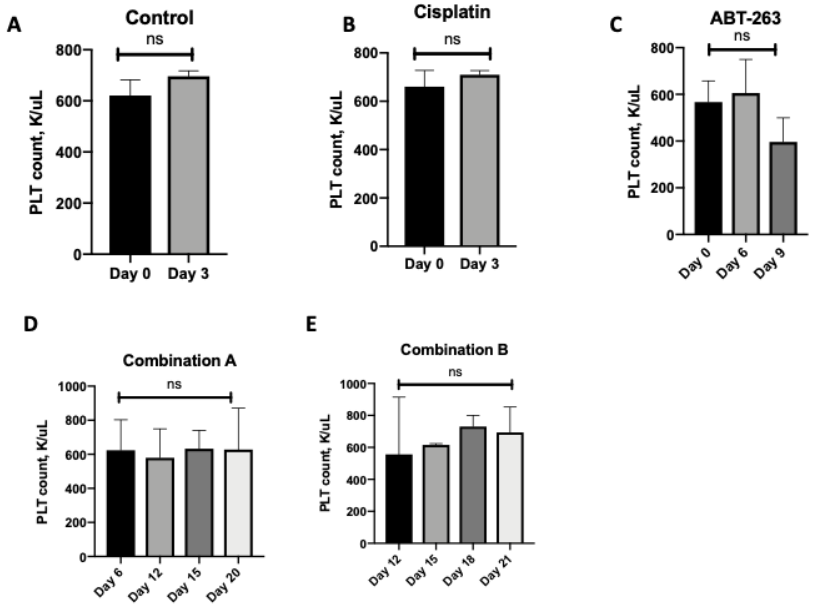

Figure 3.10. Platelet cell count (K/ µl) in mice treated with **A)** vehicle, **B)** cisplatin alone, **C)** ABT-263 alone or **D** and **E)** in combination with cisplatin over a period of 21 days. All quantitative graphs are mean ± SD from at least three independent experiments. * $p \leq 0.05$, ** $p \leq 0.01$, *** $p \leq 0.001$, **** $p \leq 0.0001$ indicate statistical significance of each condition compared to indicated condition as determined using two-way ANOVA with Sidak's post hoc test.

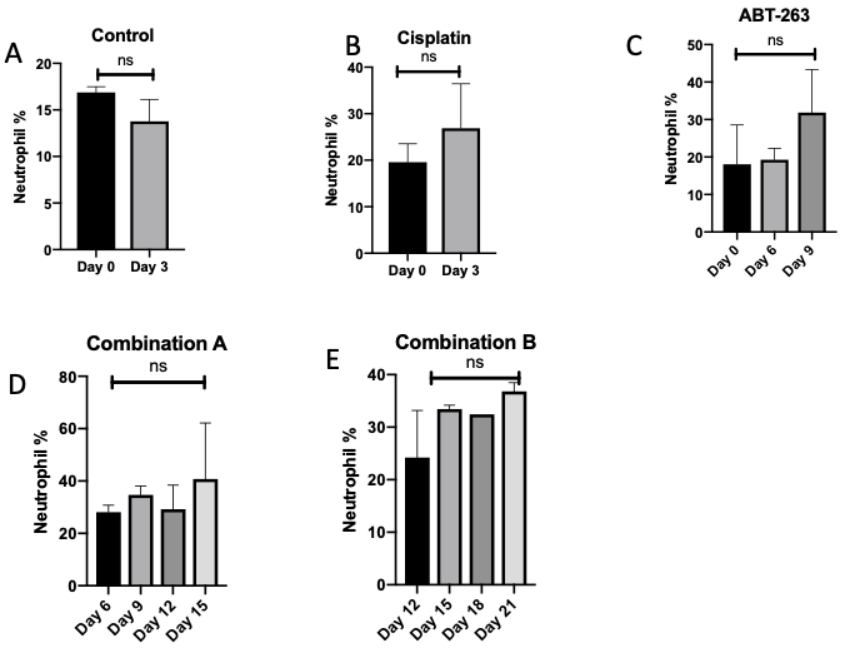

Figure 3.11. Cisplatin and ABT-263 treatment alone or in combination did not result in significant Neutropenia. Blood samples were analyzed for neutrophil percentage at different time points in different groups of **A)** control, **B)** Cisplatin alone, **C)** ABT-263, **D,** and **E)** cisplatin in combination with ABT-263. Control vs ABT, cisplatin, Combination A or B: $p > 0.05$ All quantitative graphs are mean ± SEM from at least three independent experiments. * $p \leq 0.05$, ** $p \leq 0.01$, *** $p \leq 0.001$, **** $p \leq 0.0001$ 0001 indicate the statistical significance of each condition compared to the indicated condition as determined using two-way ANOVA with Sidak's post hoc test.

3.3. Discussion

Locoregional and distant recurrence is the most common cause of death in HNSCC patients, and it has been suggested that the morbidity and mortality is mediated by the progression from residual tumor cells that survive from the assault of chemotherapy or radiotherapy (175). Such contribution to recurrence from residual tumor

cells is also observed in breast, prostate, and lung cancer; more specifically, whereas the initial therapies result in both tumor regression and stasis, a residual cell population can proliferate at secondary local or distant sites with equal or more aggressiveness (176–178). This residual and dormant cell population could potentially be linked to senescent and quiescent tumor cells as well as cancer stem cells (179–181).

Despite the fact that therapy-induced senescence has been investigated for decades, the contribution of senescent tumor cells to disease recurrence is still obscure (182). The senescence phenotype was initially considered as a favorable outcome of cancer therapy, as it likely represents a primary response to chemotherapy or radiation and cells in this state manifest characteristics such as prolonged growth arrest, which may lead to tumor regression (183). However, as senescent cells are metabolically active and resistant to apoptosis(184,185), it is anticipated that the considerable heterogeneity of senescent tumor populations would allow for proliferative recovery of some tumor subpopulations from the state of growth arrest (185,186). Additionally, the ability of senescent cells to secrete pro-inflammatory cytokines and chemokines (SASP) contributes to chronic inflammation and adverse paracrine effects (187,188). Finally, the tumorigenic potential and more aggressive behavior of post-senescent cells, including frequent epithelium-to-mesenchymal transition (EMT) and genomic instability, argues for the central involvement of senescent cells in disease recurrence (189). To combat these potentially deleterious long-term effects of therapy-induced senescence, a new class of compounds, termed “senolytics” which selectively induce cell death in senescent cells, has been developed (189).

In the current work, we investigated the utility of a two-hit sequential treatment approach, first with chemotherapy followed by senolysis, in head and neck cancer. We chose p53 wild-type HN30 cell line derived from pharynx and p53-null HN12 cell line derived from lymph node metastasis (190), in consideration of the fact that *p53* is most commonly mutated gene in head and neck cancer patients (132). Both cell lines showed a significant degree of senescence upon treatment with cisplatin by assessing multiple assays and markers (**Figure 3-1**). The delayed senescence in HN12 cell line likely reflects the p53-independent pathway (191). For example, it has been shown that p16 plays a critical role in senescence induction in p53-null models (191). We also confirmed senescence and tumor stasis induced by cisplatin treatment in a syngeneic mouse model (**Figures 3-9B**). Furthermore, the proliferative recovery from senescence was confirmed using fluorescence-activated cell sorting (FACS) and live cell imaging (**Figure 3-3 and Videos**) as well as in a mouse model (**Figure 3-9**). These results further support the recent paradigm shift that therapy-induced senescence is transient, but not permanent, growth arrest, which may contribute to tumor recurrence from dormancy(34).

In order to overcome the survival mechanism which senescent cells maintain, our data indicates that a BCL-2/BCL-X_L inhibitor, ABT-263 (navitoclax) efficiently induces apoptosis following cisplatin treatment in *in vitro* and *in vivo* head and neck cancer models (**Figures 3-5 and 3-9D**); these studies are consistent with previous reports showing effectiveness of ABT-263 in breast and lung tumors (81,86,192–194). We extensively investigated the selectivity of ABT-263, determining that this compound induces apoptosis only in the cisplatin-induced senescence population, but not in the proliferating population (**Figures 3-4**). Additionally, our growth curve data with multiple exposures to

cisplatin after proliferative recovery confirms that ABT-263 shows selectivity for the cells that are exposed to a second dose of cisplatin after recovery, but not the population recovered from the first cisplatin exposure (**Figure 3-4 D**). In mechanistic studies, we showed that (i) BCL-X_L is the primary target for apoptosis induce by ABT-263 in senescent cells (**Figure 3-7**), and that (ii) the inhibition of BCL-X_L/BAX interaction by ABT-263 followed by BAX activation is critical for this apoptosis induction (**Figure 3-8**). We and others have shown that BCL-X_L expression increases gradually after senescence induction (117,195,196) and the sensitization induced by ABT-263 is BCL-X_L-dependent in breast and lung tumors (117). Our results indicate that BAX, but not BAK, is a critical pro-apoptotic protein for ABT-263-induced apoptosis in senescent cells in which the level of BCL-X_L is induced and BAX is accumulated at the mitochondria. It has been shown that an increase of BCL-X_L levels by overexpression leads to an increase of BAX at the mitochondria and sensitizes cells treated with ABT-737, a prototype BCL-2/BCL-X_L inhibitor of ABT-263, to apoptosis(197). We speculate that the physiological levels of BCL-X_L increased by senescence induction also led to BAX accumulation at the mitochondria, which shifts the dependency of ABT-263-induced apoptosis toward BAX. Consistently, studies have shown that BCL-X_L is qualitatively and quantitively ten times more active than BCL-2 and is more effective in apoptosis inhibition (198,199). Moreover, the majority of head and neck cancer patient's tumor biopsies have shown a significant up-regulation in BCL-X_L and not BCL-2 protein levels. BCL-X_L levels was shown to be directly associated with worse therapy outcomes, whereas BCL-2 positive tumors, even after locoregional metastasis, demonstrated better therapy outcomes (200). Carter et.al also showed that BCL-X_L is significantly over-expressed in head and neck cancer patients

tumor samples, while BCL-2 levels doesn't show any increase(201). These data suggest that BCL-XL would play a major role, particularly in head and neck cancer, for drug sensitivity and treatment outcome. However, more additional work is needed to define the precise role(s) of BCL-XL and BCL-2, since our findings in this report along with publications in this area clearly show that BCL-2 and BCL-XL are functionally different (117,199,202).

Our data with a syngeneic mouse model (**Figure 3-9**) clearly indicate that two rounds of sequential cisplatin followed by ABT-263 treatment has a distinct therapeutic benefit with delayed tumor recurrence and longer survival. Cycling treatments with drugs and/or radiation are common procedure and often show clinical benefits. One concern regarding ABT-263 in the clinic is the thrombocytopenia that has been a predominant dose limiting toxicity as both a monotherapy and in combination. This has been managed successfully in several recent trials, allowing for tolerated and biologically active combinations with kinase inhibitors such as Osimertinib (203) and ruxolitinib(204). However, neutropenia has been reported as a dose limiting toxicity when navitoclax was administered with chemotherapy(205); this toxicity has been particularly limiting for these combinations, none of which have progressed beyond Phase 1. Our data indicate that sequential exposures to ABT-263 after cisplatin treatment can effectively reduce tumor burden, and therefore alleviate the need to dose both agents concomitantly. This sequential dosing approach thus has the potential to effectively treat head and neck cancer patients while circumventing the limiting hematological toxicity that would be anticipated by simultaneous dosing of the two agents. Next-generation BCL-2/BCL-XL inhibitors such as AZD0466 (206), APG-1252 (207), and DT2216 (BCL-X_L-PROTAC)

(208) have been designed to mitigate thrombocytopenia and clinical trials have recently started with these agents. Thus, these compounds also need to be verified as senolytics to be combined with existing chemotherapy/targeting drugs in the future. It is also imperative to determine the senolytic efficacy following chemoradiation, which is commonly used as the first-line treatment for HNSCC patients.

Taken together, our study provides a clear foundation upon which to develop therapeutic approaches for senescence clearance to potentially prevent or delay cancer relapse in HNSCC. Additionally, our *in-vitro* and *in-vivo* data show that sequential treatment of cisplatin and navitoclax can provide a potentially effective treatment strategy with mitigated toxicity for HNSCC patients. However, there are still key questions that need to be answered in future studies, such as the recovery mechanism in senescence cells, the interplay between navitoclax and immune system, and resistance to navitoclax in a subpopulation of cancer cells after acquiring cisplatin induced resistance. Our preliminary data (not published) shows that navitoclax is not effective in head and neck cancer resistant models. Resistance mechanism and a new strategy to eliminate the resistant population is of great importance to improve patients therapy outcome in the future.

Chapter 4: Elimination of cisplatin-treated head and neck cancer cells to delay resistance to therapy

4.1. Introduction

4.1.1. Therapy options and outcomes in Head and Neck cancer patients

Despite all multimodal treatment strategies that have been developed in recent years, treatment of locally advanced squamous cell carcinoma of the head and neck is still a challenge. After the introduction of alternative approaches such as immunotherapeutic and targeted therapy compounds, pembrolizumab and cetuximab, respectively, cisplatin remains the most cost-efficient and effective treatment for the majority of head and neck cancer patients (209,210). Most HNC patients initially respond to cisplatin therapy, but the fatal proliferation and chemoresistance are the limiting factors in the first-line therapy in these patients which consequently results in cancer recurrence and poor outcomes. Additionally, the local or distant relapse has been associated with higher morbidity, lower median survival, and an increase in financial burden in cancer care (136,211).

4.1.2. Cisplatin-induced resistance

Chemoresistance, especially cisplatin resistance, has been known as a manifold and complex phenomenon that is not yet fully understood. However, this complex and multilevel process has been potentially associated with alterations in drug import and

export, DNA repair response, and glutathione-dependent detoxification (153,212). It is also worth mentioning that the impact of pre-existing factors and high mutational loads that contribute to resistance to chemotherapeutic agents has been studied but are still not completely understood.

Understanding the underlying mechanisms of resistance to chemotherapeutic agents such as cisplatin, has continued to represent a challenge in cancer research. Chemotherapy resistance takes place due to a variety of events in cancer cells that includes extrinsic factors (such as tumor microenvironment and immune system response) and intrinsic factors such as development and selection of a subpopulation of cells with stem-like features, alterations in drug transport and metabolism, enhanced DNA repair, improved capacity for drug detoxification, and epigenetic changes (212). Therefore, cisplatin treatment often selects for a subset cellular population that can escape senescence and apoptosis and emerge as a more aggressive sub-population (213). Additionally, since cisplatin has been recognized as the most efficient and cost-effective first-line therapy for head and neck cancer patients, identifying a secondary compound to target the resistant sub-population in the primary tumor would likely represent a breakthrough approach for treating these patients.

As was discussed in chapter one, senolytics are one of the most effective secondary compounds that eliminate senescent cells. However, senolytics are not the only secondary compounds that have been reported to be effective in cancer treatment. In 2015, Jing Lu et.al designed ARV-825, a hetero-bifunctional (Proteolysis Targeting Chimera) PROTAC, that recruits BRD4 to the E3 ubiquitin ligase cereblon, resulting in fast, efficient, and prolonged degradation of BRD4 in all Burkitt's lymphoma cell lines

(111). This compound was developed in order to overcome limitations associated with JQ1, the primary BRD4 inhibitor, which is lacking in selectivity and is associated with unacceptable toxicity (214). These compounds became attractive alternatives to JQ1 to inhibit or degrade BET family proteins.

Bromodomain-containing proteins are known as essential components of epigenetic readers and erasers (215). An accumulating body of evidence has shown that ARV-825 has been effective as monotherapy in neuroblastoma, thyroid cancer, leukemia, lung carcinoma, and more models (110–112). The mechanism of action of ARV-825 greatly varies between cell lines and the treatment strategy that is being applied. Moreover, the concentration of ARV-825 and whether it is being used in combination with a chemotherapeutic compound also influence the mechanism of action (112,113,115,216). In the current work, we established a cisplatin-resistant head and neck cancer model and studied ARV-825 effectiveness and mechanism of action as a secondary compound combined with cisplatin.

4.1.3. Objectives

The objectives of this study were to i) Confirm cisplatin-induced resistance in head and neck cancer models, ii) Identify the mechanism by which resistance is acquired iii) assess ARV-825's effectiveness in eliminating both resistant and non-resistant cells, iv) investigate the mechanism by which ARV-825 eliminates cisplatin-treated cells.

4.2. Results

4.2.1. Cisplatin treatment results in acquired resistance in head and neck cancer cell lines

Based on the standard of care treatment regimen approved by the FDA, cisplatin is still the first-line chemotherapeutic agent being used in head and neck cancer patients. The concentration and administration of cisplatin are determined according to the stage and grade of the tumor, but in almost all patients, the regimen includes multiple cycles of cisplatin infusion. In the previous chapter, we showed that HN30 and HN12 cell lines underwent a temporary senescent state after cisplatin treatment, and sequential treatment with the senolytic, navitoclax significantly eradicated the senescent population. However, a small subpopulation of the HN30 cell line still survived and contributed to the proliferative recovery we observed at approximately day 12 after cisplatin treatment. Literature mining and data analysis on senescent cells and the phenomenon behind the recovery suggested the possibility in which exposure to cisplatin can lead to cisplatin-induced resistance (217–219). To assess this possibility, we exposed our previously analyzed head and neck cancer cell line, HN30, to multiple cycles of cisplatin and analyzed their growth arrest and IC50 using MTS and trypan blue exclusion viability, and β-galactosidase (SA-β-gal) activity assays. **(Figures 4-1)**. IC50 values increased from 3.7 in parental cells compared to 10.48 in the resistant model **(Figure 4-1 A)**. The newly generated cell line, HN30R, also showed lower growth rate with proliferative recovery at day 8 **(Figure 4-1 B)**. Histological and FACS based β-galactosidase (SA-β-gal) activity assay in panel C also shows that different concentrations of cisplatin induce around 80%

senescence in HN30 cells, while in the resistant cell line the maximum amount of senescence quantified is 20%.

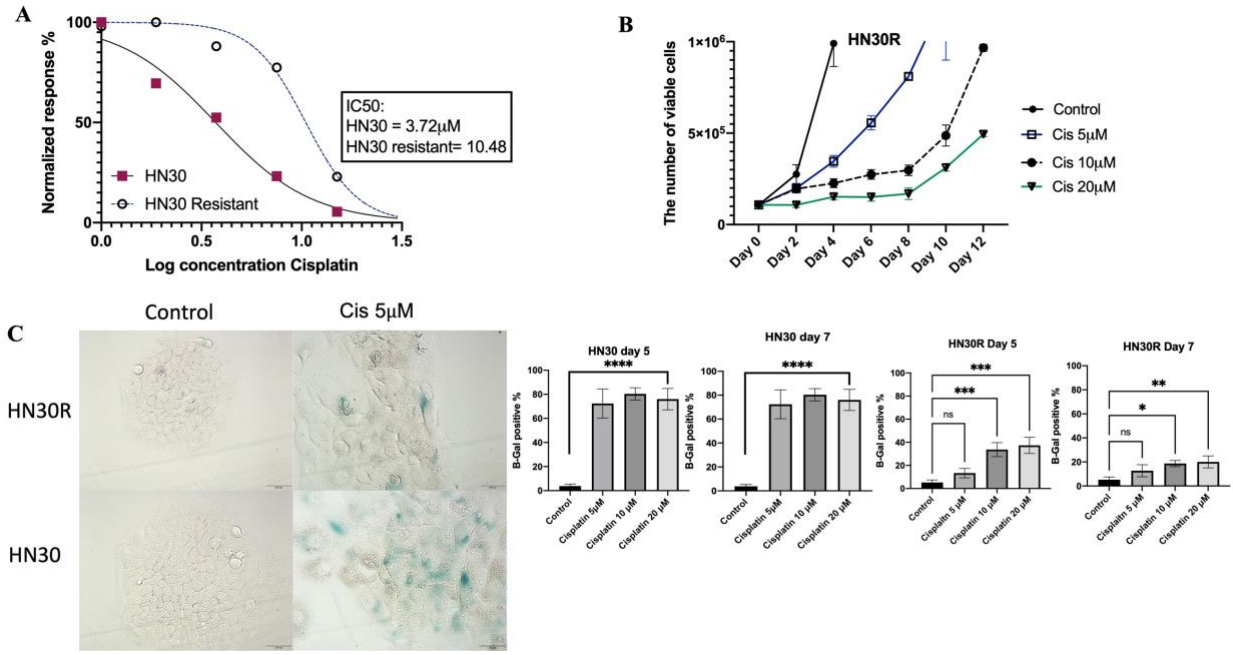

Figure 4-1. Cisplatin treatment induces acquired resistance in HN30 cells. A) IC50 was determined for both parental and resistant cell lines using MTS assay. IC50 increased more than 3 fold in the resistant cell line after continuous cisplatin treatment. **B)** HN30R time course cell viability assay after treatment with 5, 10, and 20µM cisplatin indicates that the cisplatin effect is dose-dependent and 5µM concentration induces a temporary senescence associated growth arrest with a rapid recovery. **C)** beta-galactosidase (SA-βgal) activity was assessed using X-gal staining and C12FDG assay in both parental and resistant cells at day 5. According to the morphological changes and SA-βgal signal, HN30R undergo a brief senescence state.

4.2.2. Cisplatin-Resistant cells are resistant to Navitoclax

ABT-263 or Navitoclax has been one of the most effective senolytics in cancer research and clinical trials investigating more efficient combination therapies to improve

therapy outcomes in patients (NCT01828476, NCT02591095, NCT00891605, NCT04041050) However, the heterogeneous nature of tumor cells can contribute to differential responses to therapy. In our previous study, we showed that almost 80% of HN30 cells undergo senescence after cisplatin treatment, with approximately 55% undergoing apoptosis after Navitoclax treatment. The difference between the percentage of cells that are in a state of senescence and the overall extent of apoptosis suggests that there is a subpopulation of senescent cells that either recover rapidly after cisplatin treatment and consequently fail to demonstrate sensitivity to navitoclax or that are intrinsically resistant to this compound. Understanding the origin of this subpopulation needs to be further investigated, however, to confirm that HN30R cell line does not respond to the combination treatment with cisplatin and navitoclax, we monitored the number of HN30R cells after treatment with 5 and 10 μM cisplatin alone or in combination with 2 μM navitoclax. Figure 4-2A shows that increasing the concentration of cisplatin does not increase the cellular response to navitoclax.

We utilized a trypan blue exclusion/ cell viability assay and Annexin V/PI flow cytometry to analyze the number of viable cells and apoptosis, respectively, upon exposure of the HN30R cells to cisplatin followed by navitoclax. **Figure 4-2-A and B** indicate that, as shown in **Figure 3**, exposure to 5μM cisplatin slows HN30R cell growth but does not arrest the cells; furthermore, as would have been anticipated based on the senolytic properties of navitoclax, HN30R cells do not respond to navitoclax treatment as the cells continue to proliferate and there is no increase in apoptosis.

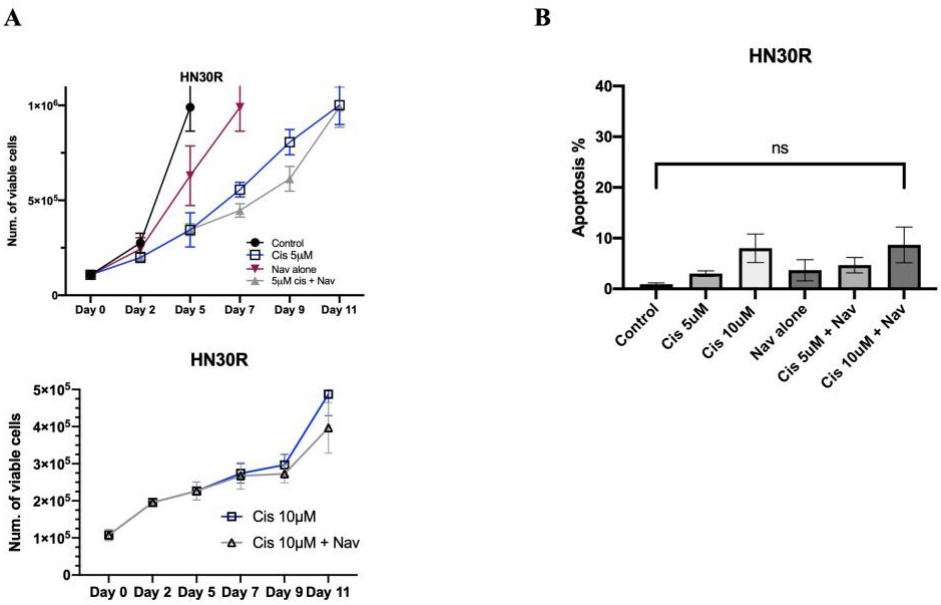

Figure 4-2. HN30R cells do not respond to cisplatin in combination with Navitoclax. **A)** Time course cell viability assay of HN30R cells treated with cisplatin 5 and 10 μM for 24 hours, followed by 2 μM navitoclax for 48 hours does not show any significant cell death. Note that in the previous section, we showed that the parental cell line, HN30, dramatically underwent apoptosis after the combination treatment. **B)** Apoptosis using Annexin V/PI staining in HN30R cells treated with the same strategy. HN30R cells, unlike the parental cell line, do not show any sensitivity to the senolytic, navitoclax.

4.2.3. Parental HN30 and resistant HN30 cell lines fail to exhibit CSC characteristics

Cisplatin resistance can be a multifactorial phenomenon in which various molecular pathways are involved. Whether drug resistance is intrinsic or acquired, it is clinically relevant to identify strategies for overcoming the drug resistance phenotype, and characterizing and identifying cancer stem cells have been correlated with diagnosis, therapy, and prognosis (220).

One possibility that has received extensive attention in the literature is the Cancer Stem Cell hypothesis (CSC), which suggests the existence of a rare subpopulation with stem cell-like characteristics, particularly that of self-renewal that is essential for cancer initiation, progression, and survival after therapy (221–224). The CSC population characteristics have been broadly investigated and it has been shown that this subpopulation survives and thrives during therapy-induced stress conditions, thereby resulting in the expansion of the resistant subpopulation (225,226). As a result of many reports published on cancer stem cells, few characteristics have been identified including Slow proliferation, differentiation properties, distinguished surface markers, and resistance to conventional chemotherapy and radiotherapy.

In order to test the cancer stem cell hypothesis in our models, we analyzed the expression of CD44 surface marker and ALDH enzyme in the parental and resistant HN30 cells. UM1-SCC and A549 cells were previously shown to contain a subpopulation expressing CD44 surface marker and ALDH, respectively (70,212,227–230), and were used as positive markers **(Figure 4-3).** These markers have been shown to be significantly expressed in small subpopulations in head and neck cancer cells (231), however, in our models, Immunofluorescent microscopy and flow cytometry showed that HN30 and HN30R cells do not express CD44 and ALDH markers.

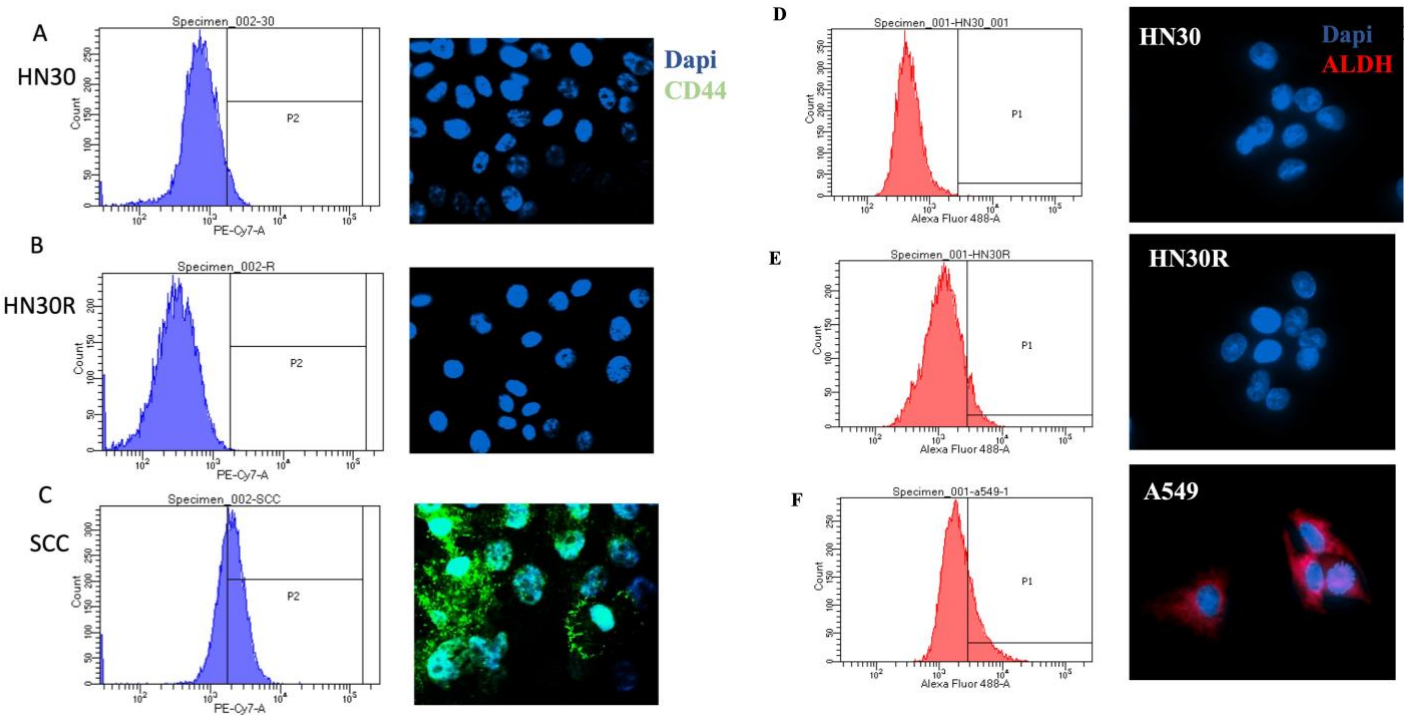

Figure 4-3. HN30 resistant cell line does not exhibit stemness characteristics. CD44 surface marker was assessed using flow cytometry (left panels) and immunofluorescent microscopy (right panels) on **A)** HN30, **B)** HN30R, and **C)** SCC cell line as a positive control. Additionally, ALDH marker existence was also evaluated as an additional marker for cancer cell stemness in **D)** HN30R, **E)** HN30, and **F)** A549s as a positive control. All images are representative fields or blots from at least three independent experiments, and all quantitative graphs are mean ± SEM from at least three independent experiments.

4-2-4. Cisplatin transporter, CTR1/SLC22A2 role in resistance

A decreased intracellular accumulation of cisplatin is also one of the mechanisms identified in cisplatin-resistant cell lines (232). Studies have described CTR1/SLC22A2 as a significant uptake transporter in yeast and mammalian cells (233). The extracellular methionine cluster of this transporter activates cisplatin and overexpression, or blockade of this molecule has been associated with cisplatin sensitivity and resistance, respectively (230,233,234). Additionally, CTR1 expression profile was shown to be correlated with higher intracellular cisplatin (233). Here we performed immunofluorescence imaging on HN30 parental and resistant cell lines for the CTR1 surface marker. **Figure 4-4** indicates the surface expression of CTR1 was not downregulated in the HN30R compared to HN30 parental cells. This observation indicates that both cell lines express CTR1 and presumably are equaly efficient in cisplatin uptake. However, intracellular concentration of cisplatin needs to be analyzed in future experiments to confirm the equal uptake efficacy.

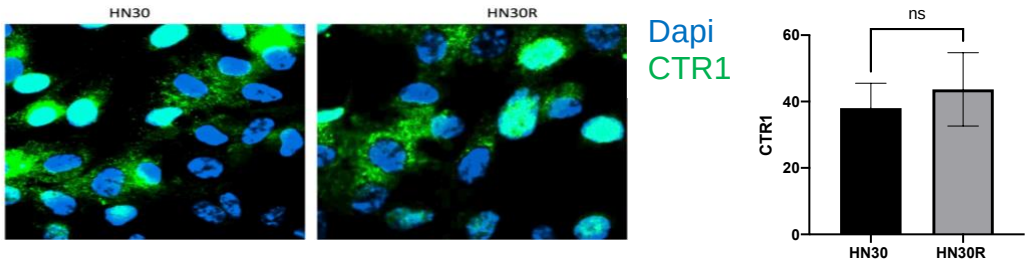

Figure 4-4. CTR1/SLC22A2, as the cisplatin major influx transporter, is not differentially expressed on the surface of HN30R cells compared to HN30s. All images are representative fields from at least three independent experiments, and all quantitative graphs are mean ± SEM from at least three independent experiments.

4.2.5. BRD4 overexpression decreases disease-free and overall survival in Head and Neck cancer patients

To further explore the characteristics of resistance in HN30R cells, we analyzed head and neck cancer patients' clinical gene expression data and observed a significant increase in BET family proteins in two data sets. BET family proteins, specifically BRD4, are bromodomain-containing proteins and epigenetic readers that play critical roles in transcription activation and various molecular pathways in cells, including tumorigenesis. Studies have shown a recurrent translocation of BRD4 in human squamous carcinomas (235). Such translocations result in the expression of the tandem N-terminal bromodomains of BRD4 as an in-frame chimera with the NUT (a nuclear protein. Functional studies in patient-derived cell lines have clarified the critical role of the BRD4-NUT oncoprotein in maintaining the proliferation advantage and in this fatal malignancy (236). Additionally, BRD4 overexpression has been clinically associated with different types of human cancers (237–240). To explore the expression profile of BET family proteins in head and neck cancer patients' clinical data, we utilized GEPIA bioinformatics as a resource to analyze The Cancer Genome Atlas (TCGA portal) human datasets. According to two different datasets with a total of 701 patients with Head and Neck Squamous cell carcinoma (HNSC) and Esophageal carcinoma (ESCA), BRD4, BRD3, and BRD2 are overexpressed in HNSC and ESCA tumors as compared to their normal counterparts (*P* value< 0.05) (**Figure 4-5A, B, and C**).

Moreover, the role of BRD4 in survival (disease-free and overall) was analyzed in the same database. Figures **4-5D** indicate that overexpression of BRD4 is associated with worse disease-free and overall survival in head and neck cancer patients.

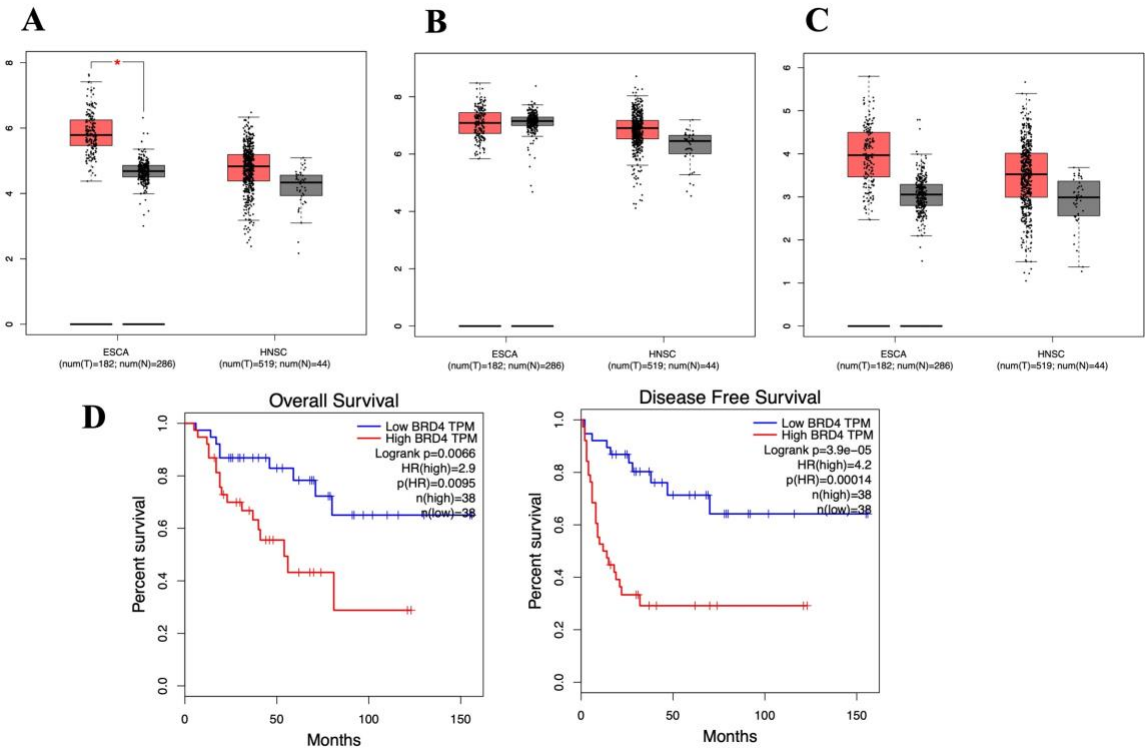

Figure 4-5. BET family proteins are over-expressed in head and neck cancer clinical data and contribute to worse outcomes in patients. mRNA expression of **A)** BRD4 **B)** BRD3, and **C)** BRD2 in two datasets from GEPIA and TCGA database. 182 tumors samples VS 44 normal tissues, *p* value <0.05. **D)** Disease-free and overall survival are significantly decreased in patients with higher BRD4 expression.

4-2-6. ARV-825, BRD4 PROTAC degrader sensitizes the parental and resistant cells to Cisplatin

ARV-825 is a newly developed PROTAC compound that contains OTX015 (small molecule inhibitor of BRD4) with an E3 ligase cereblon. This compound has been shown to be effective in several cancer models alone and in combination with chemotherapeutic drugs (112,115,216). In order to evaluate the effectiveness of ARV-825 alone and in combination with cisplatin in head and neck cancer parental and resistant models, the number of viable cells was monitored using trypan blue exclusion after treatment with cisplatin, with and without ARV-825. Both cell lines were sequentially treated with 5 μM cisplatin for 24 hours, and ARV-825 100nM for 96 hours. Cisplatin induces senescence in HN30 parental cells, while in the resistant model, the cells begin to recover from the growth arrest by day 5. ARV-825 alone clearly has transient senescence-inducing properties, as cell growth is arrested for ~ 4 days with increased bet-gal staining, followed by proliferative recovery. However, the combination treatment induces a significant level of cell death in both cell lines, accompanied by a pronounced interference with proliferative recovery. (**Figure 4-6 A and B**).

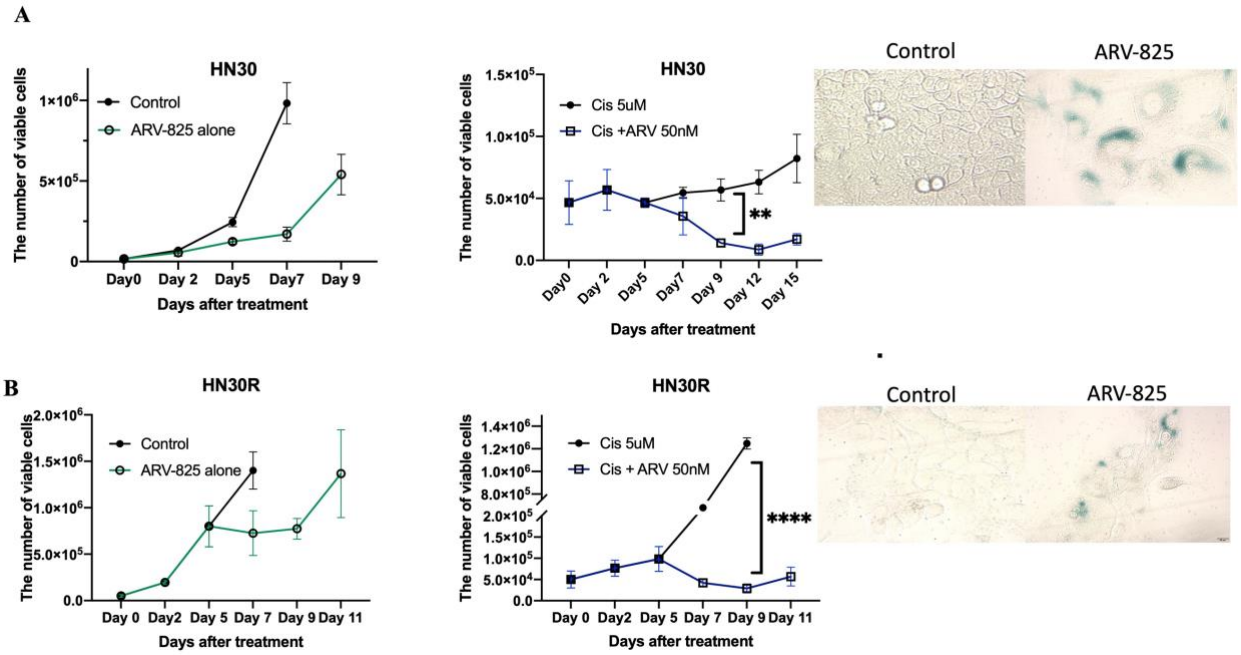

Figure 4-6. ARV-825 effectively eliminates cisplatin-treated parental and resistant cells. Growth curves for both **A)** HN30 and **B)** HN30R cells left panels, show that cisplatin treatment (5μM for 24 hours) followed by ARV-825 (50nM for 96 hours) significantly induces cell death. Beta-gal staining after ARV-825 treatment 96 hours shows senescence induction in both cell lines (right panel). for *** $p \leq 0.001$, **** $p \leq 0.0001$ indicate statistical significance of each condition compared to indicated condition as determined using two-way ANOVA with Sidak's post hoc test.

To better understand the nature of cell death in this treatment strategy, using flow cytometry, we analyzed Annexin V/PI staining on day 9 after initial treatment. **Figure 4-7** suggests that apoptosis is the major mechanism of cell death in both models when they are sequentially treated with a combination of cisplatin and ARV-825.

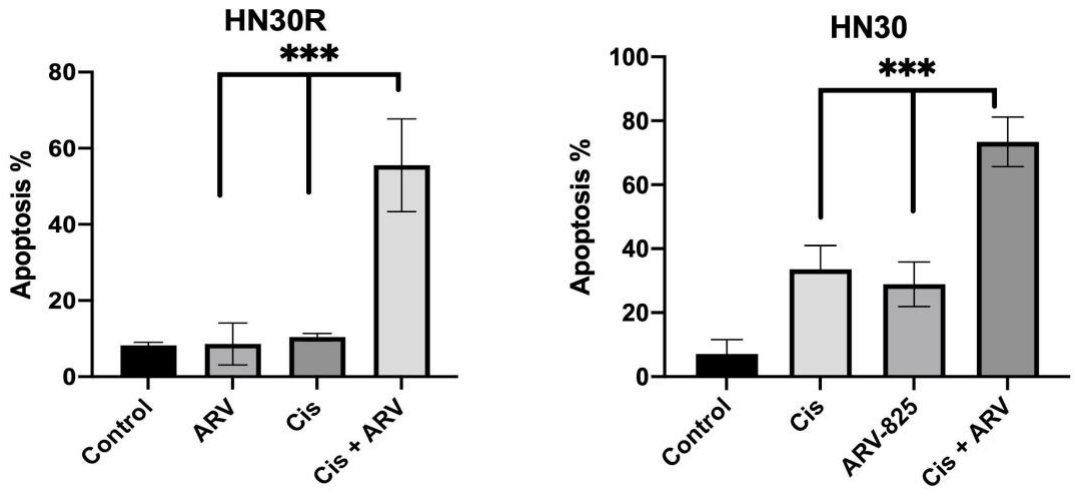

Figure 4-7. Apoptosis induction after combination treatment in **A)** HN30R and **B)** HN30. Annexin-V/PI quantification of apoptosis induced by 50nM ARV-825 with 96 hours of exposure after 5μM cisplatin in HN30 and HN12 cells. All quantitative graphs are mean ± SEM from at least three independent experiments. * $p \leq 0.05$, ** $p \leq 0.01$, *** $p \leq 0.001$, **** $p \leq 0.0001$ indicate statistical significance of each condition compared to control as determined using two-way ANOVA with Sidak's post hoc test.

4.2.7. The DNA repair response in cells treated with cisplatin and ARV-825

One major role attributed to BRD4 is contributing to the DNA damage response at double/single-strand DNA break sites (241–243). Studies have shown that BRD4 binds to acetylated histones near breakpoints on DNA strands and initiates the assembly of DNA repair machinery. We hypothesized that ARV-825 treatment degrades the BRD4 protein and thereby interferes with the DNA repair response in cisplatin-treated cells. Using western blot analysis, we first confirmed that 50nM of ARV-825 degrades the BRD4 protein in both cell lines (**Figure 4-8A**). Consequently, immunofluorescent microscopy

and its quantification showed that sequential treatment with cisplatin and ARV-825 in both cell lines increases DNA double-strand breaks (**Figure 4-8B**). DNA double-strand breaks peak at day 5 in both cell lines and resolve by day 9 after cisplatin treatment. However, after combination treatment, γ-H2AX foci signal significantly increased compared to cisplatin and ARV alone.

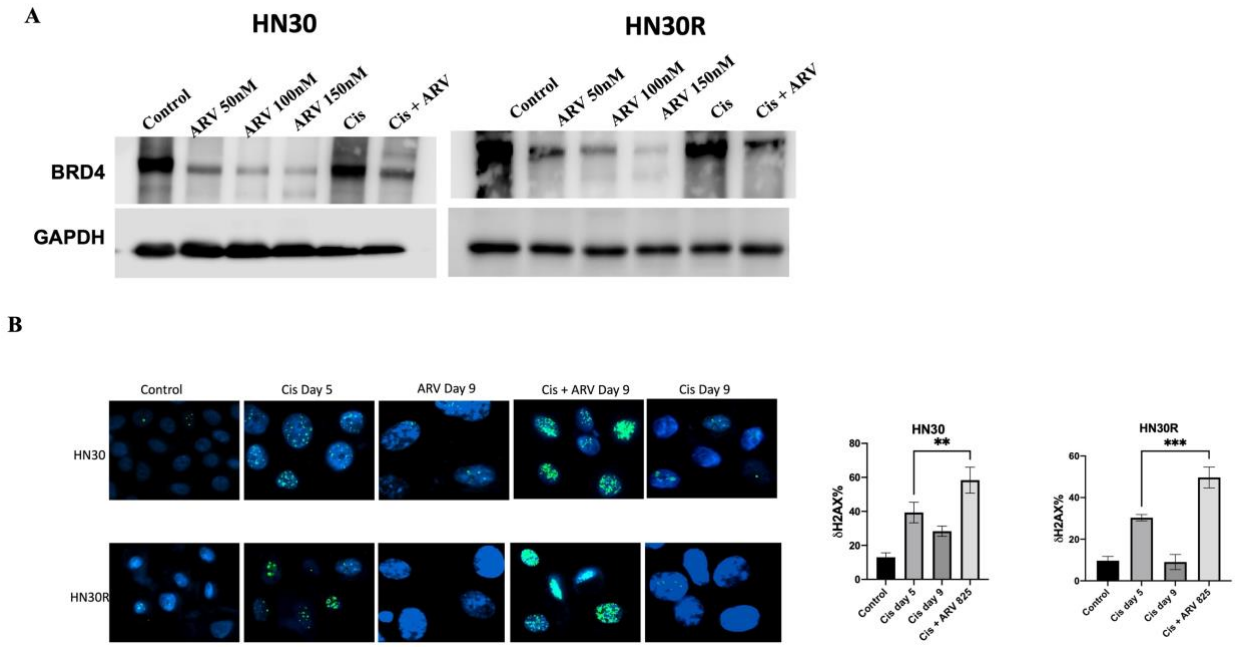

Figure 4-8. BRD4 degradation results in increased γ-H2AX foci after cisplatin treatment. **A)** Western blot shows that BRD4 is degraded in a dose-dependent manner by ARV-825 at concentrations 50, 100, and 150nM after 96 hours. **B)** Immunofluorescence imaging and quantification of γ-H2AX in HN30 and at indicated time points and treatment conditions. All images are representative fields or blots from at least three independent experiments, and all quantitative graphs are mean ± SEM from at least three independent experiments.

4.2.8. ARV-825 is not acting as a senolytic

To identify the mechanism of ARV-825-induced cell death in both models, we assessed the senolytic activity of this compound after cisplatin-mediated senescence induction. To perform this study, cisplatin treated HN30 and HN30R cells were sorted using our C12FDG sorting protocol by FACS into the highest 30% and lowest 20% senescent population. We confirmed the senescence state in sorted cells using an SA-βgal staining assay and C12FDG FACS analysis **(Figure 4-9A).** We then exposed both populations to ARV-825 and monitored cell death using Annexin V/PI staining. **Figure 4-9 B** show that both the senescence high and the senescence-low populations from both cell lines exhibit almost the same levels of sensitivity to ARV-825. The high senescence population in both cell lines does not show significant cell death before ARV-825 treatment. However, after sequential treatment with ARV-825, both high and low-senescence populations undergo apoptosis. This indicates that ARV-825, unlike ABT-263 is not specifically targeting the senescent population. Hence this BRD4 inhibitor/degrader has a greater potential to target a broad range of tumor cells, not necessarily limited to senescent cells.

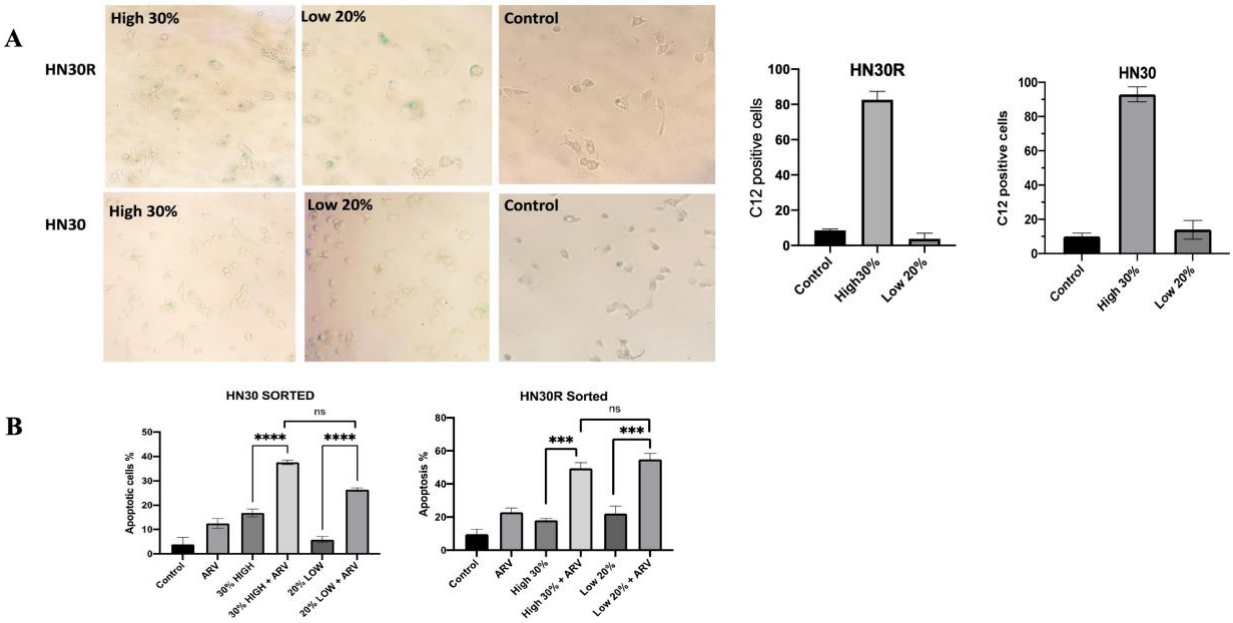

Figure 4.9. ARV-825 is not a senolytic. A) SA-βgal staining assay and C12FDG FACS analysis of sorted HN30R (Top panel) and HN30 (bottom panel) cells. Cells were treated with 5μM cis and sorted on day 3 and stained with X-gal (Top panel) and C12FDG (right graphs) and analyzed via FACS. **B)** Cells were re-plated and treated with 50nM ARV-825 for 96 hours and apoptosis was assessed using Annexin V/PI staining method and FACS analysis.

the same levels of sensitivity to ARV-825. This indicates that ARV-825, unlike ABT-263 is not specifically targeting the senescent population, hence it has a higher potential to target a broader range of cells not necessarily only senescent cells.

4.2.9. ARV-825 combination with cisplatin results in tumor regression in-vivo

To investigate ARV-825 effectiveness *in-vivo,* we established an orthotopic head and neck cancer mouse model using NSG mice and HN30 parental cell as a xenograft. Cisplatin treatment as monotherapy did not result in significant tumor stasis or regression; in dramatic contrast, the sequential addition of ARV-825 to the regimen resulted in a distinct and significant delay in tumor growth. As shown in **Figure 4-10A**, tumor regression and growth delay are detectable after the first round of ARV-825 injection. The endpoint tumor weight and volume also confirm the measurements collected throughout the experiment **Figure 4-10 B and C.**

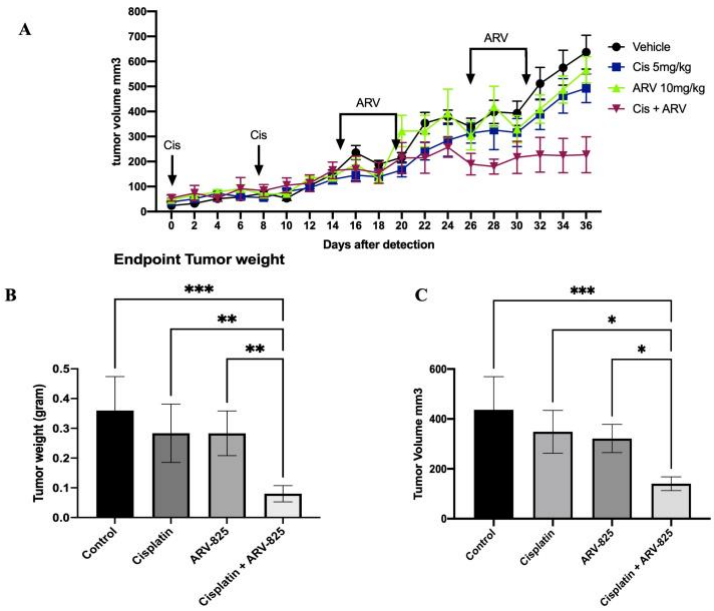

Figure 4.10. Sequential administration of ARV-825 following cisplatin delays tumor growth in an orthotopic mouse model of HN30 cells. A) NSG mice were treated with two doses of cisplatin 5 mg/kg/vehicle after tumor detection on days 0 and day 8, followed by two cycles of ARV-825 (10mg/kg)/vehicle injection containing three doses each, every other day. Caliper measurement of tumors shows that despite monotherapy groups,

tumors treated with the combination of cisplatin and ARV-825, enter a regression/stasis phase after the first round of ARV-825 injections. Endpoint **B)** tumor weight and **C)** tumor volume was also analyzed to confirm the previous observations.

We further extracted and analyzed HN30 tumors to investigate the ARV-825 mechanism of action. **Figure 4-11A** shows that cisplatin induces DNA single- or double-strand breaks (DSBs). The phosphorylated form of histone H2AX (γ-H2AX) marks sites of DNA DSB repair. Compared to the control, γ-H2AX was strongly stained in tumors exposed to cisplatin. However, in tumors treated with a combination of cisplatin and ARV-825, we observed even higher levels of γ-H2AX staining indicating that ARV-825 inhibits DNA repair pathways and consequently, induces apoptosis. The levels of cleaved-caspase-3 (c-casp3), indicative of apoptosis, were markedly increased in tumors treated with cisplatin followed by ARV-825 (**Figure 4-11 B).** These results suggest that the benefit of sequential treatment is a result of apoptosis by ARV-825 in cisplatin-treated tumors.

Additionally, we confirmed that ARV-825 at the indicated dose inhibits BRD4 (**Figure 4-11C**).

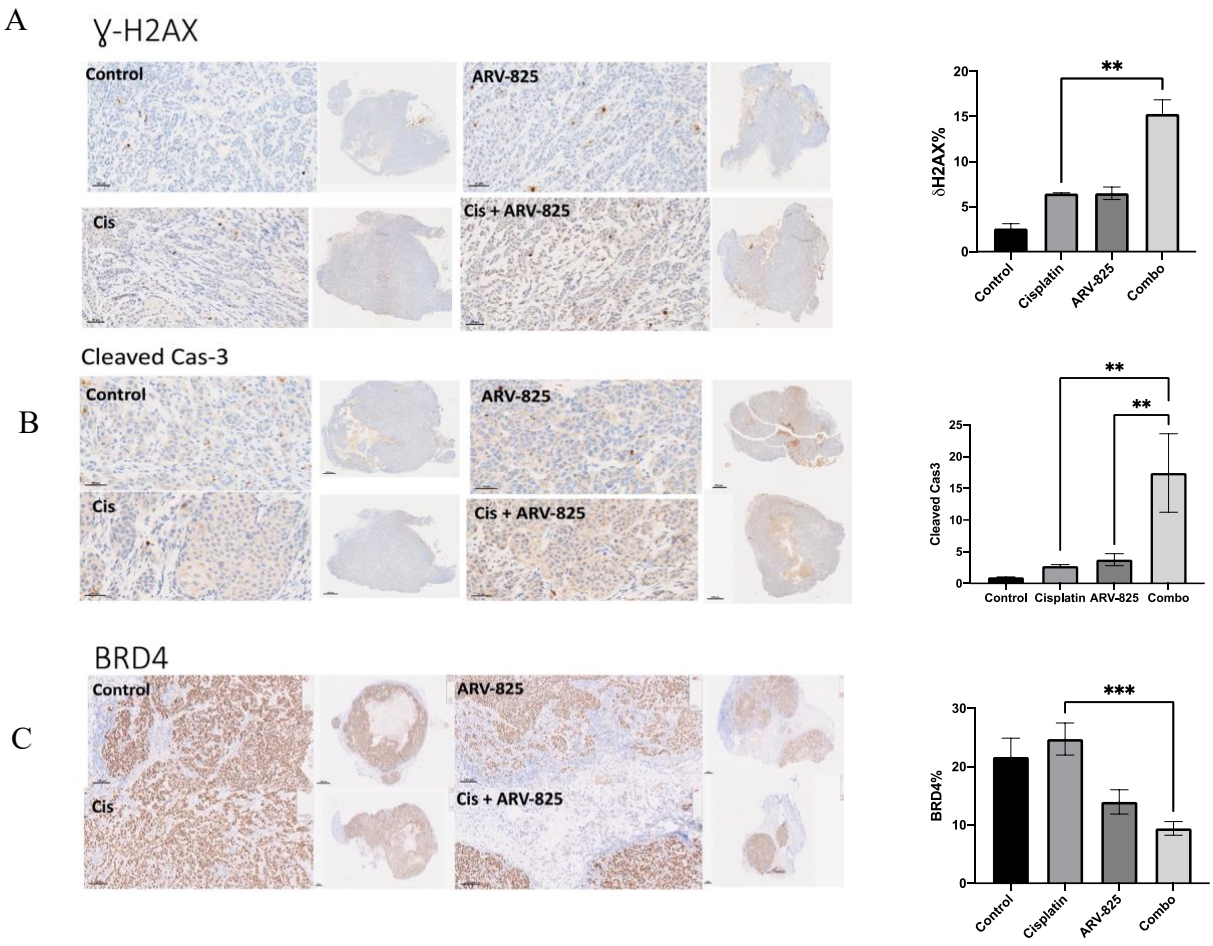

Figure 4.11. Immunohistochemical staining and quantification of mouse tumor tissues indicate apoptosis, DNA damage, and BRD4 inhibition. Tumors were extracted at the endpoint of the study and fixed in formalin, and stained with antibodies against **A)** δH2AX, **B)** Cleave-Caspase 3, and **C)** BRD4. (Original magnification = 20X). All tumor images are representative fields from four tumor slices (n = 3) taken from three mice per group (n = 3). Signal quantification was done using Image j software.

Finally, we evaluated the safety and potential toxicity of the combination of cisplatin and ARV-825 in this study by monitoring mouse body weight and analyzing Complete

Blood Count (CBC) by focusing on platelet counts and neutrophil percentages in the blood collected from a cardiac puncture in mice at the endpoint of the experiment. We did not observe any significant effects of treatment on these parameters **(Figure 4-12A, B, and C).**

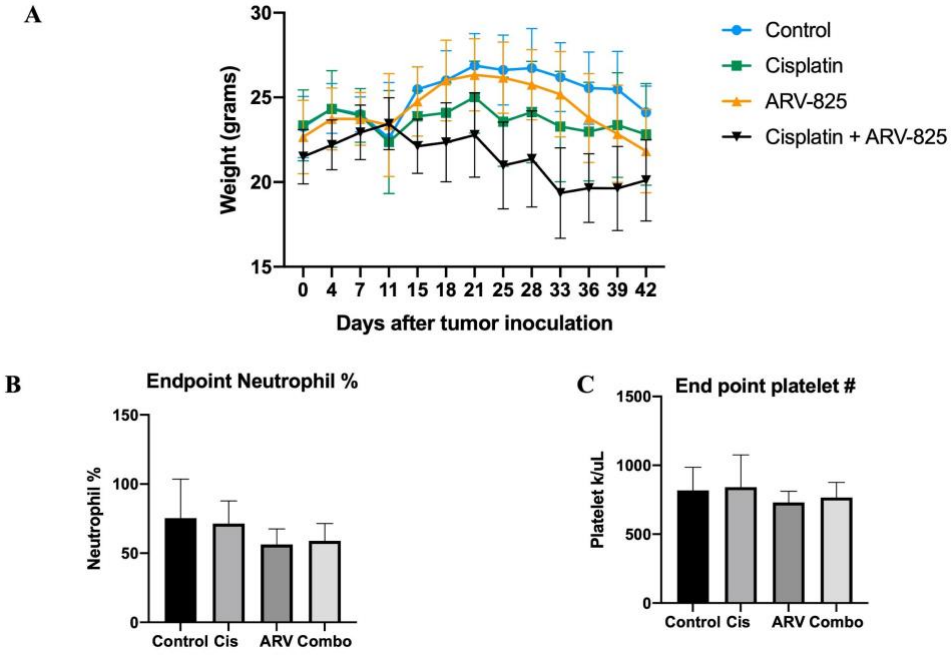

Figure 4.12. ARV-825 in combination with cisplatin does not induce significant toxicity. A) Individual body weight of mice was monitored throughout the experiment. Mice treated with the combination regimen showed temporary and non-lethal weight loss, with instant recovery. Endpoint CBC analysis of **B)** Neutrophil and **C)** Platelet counts did not show any significant decrease in the combination group compared with the vehicle-treated mice. All quantitative graphs are mean ± SEM from at least three independent experiments. * $p \leq 0.05$, ** $p \leq 0.01$, *** $p \leq 0.001$, **** $p \leq 0.0001$ indicate statistical significance of each condition compared to indicated condition as determined using two-way ANOVA with Sidak's post hoc test.

4.3. Discussion and future direction

Response to cisplatin-based chemotherapy is critical for not only head and neck cancer patients, but also for other solid tumors such as ovarian, lung, and testicular cancer (244). However, cisplatin-induced resistance is one of the major obstacles to achieving desirable outcomes from cisplatin in cancer patients (245). The first-line chemotherapy regimen for head and neck cancer patients requires multiple rounds of cisplatin infusion after surgery, with or without radiotherapy, depending on the type and stage of the tumor (246–248). Both *in-vivo* and *in-vitro* studies, along with clinical data have shown that cisplatin treatment induces resistance in the tumor cell population, resulting in tumor recurrence and metastasis (249,250). Studies and clinical trials investigating alternative regimens as first-line therapy for head and neck cancer patients concluded that cisplatin based therapy is still superior to multiple chemotherapy drugs such as carboplatin, and docetaxel in the rate of objective response (251,252). Moreover, economic analysis of cisplatin has also shown that this chemotherapeutic agent, alone or in combination with a secondary compound, is the most cost-effective approach for patients (253,254).

In the previous chapter, we investigated the effectiveness of navitoclax on head and neck cancer cells induced into senescence by cisplatin, showed that cisplatin does not induce a significant amount of cell death in either HN30 or HN12 cell lines, and observed high levels of senescence induction in both cell lines (**Figure 3-1**). Using a senolytic, navitoclax, we were able to induce tumor cell death *in-vitro* and *in-vivo.* However, the recovery of a small subpopulation of cells was unavoidable (**Figures 3-4A**

and D). Due to the heterogeneous nature of tumor cells, we hypothesized that there is a subpopulation in the HN30 cell line from which resistant cells develop after cisplatin treatment. Thus, we established HN30R cells from the HN30 cell line to investigate their sensitivity to cisplatin and senolytics or secondary compounds. Even though cisplatin was still able to induce a brief senescence-associated growth arrest peaking on day 5, we showed that HN30R cells did not show any sensitivity to navitoclax (**Figure 4-2**). Hence, we investigated the resistance mechanism in HN30R cells. Studies have shown that cisplatin resistance can result from one or multiple mechanisms resulting from epigenetic changes, downregulation of cisplatin transporters, cancer stem cell sub-population, and higher pace in DNA repair responses (70). Thus, we screened a number of secondary compounds such as Fisetin, Venetoclax, Curcumin, and BRD4 protein degrader to sensitize the resistant population from which only BRD4 degrader, ARV-825 showed effectiveness in both HN30 parental and resistant cell line.

Our *in-vitro* and *in-vivo* data indicate that cisplatin induces double-strand breaks in HN30 and HN30R cells, with a peak on day 5 after cisplatin treatment (**Figure 3-9, 4-8**). Consistently, studies have shown that cisplatin as an alkylating agent, crosslinks with urine bases on the DNA and forms DNA adducts. By exploiting Nucleotide Excision Base repair, or NER, cells remove the adducts from DNA strands and leave DNA strand breaks behind (154). This illustrates the underlying reason for the observed DNA damage signals on day 5 after cisplatin treatment in our models. We then investigated the effectiveness of ARV-825 treatment at different time points in both HN30 and HN30R cells. The addition of ARV-825 concurrently with cisplatin, or on day 1 to day 4 after cisplatin treatment did not induce any form of cell death (data not shown). However, administration of ARV-825

on day 5 after cisplatin treatment, induced apoptotic cell death in both cell lines. By investigating the DNA double-strand markers, γH2AX, we showed that ARV-825 addition significantly increases the DNA double-strand breaks in both models. We confirmed our observations in-vivo in NSG mice bearing HN30 tumors. Our observations indicate that the primary mechanism of action of ARV-825 in combination with cisplatin is through inhibiting DNA repair mechanisms; however, the complex nature of BRD4 and its downstream target genes have been shown to play significant roles in ARV-825 effectiveness. We conclude that ARV-825 halts the assembly of DNA repair machinery by degrading BRD4 as it was previously reported as a mechanism of action for ARV-825 (104). Finally, this study provides primary insight into the effectiveness and mechanism of ARV-825 in combination with cisplatin in head and neck cancer models, and further investigations will be required in the future to clarify the role of downstream ARV-825 target genes and involved molecular pathways.

References

1. Hayflick L. The limited in vitro lifetime of human diploid cell strains. Experimental Cell Research. 1965 Mar;37(3):614–36.

2. Shay JW, Wright WE. Hayflick, his limit, and cellular ageing. Nat Rev Mol Cell Biol. 2000 Oct;1(1):72–6.

3. Watson JD. Origin of Concatemeric T7DNA. Nature New Biology. 1972 Oct;239(94):197–201.

4. Shay JW, Wright WE. Senescence and immortalization: role of telomeres and telomerase. Carcinogenesis. 2005 May 1;26(5):867–74.

5. Kumari R, Jat P. Mechanisms of Cellular Senescence: Cell Cycle Arrest and Senescence Associated Secretory Phenotype. Front Cell Dev Biol. 2021 Mar 29;9:645593.

6. Di Micco R, Fumagalli M, Cicalese A, Piccinin S, Gasparini P, Luise C, et al. Oncogene-induced senescence is a DNA damage response triggered by DNA hyper-replication. Nature. 2006 Nov;444(7119):638–42.

7. Mallette FA, Gaumont-Leclerc MF, Ferbeyre G. The DNA damage signaling pathway is a critical mediator of oncogene-induced senescence. Genes Dev. 2007 Jan 1;21(1):43–8.

8. Reddy JP, Li Y. Oncogene-Induced Senescence and its Role in Tumor Suppression. J Mammary Gland Biol Neoplasia. 2011 Sep;16(3):247–56.

9. Bartkova J, Rezaei N, Liontos M, Karakaidos P, Kletsas D, Issaeva N, et al. Oncogene-induced senescence is part of the tumorigenesis barrier imposed by DNA damage checkpoints. Nature. 2006 Nov;444(7119):633–7.

10. Oubaha M, Miloudi K, Dejda A, Guber V, Mawambo G, Germain MA, et al. Senescence-associated secretory phenotype contributes to pathological angiogenesis in retinopathy. Science Translational Medicine. 2016 Oct 26;8(362):362ra144-362ra144.

11. Serrano M, Lin AW, McCurrach ME, Beach D, Lowe SW. Oncogenic ras Provokes Premature Cell Senescence Associated with Accumulation of p53 and p16INK4a. Cell. 1997 Mar;88(5):593–602.

12. Narita M, Nuñez S, Heard E, Narita M, Lin AW, Hearn SA, et al. Rb-Mediated Heterochromatin Formation and Silencing of E2F Target Genes during Cellular Senescence. Cell. 2003 Jun;113(6):703–16.

13. Coppé JP, Patil CK, Rodier F, Sun Y, Muñoz DP, Goldstein J, et al. Senescence-Associated Secretory Phenotypes Reveal Cell-Nonautonomous Functions of Oncogenic RAS and the p53 Tumor Suppressor. Downward J, editor. PLoS Biol. 2008 Dec 2;6(12):e301.

14. Dimri GP, Lee X, Basile G, Acosta M, Scott G, Roskelley C, et al. A biomarker that identifies senescent human cells in culture and in aging skin in vivo. Proceedings of the National Academy of Sciences. 1995 Sep 26;92(20):9363–7.

15. Childs BG, Durik M, Baker DJ, van Deursen JM. Cellular senescence in aging and age-related disease: from mechanisms to therapy. Nat Med. 2015 Dec;21(12):1424–35.

16. Sharpless NE, Sherr CJ. Forging a signature of in vivo senescence. Nat Rev Cancer. 2015 Jul;15(7):397–408.

17. Salama R, Sadaie M, Hoare M, Narita M. Cellular senescence and its effector programs. Genes & Development. 2014 Jan 15;28(2):99–114.

18. Serrano M. Shifting senescence into quiescence by turning up p53. Cell Cycle. 2010 Nov;9(21):4256–7.

19. Leontieva OV, Demidenko ZN, Gudkov AV, Blagosklonny MV. Elimination of Proliferating Cells Unmasks the Shift from Senescence to Quiescence Caused by Rapamycin. El-Deiry WS, editor. PLoS ONE. 2011 Oct 11;6(10):e26126.

20. Blagosklonny MV. Cell cycle arrest is not senescence. Aging. 2011 Feb 6;3(2):94–101.

21. Terzi MY, Izmirli M, Gogebakan B. The cell fate: senescence or quiescence. Mol Biol Rep. 2016 Nov;43(11):1213–20.

22. Gil J, Peters G. Regulation of the INK4b–ARF–INK4a tumour suppressor locus: all for one or one for all. Nat Rev Mol Cell Biol. 2006 Sep;7(9):667–77.

23. Yao G. Modelling mammalian cellular quiescence. Interface Focus. 2014 Jun 6;4(3):20130074.

24. Madan E, Gogna R, Kuppusamy P, Bhatt M, Pati U, Mahdi AA. TIGAR induces p53-mediated cell-cycle arrest by regulation of RB–E2F1 complex. Br J Cancer. 2012 Jul;107(3):516–26.

25. Fujimaki K, Li R, Chen H, Della Croce K, Zhang HH, Xing J, et al. Graded regulation of cellular quiescence depth between proliferation and senescence by a lysosomal dimmer switch. Proc Natl Acad Sci USA. 2019 Nov 5;116(45):22624–34.

26. Pereira SFF, Gonzalez RL, Dworkin J. Protein synthesis during cellular quiescence is inhibited by phosphorylation of a translational elongation factor. Proc Natl Acad Sci USA [Internet]. 2015 Jun 23 [cited 2022 Nov 7];112(25). Available from: https://pnas.org/doi/full/10.1073/pnas.1505297112

27. He S, Sharpless NE. Senescence in Health and Disease. Cell. 2017 Jun;169(6):1000–11.

28. Muñoz-Espín D, Cañamero M, Maraver A, Gómez-López G, Contreras J, Murillo-Cuesta S, et al. Programmed Cell Senescence during Mammalian Embryonic Development. Cell. 2013 Nov;155(5):1104–18.

29. Martin JA, Buckwalter JA. Roles of articular cartilage aging and chondrocyte senescence in the pathogenesis of osteoarthritis. Iowa Orthop J. 2001;21:1–7.

30. Childs BG, Baker DJ, Wijshake T, Conover CA, Campisi J, van Deursen JM. Senescent intimal foam cells are deleterious at all stages of atherosclerosis. Science. 2016 Oct 28;354(6311):472–7.

31. Schafer MJ, White TA, Iijima K, Haak AJ, Ligresti G, Atkinson EJ, et al. Cellular senescence mediates fibrotic pulmonary disease. Nat Commun. 2017 Apr;8(1):14532.

32. Ogrodnik M, Zhu Y, Langhi LGP, Tchkonia T, Krüger P, Fielder E, et al. Obesity-Induced Cellular Senescence Drives Anxiety and Impairs Neurogenesis. Cell Metabolism. 2019 May;29(5):1061-1077.e8.

33. Tan H, Xu J, Liu Y. Ageing, cellular senescence and chronic kidney disease: experimental evidence. Current Opinion in Nephrology & Hypertension. 2022 May;31(3):235–43.

34. Saleh T, Bloukh S, Carpenter VJ, Alwohoush E, Bakeer J, Darwish S, et al. Therapy-Induced Senescence: An “Old” Friend Becomes the Enemy. Cancers. 2020 Mar 29;12(4):822.

35. Li M, You L, Xue J, Lu Y. Ionizing Radiation-Induced Cellular Senescence in Normal, Non-transformed Cells and the Involved DNA Damage Response: A Mini Review. Front Pharmacol. 2018 May 22;9:522.

36. Saleh T, Tyutyunyk-Massey L, Murray GF, Alotaibi MR, Kawale AS, Elsayed Z, et al. Tumor cell escape from therapy-induced senescence. Biochemical Pharmacology. 2019 Apr;162:202–12.

37. Acosta JC, O'Loghlen A, Banito A, Guijarro MV, Augert A, Raguz S, et al. Chemokine Signaling via the CXCR2 Receptor Reinforces Senescence. Cell. 2008 Jun;133(6):1006–18.

38. Acosta JC, Banito A, Wuestefeld T, Georgilis A, Janich P, Morton JP, et al. A complex secretory program orchestrated by the inflammasome controls paracrine senescence. Nat Cell Biol. 2013 Aug;15(8):978–90.

39. Di X, Bright AT, Bellott R, Gaskins E, Robert J, Holt S, et al. A chemotherapy-associated senescence bystander effect in breast cancer cells. Cancer Biology & Therapy. 2008 Jun;7(6):864–72.

40. Nelson G, Wordsworth J, Wang C, Jurk D, Lawless C, Martin-Ruiz C, et al. A senescent cell bystander effect: senescence-induced senescence. Aging Cell. 2012 Apr;11(2):345–9.

41. Carpenter VJ, Patel BB, Autorino R, Smith SC, Gewirtz DA, Saleh T. Senescence and castration resistance in prostate cancer: A review of experimental evidence and clinical implications. Biochimica et Biophysica Acta (BBA) - Reviews on Cancer. 2020 Dec;1874(2):188424.

42. Carrière C, Gore AJ, Norris AM, Gunn JR, Young AL, Longnecker DS, et al. Deletion of Rb Accelerates Pancreatic Carcinogenesis by Oncogenic Kras and Impairs Senescence in Premalignant Lesions. Gastroenterology. 2011 Sep;141(3):1091–101.

43. Sarkisian CJ, Keister BA, Stairs DB, Boxer RB, Moody SE, Chodosh LA. Dose-dependent oncogene-induced senescence in vivo and its evasion during mammary tumorigenesis. Nat Cell Biol. 2007 May;9(5):493–505.

44. Beausejour CM. Reversal of human cellular senescence: roles of the p53 and p16 pathways. The EMBO Journal. 2003 Aug 15;22(16):4212–22.

45. Kansara M, Leong HS, Lin DM, Popkiss S, Pang P, Garsed DW, et al. Immune response to RB1-regulated senescence limits radiation-induced osteosarcoma formation. J Clin Invest. 2013 Dec 2;123(12):5351–60.

46. Kang TW, Yevsa T, Woller N, Hoenicke L, Wuestefeld T, Dauch D, et al. Senescence surveillance of pre-malignant hepatocytes limits liver cancer development. Nature. 2011 Nov;479(7374):547–51.

47. Lujambio A, Akkari L, Simon J, Grace D, Tschaharganeh DF, Bolden JE, et al. Non-Cell-Autonomous Tumor Suppression by p53. Cell. 2013 Apr;153(2):449–60.

48. Medema JP. Escape from senescence boosts tumour growth. Nature. 2018 Jan;553(7686):37–8.

49. De Blander H, Morel AP, Senaratne AP, Ouzounova M, Puisieux A. Cellular Plasticity: A Route to Senescence Exit and Tumorigenesis. Cancers. 2021 Sep 11;13(18):4561.

50. Zampetidis CP, Papantonis A, Gorgoulis VG. Escape from senescence: revisiting cancer therapeutic strategies. Molecular & Cellular Oncology. 2022 Dec 31;9(1):2030158.

51. Yang J, Liu M, Hong D, Zeng M, Zhang X. The Paradoxical Role of Cellular Senescence in Cancer. Front Cell Dev Biol. 2021 Aug 12;9:722205.

52. Campisi J. Cellular senescence as a tumor-suppressor mechanism. Trends in Cell Biology. 2001 Nov;11(11):S27–31.

53. Allsopp RC, Harley CB. Evidence for a Critical Telomere Length in Senescent Human Fibroblasts. Experimental Cell Research. 1995 Jul;219(1):130–6.

54. Saleh T, Tyutyunyk-Massey L, Murray GF, Alotaibi MR, Kawale AS, Elsayed Z, et al. Tumor cell escape from therapy-induced senescence. Biochemical Pharmacology. 2019 Apr;162:202–12.

55. Ou H, Hoffmann R, González-López C, Doherty GJ, Korkola JE, Muñoz-Espín D. Cellular senescence in cancer: from mechanisms to detection. Molecular Oncology. 2021 Oct;15(10):2634–71.

56. Saleh T, Tyutyunyk-Massey L, Murray GF, Alotaibi MR, Kawale AS, Elsayed Z, et al. Tumor cell escape from therapy-induced senescence. Biochemical Pharmacology. 2019 Apr;162:202–12.

57. Roberson RS, Kussick SJ, Vallieres E, Chen SYJ, Wu DY. Escape from Therapy-Induced Accelerated Cellular Senescence in p53-Null Lung Cancer Cells and in Human Lung Cancers. Cancer Res. 2005 Apr 1;65(7):2795–803.

58. Olszewska A, Borkowska A, Granica M, Karolczak J, Zglinicki B, Kieda C, et al. Escape From Cisplatin-Induced Senescence of Hypoxic Lung Cancer Cells Can Be Overcome by Hydroxychloroquine. Front Oncol. 2022 Jan 21;11:738385.

59. Ahmadinejad F, Bos T, Hu B, Britt E, Koblinski J, Souers AJ, et al. Senolytic-Mediated Elimination of Head and Neck Tumor Cells Induced Into Senescence by Cisplatin. Mol Pharmacol. 2022 Mar;101(3):168–80.

60. Alotaibi M, Sharma K, Saleh T, Povirk LF, Hendrickson EA, Gewirtz DA. Radiosensitization by PARP Inhibition in DNA Repair Proficient and Deficient Tumor Cells: Proliferative Recovery in Senescent Cells. Radiation Research. 2016 Mar 2;185(3):229.

61. Lim ZF, Ma PC. Emerging insights of tumor heterogeneity and drug resistance mechanisms in lung cancer targeted therapy. J Hematol Oncol. 2019 Dec;12(1):134.

62. Wu D, Wang DC, Cheng Y, Qian M, Zhang M, Shen Q, et al. Roles of tumor heterogeneity in the development of drug resistance: A call for precision therapy. Seminars in Cancer Biology. 2017 Feb;42:13–9.

63. Guillon J, Petit C, Toutain B, Guette C, Lelièvre E, Coqueret O. Chemotherapy-induced senescence, an adaptive mechanism driving resistance and tumor heterogeneity. Cell Cycle. 2019 Oct 2;18(19):2385–97.

64. Luqmani YA. Mechanisms of Drug Resistance in Cancer Chemotherapy. Med Princ Pract. 2005;14(Suppl. 1):35–48.

65. Saleh T, Tyutyunyk-Massey L, Gewirtz DA. Tumor Cell Escape from Therapy-Induced Senescence as a Model of Disease Recurrence after Dormancy. Cancer Research. 2019 Mar 15;79(6):1044–6.

66. Elmore LW. Evasion of a Single-Step, Chemotherapy-Induced Senescence in Breast Cancer Cells: Implications for Treatment Response. Clinical Cancer Research. 2005 Apr 1;11(7):2637–43.

67. Christian F, Smith E, Carmody R. The Regulation of NF-κB Subunits by Phosphorylation. Cells. 2016 Mar 18;5(1):12.

68. Salunkhe S, Mishra SV, Nair J, Shah S, Gardi N, Thorat R, et al. Nuclear localization of p65 reverses therapy-induced senescence. Journal of Cell Science. 2021 Mar 15;134(6):jcs253203.

69. Guillon J, Petit C, Moreau M, Toutain B, Henry C, Roché H, et al. Regulation of senescence escape by TSP1 and CD47 following chemotherapy treatment. Cell Death Dis. 2019 Mar;10(3):199.

70. Chen SH, Chang JY. New Insights into Mechanisms of Cisplatin Resistance: From Tumor Cell to Microenvironment. IJMS. 2019 Aug 24;20(17):4136.

71. Milanovic M, Fan DNY, Belenki D, Däbritz JHM, Zhao Z, Yu Y, et al. Senescence-associated reprogramming promotes cancer stemness. Nature. 2018 Jan;553(7686):96–100.

72. Lim JS, Lee DY, Kim HS, Park SC, Park JT, Kim HS, et al. Identification of a novel senomorphic agent, avenanthramide C, via the suppression of the senescence-associated secretory phenotype. Mechanisms of Ageing and Development. 2020 Dec;192:111355.

73. Wissler Gerdes EO, Zhu Y, Tchkonia T, Kirkland JL. Discovery, development, and future application of senolytics: theories and predictions. FEBS J. 2020 Jun;287(12):2418–27.

74. Short S, Fielder E, Miwa S, von Zglinicki T. Senolytics and senostatics as adjuvant tumour therapy. EBioMedicine. 2019 Mar;41:683–92.

75. Wang Y, Zhao H, Jia S, Wang Q, Yao W, Yang Y, et al. Senomorphic agent pterostilbene ameliorates osteoarthritis through the PI3K/AKT/NF-κB axis: an in vitro and in vivo study. Am J Transl Res. 2022;14(8):5243–62.

76. Moiseeva O, Deschênes-Simard X, St-Germain E, Igelmann S, Huot G, Cadar AE, et al. Metformin inhibits the senescence-associated secretory phenotype by interfering with IKK / NF -κ B activation. Aging Cell. 2013 Jun;12(3):489–98.

77. Laberge RM, Zhou L, Sarantos MR, Rodier F, Freund A, de Keizer PLJ, et al. Glucocorticoids suppress selected components of the senescence-associated secretory phenotype: Glucocorticoids suppress the SASP. Aging Cell. 2012 Aug;11(4):569–78.

78. Xu M, Tchkonia T, Ding H, Ogrodnik M, Lubbers ER, Pirtskhalava T, et al. JAK inhibition alleviates the cellular senescence-associated secretory phenotype and frailty in old age. Proc Natl Acad Sci USA [Internet]. 2015 Nov 17 [cited 2022 Nov 8];112(46). Available from: https://pnas.org/doi/full/10.1073/pnas.1515386112

79. Xu M, Palmer AK, Ding H, Weivoda MM, Pirtskhalava T, White TA, et al. Targeting senescent cells enhances adipogenesis and metabolic function in old age. eLife. 2015 Dec 19;4:e12997.

80. Wang C, Vegna S, Jin H, Benedict B, Lieftink C, Ramirez C, et al. Inducing and exploiting vulnerabilities for the treatment of liver cancer. Nature. 2019 Oct 10;574(7777):268–72.

81. Zhu Y, Tchkonia T, Pirtskhalava T, Gower AC, Ding H, Giorgadze N, et al. The Achilles' heel of senescent cells: from transcriptome to senolytic drugs. Aging Cell. 2015 Aug;14(4):644–58.

82. Abbas T, Dutta A. p21 in cancer: intricate networks and multiple activities. Nat Rev Cancer. 2009 Jun;9(6):400–14.

83. Musi N, Valentine JM, Sickora KR, Baeuerle E, Thompson CS, Shen Q, et al. Tau protein aggregation is associated with cellular senescence in the brain: XXXX. Aging Cell. 2018 Dec;17(6):e12840.

84. Zhang P, Kishimoto Y, Grammatikakis I, Gottimukkala K, Cutler RG, Zhang S, et al. Senolytic therapy alleviates Aβ-associated oligodendrocyte progenitor cell senescence and cognitive deficits in an Alzheimer's disease model. Nat Neurosci. 2019 May;22(5):719–28.

85. Ogrodnik M, Miwa S, Tchkonia T, Tiniakos D, Wilson CL, Lahat A, et al. Cellular senescence drives age-dependent hepatic steatosis. Nat Commun. 2017 Aug;8(1):15691.

86. Zhu Y, Tchkonia T, Fuhrmann-Stroissnigg H, Dai HM, Ling YY, Stout MB, et al. Identification of a novel senolytic agent, navitoclax, targeting the Bcl-2 family of anti-apoptotic factors. Aging Cell. 2016 Jun;15(3):428–35.

87. Mikawa R, Suzuki Y, Baskoro H, Kanayama K, Sugimoto K, Sato T, et al. Elimination of p19 ^{ARF} -expressing cells protects against pulmonary emphysema in mice. Aging Cell. 2018 Oct;17(5):e12827.

88. Xu X, Kim JJ, Li Y, Xie J, Shao C, Wei JJ. Oxidative stress-induced miRNAs modulate AKT signaling and promote cellular senescence in uterine leiomyoma. J Mol Med. 2018 Oct;96(10):1095–106.

89. Bussian TJ, Aziz A, Meyer CF, Swenson BL, van Deursen JM, Baker DJ. Clearance of senescent glial cells prevents tau-dependent pathology and cognitive decline. Nature. 2018 Oct;562(7728):578–82.

90. Yabluchanskiy A, Tarantini S, Balasubramanian P, Kiss T, Csipo T, Fülöp GA, et al. Pharmacological or genetic depletion of senescent astrocytes prevents whole brain irradiation–induced impairment of neurovascular coupling responses protecting cognitive function in mice. GeroScience. 2020 Jan 20;1–20.

91. van der Feen DE, Bossers GPL, Hagdorn QAJ, Moonen JR, Kurakula K, Szulcek R, et al. Cellular senescence impairs the reversibility of pulmonary arterial hypertension. Sci Transl Med. 2020 Jul 29;12(554):eaaw4974.

92. Sessions GA, Copp ME, Liu J, Sinkler MA, D'Costa S, Diekman BO. Controlled induction and targeted elimination of p16 ^{INK4a} -expressing chondrocytes in cartilage explant culture. FASEB j. 2019 Nov;33(11):12364–73.

93. Yang H, Chen C, Chen H, Duan X, Li J, Zhou Y, et al. Navitoclax (ABT263) reduces inflammation and promotes chondrogenic phenotype by clearing senescent osteoarthritic chondrocytes in osteoarthritis. Aging. 2020 Jul 1;12(13):12750–70.

94. Chung L, Maestas DR, Lebid A, Mageau A, Rosson GD, Wu X, et al. Interleukin 17 and senescent cells regulate the foreign body response to synthetic material implants in mice and humans. Sci Transl Med. 2020 Apr 15;12(539):eaax3799.

95. Yousefzadeh MJ, Zhu Y, McGowan SJ, Angelini L, Fuhrmann-Stroissnigg H, Xu M, et al. Fisetin is a senotherapeutic that extends health and lifespan. EBioMedicine. 2018 Oct;36:18–28.

96. Zhu Y, Doornebal EJ, Pirtskhalava T, Giorgadze N, Wentworth M, Fuhrmann-Stroissnigg H, et al. New agents that target senescent cells: the flavone, fisetin, and the BCL-XL inhibitors, A1331852 and A1155463. Aging. 2017 Mar 8;9(3):955–63.

97. Cherif H, Bisson D, Jarzem P, Weber M, Ouellet J, Haglund L. Curcumin and o-Vanillin Exhibit Evidence of Senolytic Activity in Human IVD Cells In Vitro. JCM. 2019 Mar 29;8(4):433.

98. Li W, He Y, Zhang R, Zheng G, Zhou D. The curcumin analog EF24 is a novel senolytic agent. Aging. 2019 Jan 28;11(2):771–82.

99. Ferrari AC, Alumkal JJ, Stein MN, Taplin ME, Babb J, Barnett ES, et al. Epigenetic Therapy with Panobinostat Combined with Bicalutamide Rechallenge in Castration-Resistant Prostate Cancer. Clinical Cancer Research. 2019 Jan 1;25(1):52–63.

100. Samaraweera L, Adomako A, Rodriguez-Gabin A, McDaid HM. A Novel Indication for Panobinostat as a Senolytic Drug in NSCLC and HNSCC. Sci Rep. 2017 Dec;7(1):1900.

101. Fuhrmann-Stroissnigg H, Ling YY, Zhao J, McGowan SJ, Zhu Y, Brooks RW, et al. Identification of HSP90 inhibitors as a novel class of senolytics. Nat Commun. 2017 Dec;8(1):422.

102. Chen L, Li J, Farah E, Sarkar S, Ahmad N, Gupta S, et al. Cotargeting HSP90 and Its Client Proteins for Treatment of Prostate Cancer. Molecular Cancer Therapeutics. 2016 Sep 1;15(9):2107–18.

103. Śmieszek A, Stręk Z, Kornicka K, Grzesiak J, Weiss C, Marycz K. Antioxidant and Anti-Senescence Effect of Metformin on Mouse Olfactory Ensheathing Cells (mOECs) May Be Associated with Increased Brain-Derived Neurotrophic Factor Levels—An Ex Vivo Study. IJMS. 2017 Apr 20;18(4):872.

104. Wakita M, Takahashi A, Sano O, Loo TM, Imai Y, Narukawa M, et al. A BET family protein degrader provokes senolysis by targeting NHEJ and autophagy in senescent cells. Nat Commun. 2020 Dec;11(1):1935.

105. Doroshow DB, Eder JP, LoRusso PM. BET inhibitors: a novel epigenetic approach. Annals of Oncology. 2017 Aug;28(8):1776–87.

106. Itzen F, Greifenberg AK, Bösken CA, Geyer M. Brd4 activates P-TEFb for RNA polymerase II CTD phosphorylation. Nucleic Acids Res. 2014 Jul 8;42(12):7577–90.

107. Liu B, Liu X, Han L, Chen X, Wu X, Wu J, et al. BRD4-directed super-enhancer organization of transcription repression programs links to chemotherapeutic

efficacy in breast cancer. Proc Natl Acad Sci USA. 2022 Feb 8;119(6):e2109133119.

108. Hong SH, Eun JW, Choi SK, Shen Q, Choi WS, Han JW, et al. Epigenetic reader BRD4 inhibition as a therapeutic strategy to suppress E2F2-cell cycle regulation circuit in liver cancer. Oncotarget. 2016 May 31;7(22):32628–40.

109. Rodriguez RM, Huidobro C, Urdinguio RG, Mangas C, Soldevilla B, Domínguez G, et al. Aberrant epigenetic regulation of bromodomain Brd4 in human colon cancer. J Mol Med. 2012 May;90(5):587–95.

110. Zhou S, Zhang S, Wang L, Huang S, Yuan Y, Yang J, et al. BET protein inhibitor JQ1 downregulates chromatin accessibility and suppresses metastasis of gastric cancer via inactivating RUNX2/NID1 signaling. Oncogenesis. 2020 Mar;9(3):33.

111. Lu J, Qian Y, Altieri M, Dong H, Wang J, Raina K, et al. Hijacking the E3 Ubiquitin Ligase Cereblon to Efficiently Target BRD4. Chemistry & Biology. 2015 Jun;22(6):755–63.

112. Li Z, Lim SL, Tao Y, Li X, Xie Y, Yang C, et al. PROTAC Bromodomain Inhibitor ARV-825 Displays Anti-Tumor Activity in Neuroblastoma by Repressing Expression of MYCN or c-Myc. Front Oncol. 2020 Nov 26;10:574525.

113. He L, Chen C, Gao G, Xu K, Ma Z. ARV-825-induced BRD4 protein degradation as a therapy for thyroid carcinoma. Aging. 2020 Mar 12;12(5):4547–57.

114. Wu S, Jiang Y, Hong Y, Chu X, Zhang Z, Tao Y, et al. BRD4 PROTAC degrader ARV-825 inhibits T-cell acute lymphoblastic leukemia by targeting “Undruggable” Myc-pathway genes. Cancer Cell Int. 2021 Dec;21(1):230.

115. Vartak R, Saraswat A, Yang Y, Chen ZS, Patel K. Susceptibility of Lung Carcinoma Cells to Nanostructured Lipid Carrier of ARV-825, a BRD4 Degrading Proteolysis Targeting Chimera. Pharm Res. 2022 Nov;39(11):2745–59.

116. Lim SL, Damnernsawad A, Shyamsunder P, Chng WJ, Han BC, Xu L, et al. Proteolysis targeting chimeric molecules as therapy for multiple myeloma: efficacy, biomarker and drug combinations. Haematologica. 2019 Jun;104(6):1209–20.

117. Saleh T, Carpenter VJ, Tyutyunyk-Massey L, Murray G, Leverson JD, Souers AJ, et al. Clearance of therapy-induced senescent tumor cells by the senolytic ABT-263 via interference with BCL-X $_L$ –BAX interaction. Mol Oncol. 2020 Oct;14(10):2504–19.

118. Go S, Kang M, Kwon SP, Jung M, Jeon OH, Kim B. The Senolytic Drug JQ1 Removes Senescent Cells via Ferroptosis. Tissue Eng Regen Med. 2021 Oct;18(5):841–50.

119. Kale J, Osterlund EJ, Andrews DW. BCL-2 family proteins: changing partners in the dance towards death. Cell Death & Differentiation. 2018 Jan;25(1):65–80.

120. Elmore S. Apoptosis: A Review of Programmed Cell Death. Toxicol Pathol. 2007 Jun;35(4):495–516.

121. Banfalvi G. Methods to detect apoptotic cell death. Apoptosis. 2017 Feb;22(2):306–23.

122. Wlodkowic D, Telford W, Skommer J, Darzynkiewicz Z. Apoptosis and Beyond: Cytometry in Studies of Programmed Cell Death. In: Methods in Cell Biology [Internet]. Elsevier; 2011 [cited 2020 Sep 30]. p. 55–98. Available from: https://linkinghub.elsevier.com/retrieve/pii/B9780123854933000048

123. Wakita M, Takahashi A, Sano O, Loo TM, Imai Y, Narukawa M, et al. A BET family protein degrader provokes senolysis by targeting NHEJ and autophagy in senescent cells. Nature Communications [Internet]. 2020 Dec [cited 2020 Jul 6];11(1). Available from: http://www.nature.com/articles/s41467-020-15719-6

124. Gewirtz DA. The Four Faces of Autophagy: Implications for Cancer Therapy. Cancer Res. 2014 Feb 1;74(3):647–51.

125. Sharma K, Le N, Alotaibi M, Gewirtz D. Cytotoxic Autophagy in Cancer Therapy. IJMS. 2014 Jun 5;15(6):10034–51.

126. Patel NH, Xu J, Saleh T, Wu Y, Lima S, Gewirtz DA. Influence of nonprotective autophagy and the autophagic switch on sensitivity to cisplatin in non-small cell lung cancer cells. Biochemical Pharmacology. 2020 May;175:113896.

127. Saleh T, Tyutyunyk-Massey L, H. Patel N, K. Cudjoe E, Alotaibi M, A. Gewirtz D. Studies of Non-Protective Autophagy Provide Evidence that Recovery from

Therapy-Induced Senescence is Independent of Early Autophagy. IJMS. 2020 Feb 20;21(4):1427.

128. Debacq-Chainiaux F, Erusalimsky JD, Campisi J, Toussaint O. Protocols to detect senescence-associated beta-galactosidase (SA-βgal) activity, a biomarker of senescent cells in culture and in vivo. Nat Protoc. 2009 Dec;4(12):1798–806.

129. Sharma K, Goehe RW, Di X, Hicks MA, Torti SV, Torti FM, et al. A novel cytostatic form of autophagy in sensitization of non-small cell lung cancer cells to radiation by vitamin D and the vitamin D analog, EB 1089. Autophagy. 2014 Dec 2;10(12):2346–61.

130. Alotaibi M, Sharma K, Saleh T, Povirk LF, Hendrickson EA, Gewirtz DA. Radiosensitization by PARP Inhibition in DNA Repair Proficient and Deficient Tumor Cells: Proliferative Recovery in Senescent Cells. Radiation Research. 2016 Mar 2;185(3):229.

131. Saleh T, Tyutyunyk-Massey L, Murray GF, Alotaibi MR, Kawale AS, Elsayed Z, et al. Tumor cell escape from therapy-induced senescence. Biochemical Pharmacology. 2019 Apr;162:202–12.

132. Leemans CR, Braakhuis BJM, Brakenhoff RH. The molecular biology of head and neck cancer. Nat Rev Cancer. 2011 Jan;11(1):9–22.

133. Donà MG, Rollo F, Pichi B, Spriano G, Moretto S, Covello R, et al. Evolving Profile of HPV-Driven Oropharyngeal Squamous Cell Carcinoma in a National Cancer

Institute in Italy: A 10-Year Retrospective Study. Microorganisms. 2020 Sep 29;8(10):1498.

134. Cramer JD, Burtness B, Le QT, Ferris RL. The changing therapeutic landscape of head and neck cancer. Nat Rev Clin Oncol. 2019 Nov;16(11):669–83.

135. Chow LQM. Head and Neck Cancer. Longo DL, editor. N Engl J Med. 2020 Jan 2;382(1):60–72.

136. Cohen EEW, Soulières D, Le Tourneau C, Dinis J, Licitra L, Ahn MJ, et al. Pembrolizumab versus methotrexate, docetaxel, or cetuximab for recurrent or metastatic head-and-neck squamous cell carcinoma (KEYNOTE-040): a randomised, open-label, phase 3 study. The Lancet. 2019 Jan;393(10167):156–67.

137. Seiwert TY, Burtness B, Mehra R, Weiss J, Berger R, Eder JP, et al. Safety and clinical activity of pembrolizumab for treatment of recurrent or metastatic squamous cell carcinoma of the head and neck (KEYNOTE-012): an open-label, multicentre, phase 1b trial. The Lancet Oncology. 2016 Jul;17(7):956–65.

138. Bauml J, Seiwert TY, Pfister DG, Worden F, Liu SV, Gilbert J, et al. Pembrolizumab for Platinum- and Cetuximab-Refractory Head and Neck Cancer: Results From a Single-Arm, Phase II Study. JCO. 2017 May 10;35(14):1542–9.

139. Ferris RL, Blumenschein G, Fayette J, Guigay J, Colevas AD, Licitra L, et al. Nivolumab for Recurrent Squamous-Cell Carcinoma of the Head and Neck. N Engl J Med. 2016 Nov 10;375(19):1856–67.

140. Argiris A, Karamouzis MV, Raben D, Ferris RL. Head and neck cancer. The Lancet. 2008 May;371(9625):1695–709.

141. Gibson MK, Li Y, Murphy B, Hussain MHA, DeConti RC, Ensley J, et al. Randomized Phase III Evaluation of Cisplatin Plus Fluorouracil Versus Cisplatin Plus Paclitaxel in Advanced Head and Neck Cancer (E1395): An Intergroup Trial of the Eastern Cooperative Oncology Group. JCO. 2005 May 20;23(15):3562–7.

142. Goss PE, Chambers AF. Does tumour dormancy offer a therapeutic target? Nat Rev Cancer. 2010 Dec;10(12):871–7.

143. Kareva I. Escape from tumor dormancy and time to angiogenic switch as mitigated by tumor-induced stimulation of stroma. Journal of Theoretical Biology. 2016 Apr;395:11–22.

144. Sosa MS, Bragado P, Aguirre-Ghiso JA. Mechanisms of disseminated cancer cell dormancy: an awakening field. Nat Rev Cancer. 2014 Sep;14(9):611–22.

145. Yeh AC, Ramaswamy S. Mechanisms of Cancer Cell Dormancy--Another Hallmark of Cancer? Cancer Research. 2015 Dec 1;75(23):5014–22.

146. Chabner BA. Barnett Rosenberg: In Memoriam (1924–2009). Cancer Research. 2010 Jan 1;70(1):428–9.

147. Lippman AJ, Helson C, Helson L, Krakoff IH. Clinical trials of cis-diamminedichloroplatinum (NSC-119875). Cancer Chemother Rep. 1973 Apr;57(2):191–200.

148. Wang Y, Blandino G, Oren M, Givol D. Induced p53 expression in lung cancer cell line promotes cell senescence and differentially modifies the cytotoxicity of anti-cancer drugs. Oncogene. 1998 Oct 15;17(15):1923–30.

149. Rosenberg B, Van Camp L, Krigas T. Inhibition of Cell Division in Escherichia coli by Electrolysis Products from a Platinum Electrode. Nature. 1965 Feb;205(4972):698–9.

150. Cisplatin [Internet]. Available from: https://www.cancer.gov/about-cancer/treatment/drugs/cisplatin

151. Aldossary SA. Review on Pharmacology of Cisplatin: Clinical Use, Toxicity and Mechanism of Resistance of Cisplatin. Biomed Pharmacol J. 2019 Mar 28;12(1):07–15.

152. Eljack ND, Ma HYM, Drucker J, Shen C, Hambley TW, New EJ, et al. Mechanisms of cell uptake and toxicity of the anticancer drug cisplatin. Metallomics. 2014;6(11):2126–33.

153. Florea AM, Büsselberg D. Cisplatin as an Anti-Tumor Drug: Cellular Mechanisms of Activity, Drug Resistance and Induced Side Effects. Cancers. 2011 Mar 15;3(1):1351–71.

154. Bowden NA, Ashton KA, Avery-Kiejda KA, Zhang XD, Hersey P, Scott RJ. Nucleotide Excision Repair Gene Expression after Cisplatin Treatment in Melanoma. Cancer Research. 2010 Oct 15;70(20):7918–26.

155. Yimit A, Adebali O, Sancar A, Jiang Y. Differential damage and repair of DNA-adducts induced by anti-cancer drug cisplatin across mouse organs. Nat Commun. 2019 Dec;10(1):309.

156. Urien S, Lokiec F. Population pharmacokinetics of total and unbound plasma cisplatin in adult patients. Br J Clin Pharmacol. 2004 Jun;57(6):756–63.

157. Ang KK, Zhang Q, Rosenthal DI, Nguyen-Tan PF, Sherman EJ, Weber RS, et al. Randomized Phase III Trial of Concurrent Accelerated Radiation Plus Cisplatin With or Without Cetuximab for Stage III to IV Head and Neck Carcinoma: RTOG 0522. JCO. 2014 Sep 20;32(27):2940–50.

158. Farris FF, Dedrick RL, King FG. Cisplatin pharmacokinetics: applications of a physiological model. Toxicology Letters. 1988 Oct;43(1–3):117–37.

159. Basu A, Krishnamurthy S. Cellular Responses to Cisplatin-Induced DNA Damage. Journal of Nucleic Acids. 2010;2010:1–16.

160. Rezaee M, Sanche L, Hunting DJ. Cisplatin Enhances the Formation of DNA Single- and Double-Strand Breaks by Hydrated Electrons and Hydroxyl Radicals. Radiation Research. 2013 Mar;179(3):323–31.

161. Jeon JH, Kim SK, Kim HJ, Chang J, Ahn CM, Chang YS. Insulin-like growth factor-1 attenuates cisplatin-induced γH2AX formation and DNA double-strand breaks repair pathway in non-small cell lung cancer. Cancer Letters. 2008 Dec;272(2):232–41.

162. Triana-Martínez F, Loza MI, Domínguez E. Beyond Tumor Suppression: Senescence in Cancer Stemness and Tumor Dormancy. Cells. 2020 Feb 3;9(2):346.

163. Shay JW, Roninson IB. Hallmarks of senescence in carcinogenesis and cancer therapy. Oncogene. 2004 Apr;23(16):2919–33.

164. Chitikova ZV, Gordeev SA, Bykova TV, Zubova SG, Pospelov VA, Pospelova TV. Sustained activation of DNA damage response in irradiated apoptosis-resistant cells induces reversible senescence associated with mTOR downregulation and expression of stem cell markers. Cell Cycle. 2014 May;13(9):1424–39.

165. Puig PE, Guilly MN, Bouchot A, Droin N, Cathelin D, Bouyer F, et al. Tumor cells can escape DNA-damaging cisplatin through DNA endoreduplication and reversible polyploidy. Cell Biology International. 2008 Sep;32(9):1031–43.

166. Wang Q, Wu PC, Dong DZ, Ivanova I, Chu E, Zeliadt S, et al. Polyploidy road to therapy-induced cellular senescence and escape. Int J Cancer. 2013 Apr 1;132(7):1505–15.

167. Dirac AMG, Bernards R. Reversal of Senescence in Mouse Fibroblasts through Lentiviral Suppression of p53. Journal of Biological Chemistry. 2003 Apr;278(14):11731–4.

168. Rebbaa A. Targeting senescence pathways to reverse drug resistance in cancer. Cancer Letters. 2005 Feb 28;219(1):1–13.

169. Yang L, Fang J, Chen J. Tumor cell senescence response produces aggressive variants. Cell Death Discov. 2017 Dec;3(1):17049.

170. Lafontaine J, Cardin GB, Malaquin N, Boisvert JS, Rodier F, Wong P. Senolytic Targeting of Bcl-2 Anti-Apoptotic Family Increases Cell Death in Irradiated Sarcoma Cells. Cancers. 2021 Jan 21;13(3):386.

171. Tse C, Shoemaker AR, Adickes J, Anderson MG, Chen J, Jin S, et al. ABT-263: A Potent and Orally Bioavailable Bcl-2 Family Inhibitor. Cancer Research. 2008 May 1;68(9):3421–8.

172. Shoemaker AR, Mitten MJ, Adickes J, Oleksijew A, Zhang H, Bauch J, et al. The Bcl-2 Family Inhibitor ABT-263 Shows Significant but Reversible Thrombocytopenia in Mice. Blood. 2006 Nov 16;108(11):1107–1107.

173. Roberts AW, Wilson W, Gandhi L, O'Connor OA, Rudin CM, Brown JR, et al. Ongoing phase I studies of ABT-263: Mitigating Bcl-X_L induced thrombocytopenia with lead-in and continuous dosing. JCO. 2009 May 20;27(15_suppl):3505–3505.

174. Oltersdorf T, Elmore SW, Shoemaker AR, Armstrong RC, Augeri DJ, Belli BA, et al. An inhibitor of Bcl-2 family proteins induces regression of solid tumours. Nature. 2005 Jun;435(7042):677–81.

175. Lambrecht M, Dirix P, Van den Bogaert W, Nuyts S. Incidence of isolated regional recurrence after definitive (chemo-) radiotherapy for head and neck squamous cell carcinoma. Radiotherapy and Oncology. 2009 Dec;93(3):498–502.

176. Walens A, DiMarco AV, Lupo R, Kroger BR, Damrauer JS, Alvarez JV. CCL5 promotes breast cancer recurrence through macrophage recruitment in residual tumors. eLife. 2019 Apr 16;8:e43653.

177. Morgan TM, Lange PH, Porter MP, Lin DW, Ellis WJ, Gallaher IS, et al. Disseminated Tumor Cells in Prostate Cancer Patients after Radical Prostatectomy and without Evidence of Disease Predicts Biochemical Recurrence. Clinical Cancer Research. 2009 Jan 15;15(2):677–83.

178. Wu CY, Lee CL, Wu CF, Fu JY, Yang CT, Wen CT, et al. Circulating Tumor Cells as a Tool of Minimal Residual Disease Can Predict Lung Cancer Recurrence: A longitudinal, Prospective Trial. Diagnostics. 2020 Mar 6;10(3):144.

179. Wang H, Stoecklein NH, Lin PP, Gires O. Circulating and disseminated tumor cells: diagnostic tools and therapeutic targets in motion. Oncotarget. 2017 Jan 3;8(1):1884–912.

180. Phi LTH, Sari IN, Yang YG, Lee SH, Jun N, Kim KS, et al. Cancer Stem Cells (CSCs) in Drug Resistance and their Therapeutic Implications in Cancer Treatment. Stem Cells International. 2018;2018:1–16.

181. Kim RS, Avivar-Valderas A, Estrada Y, Bragado P, Sosa MS, Aguirre-Ghiso JA, et al. Dormancy Signatures and Metastasis in Estrogen Receptor Positive and Negative Breast Cancer. Minna JD, editor. PLoS ONE. 2012 Apr 18;7(4):e35569.

182. Pérez-Mancera PA, Young ARJ, Narita M. Inside and out: the activities of senescence in cancer. Nat Rev Cancer. 2014 Aug;14(8):547–58.

183. Nardella C, Clohessy JG, Alimonti A, Pandolfi PP. Pro-senescence therapy for cancer treatment. Nat Rev Cancer. 2011 Jul;11(7):503–11.

184. Seluanov A, Gorbunova V, Falcovitz A, Sigal A, Milyavsky M, Zurer I, et al. Change of the Death Pathway in Senescent Human Fibroblasts in Response to DNA Damage Is Caused by an Inability To Stabilize p53. Mol Cell Biol. 2001 Mar 1;21(5):1552–64.

185. Wiley CD, Flynn JM, Morrissey C, Lebofsky R, Shuga J, Dong X, et al. Analysis of individual cells identifies cell-to-cell variability following induction of cellular senescence. Aging Cell. 2017 Oct;16(5):1043–50.

186. Hernandez-Segura A, de Jong TV, Melov S, Guryev V, Campisi J, Demaria M. Unmasking Transcriptional Heterogeneity in Senescent Cells. Current Biology. 2017 Sep;27(17):2652-2660.e4.

187. Coppé JP, Desprez PY, Krtolica A, Campisi J. The Senescence-Associated Secretory Phenotype: The Dark Side of Tumor Suppression. Annu Rev Pathol Mech Dis. 2010 Jan;5(1):99–118.

188. Krizhanovsky V, Yon M, Dickins RA, Hearn S, Simon J, Miething C, et al. Senescence of Activated Stellate Cells Limits Liver Fibrosis. Cell. 2008 Aug;134(4):657–67.

189. Sieben CJ, Sturmlechner I, van de Sluis B, van Deursen JM. Two-Step Senescence-Focused Cancer Therapies. Trends in Cell Biology. 2018 Sep;28(9):723–37.

190. Singchat W, Hitakomate E, Rerkarmnuaychoke B, Suntronpong A, Fu B, Bodhisuwan W, et al. Genomic Alteration in Head and Neck Squamous Cell Carcinoma (HNSCC) Cell Lines Inferred from Karyotyping, Molecular Cytogenetics, and Array Comparative Genomic Hybridization. Castresana JS, editor. PLoS ONE. 2016 Aug 8;11(8):e0160901.

191. Mirzayans R, Andrais B, Hansen G, Murray D. Role of p16 INK4A in Replicative Senescence and DNA Damage-Induced Premature Senescence in p53-Deficient Human Cells. Biochemistry Research International. 2012;2012:1–8.

192. Yosef R, Pilpel N, Tokarsky-Amiel R, Biran A, Ovadya Y, Cohen S, et al. Directed elimination of senescent cells by inhibition of BCL-W and BCL-XL. Nat Commun. 2016 Sep;7(1):11190.

193. Grezella C, Fernandez-Rebollo E, Franzen J, Ventura Ferreira MS, Beier F, Wagner W. Effects of senolytic drugs on human mesenchymal stromal cells. Stem Cell Res Ther. 2018 Dec;9(1):108.

194. Yabluchanskiy A, Tarantini S, Balasubramanian P, Kiss T, Csipo T, Fülöp GA, et al. Pharmacological or genetic depletion of senescent astrocytes prevents whole brain irradiation–induced impairment of neurovascular coupling responses protecting cognitive function in mice. GeroScience. 2020 Apr;42(2):409–28.

195. Hayward RL, Macpherson JS, Cummings J, Monia BP, Smyth JF, Jodrell DI. Antisense Bcl-xl Down-Regulation Switches the Response to Topoisomerase I Inhibition from Senescence to Apoptosis in Colorectal Cancer Cells, Enhancing Global Cytotoxicity. Clin Cancer Res. 2003 Jul 1;9(7):2856.

196. Mas-Bargues C, Borrás C, Viña J. Bcl-xL as a Modulator of Senescence and Aging. IJMS. 2021 Feb 3;22(4):1527.

197. Renault TT, Teijido O, Missire F, Ganesan YT, Velours G, Arokium H, et al. Bcl-xL stimulates Bax relocation to mitochondria and primes cells to ABT-737. The International Journal of Biochemistry & Cell Biology. 2015 Jul;64:136–46.

198. Wang X, Zhang J, Kim HP, Wang Y, Choi AMK, Ryter SW. Bcl-X $_{L}$ disrupts death-inducing signal complex formation in plasma membrane induced by hypoxia/reoxygenation. FASEB j. 2004 Dec;18(15):1826–33.

199. Fiebig AA, Zhu W, Hollerbach C, Leber B, Andrews DW. Bcl-XL is qualitatively different from and ten times more effective than Bcl-2 when expressed in a breast cancer cell line. BMC Cancer. 2006 Dec;6(1):213.

200. Pena JC, Thompson CB, Recant W, Vokes EE, Rudin CM. Bcl-xL and Bcl-2 expression in squamous cell carcinoma of the head and neck. Cancer. 1999 Jan 1;85(1):164–70.

201. Carter RJ, Milani M, Butterworth M, Alotibi A, Harper N, Yedida G, et al. Exploring the potential of BH3 mimetic therapy in squamous cell carcinoma of the head and neck. Cell Death Dis. 2019 Dec;10(12):912.

202. Oliver L, Hue E, Rossignol J, Bougras G, Hulin P, Naveilhan P, et al. Distinct Roles of Bcl-2 and Bcl-Xl in the Apoptosis of Human Bone Marrow Mesenchymal Stem Cells during Differentiation. Goldberg AC, editor. PLoS ONE. 2011 May 12;6(5):e19820.

203. Bertino EM, Gentzler RD, Clifford S, Kolesar J, Muzikansky A, Haura EB, et al. Phase IB Study of Osimertinib in Combination with Navitoclax in *EGFR* -mutant NSCLC Following Resistance to Initial *EGFR* Therapy (ETCTN 9903). Clin Cancer Res. 2021 Mar 15;27(6):1604–11.

204. Harrison CN, Garcia JS, Mesa RA, Somervaille TC, Komrokji RS, Pemmaraju N, et al. Results from a Phase 2 Study of Navitoclax in Combination with Ruxolitinib in Patients with Primary or Secondary Myelofibrosis. Blood. 2019 Nov 13;134(Supplement_1):671–671.

205. Puglisi M, van Doorn L, Blanco-Codesido M, De Jonge MJ, Moran K, Yang J, et al. A phase I safety and pharmacokinetic (PK) study of navitoclax (N) in combination with docetaxel (D) in patients (pts) with solid tumors. JCO. 2011 May 20;29(15_suppl):2518–2518.

206. Patterson CM, Balachander SB, Grant I, Pop-Damkov P, Kelly B, McCoull W, et al. Design and optimisation of dendrimer-conjugated Bcl-2/xL inhibitor, AZD0466, with improved therapeutic index for cancer therapy. Commun Biol. 2021 Dec;4(1):112.

207. Lakhani NJ, Rasco DW, Tolcher AW, Huang Y, Ji J, Wang H, et al. A phase I study of novel dual Bcl-2/Bcl-xL inhibitor APG-1252 in patients with advanced small cell lung cancer (SCLC) or other solid tumor. JCO. 2018 May 20;36(15_suppl):2594–2594.

208. He Y, Koch R, Budamagunta V, Zhang P, Zhang X, Khan S, et al. DT2216—a Bcl-xL-specific degrader is highly active against Bcl-xL-dependent T cell lymphomas. J Hematol Oncol. 2020 Dec;13(1):95.

209. Burtness B, Harrington KJ, Greil R, Soulières D, Tahara M, de Castro G, et al. Pembrolizumab alone or with chemotherapy versus cetuximab with chemotherapy for recurrent or metastatic squamous cell carcinoma of the head and neck (KEYNOTE-048): a randomised, open-label, phase 3 study. The Lancet. 2019 Nov;394(10212):1915–28.

210. Vermorken J, Specenier P. Cetuximab: its unique place in head and neck cancer treatment. BTT. 2013 Apr;77.

211. Jou A, Hess J. Epidemiology and Molecular Biology of Head and Neck Cancer. Oncol Res Treat. 2017;40(6):328–32.

212. Galluzzi L, Senovilla L, Vitale I, Michels J, Martins I, Kepp O, et al. Molecular mechanisms of cisplatin resistance. Oncogene. 2012 Apr;31(15):1869–83.

213. Rizzo S, Hersey JM, Mellor P, Dai W, Santos-Silva A, Liber D, et al. Ovarian Cancer Stem Cell–Like Side Populations Are Enriched Following Chemotherapy and Overexpress *EZH2*. Molecular Cancer Therapeutics. 2011 Feb 1;10(2):325–35.

214. Lu Q, Ding X, Huang T, Zhang S, Li Y, Xu L, et al. BRD4 degrader ARV-825 produces long-lasting loss of BRD4 protein and exhibits potent efficacy against cholangiocarcinoma cells. Am J Transl Res. 2019;11(9):5728–39.

215. Sarnik J, Popławski T, Tokarz P. BET Proteins as Attractive Targets for Cancer Therapeutics. IJMS. 2021 Oct 14;22(20):11102.

216. Liao X, Qian X, Zhang Z, Tao Y, Li Z, Zhang Q, et al. ARV-825 Demonstrates Antitumor Activity in Gastric Cancer via MYC-Targets and G2M-Checkpoint Signaling Pathways. Front Oncol. 2021 Oct 18;11:753119.

217. Sirichanchuen B, Pengsuparp T, Chanvorachote P. Long-term cisplatin exposure impairs autophagy and causes cisplatin resistance in human lung cancer cells. Mol Cell Biochem. 2012 May;364(1–2):11–8.

218. Robinson AM, Rathore R, Redlich NJ, Adkins DR, VanArsdale T, Van Tine BA, et al. Cisplatin exposure causes c-Myc-dependent resistance to CDK4/6 inhibition in HPV-negative head and neck squamous cell carcinoma. Cell Death Dis. 2019 Nov;10(11):867.

219. Chen J, Wang X, Yuan Y, Chen H, Zhang L, Xiao H, et al. Exploiting the acquired vulnerability of cisplatin-resistant tumors with a hypoxia-amplifying DNA repair–inhibiting (HYDRI) nanomedicine. Sci Adv. 2021 Mar 26;7(13):eabc5267.

220. Walcher L, Kistenmacher AK, Suo H, Kitte R, Dluczek S, Strauß A, et al. Cancer Stem Cells—Origins and Biomarkers: Perspectives for Targeted Personalized Therapies. Front Immunol. 2020 Aug 7;11:1280.

221. Enderling H, Hlatky L, Hahnfeldt P. Cancer Stem Cells: A Minor Cancer Subpopulation that Redefines Global Cancer Features. Front Oncol [Internet]. 2013 [cited 2022 Dec 15];3. Available from: http://journal.frontiersin.org/article/10.3389/fonc.2013.00076/abstract

222. Pang R, Law WL, Chu ACY, Poon JT, Lam CSC, Chow AKM, et al. A Subpopulation of CD26+ Cancer Stem Cells with Metastatic Capacity in Human Colorectal Cancer. Cell Stem Cell. 2010 Jun;6(6):603–15.

223. Prince ME, Sivanandan R, Kaczorowski A, Wolf GT, Kaplan MJ, Dalerba P, et al. Identification of a subpopulation of cells with cancer stem cell properties in head and neck squamous cell carcinoma. Proc Natl Acad Sci USA. 2007 Jan 16;104(3):973–8.

224. Reynolds DS, Tevis KM, Blessing WA, Colson YL, Zaman MH, Grinstaff MW. Breast Cancer Spheroids Reveal a Differential Cancer Stem Cell Response to Chemotherapeutic Treatment. Sci Rep. 2017 Dec;7(1):10382.

225. Nishikawa S, Konno M, Hamabe A, Hasegawa S, Kano Y, Ohta K, et al. Aldehyde dehydrogenasehigh gastric cancer stem cells are resistant to chemotherapy. International Journal of Oncology. 2013 Apr;42(4):1437–42.

226. Abugomaa A, Elbadawy M, Yamawaki H, Usui T, Sasaki K. Emerging Roles of Cancer Stem Cells in Bladder Cancer Progression, Tumorigenesis, and Resistance to Chemotherapy: A Potential Therapeutic Target for Bladder Cancer. Cells. 2020 Jan 17;9(1):235.

227. Misuno K, Liu X, Feng S, Hu S. Quantitative proteomic analysis of sphere-forming stem-like oral cancer cells. Stem Cell Res Ther. 2013 Dec;4(6):156.

228. Moreb JS, Zucali JR, Ostmark B, Benson NA. Heterogeneity of aldehyde dehydrogenase expression in lung cancer cell lines is revealed by Aldefluor flow cytometry-based assay. Cytometry. 2007 Jul;72B(4):281–9.

229. Holzer AK, Manorek GH, Howell SB. Contribution of the Major Copper Influx Transporter CTR1 to the Cellular Accumulation of Cisplatin, Carboplatin, and Oxaliplatin. Mol Pharmacol. 2006 Oct;70(4):1390–4.

230. Lin X, Okuda T, Holzer A, Howell SB. The Copper Transporter *CTR1* Regulates Cisplatin Uptake in *Saccharomyces cerevisiae*. Mol Pharmacol. 2002 Nov 1;62(5):1154–9.

231. Gomez KE, Wu F, Keysar SB, Morton JJ, Miller B, Chimed TS, et al. Cancer Cell CD44 Mediates Macrophage/Monocyte-Driven Regulation of Head and Neck Cancer Stem Cells. Cancer Research. 2020 Oct 1;80(19):4185–98.

232. Brozovic A, Osmak M. Activation of mitogen-activated protein kinases by cisplatin and their role in cisplatin-resistance. Cancer Letters. 2007 Jun;251(1):1–16.

233. Ishida S, Lee J, Thiele DJ, Herskowitz I. Uptake of the anticancer drug cisplatin mediated by the copper transporter Ctr1 in yeast and mammals. Proc Natl Acad Sci USA. 2002 Oct 29;99(22):14298–302.

234. Jiang P, Wu X, Wang X, Huang W, Feng Q. NEAT1 upregulates EGCG-induced CTR1 to enhance cisplatin sensitivity in lung cancer cells. Oncotarget. 2016 Jul 12;7(28):43337–51.

235. Filippakopoulos P, Qi J, Picaud S, Shen Y, Smith WB, Fedorov O, et al. Selective inhibition of BET bromodomains. Nature. 2010 Dec;468(7327):1067–73.

236. French CA, Ramirez CL, Kolmakova J, Hickman TT, Cameron MJ, Thyne ME, et al. BRD–NUT oncoproteins: a family of closely related nuclear proteins that block epithelial differentiation and maintain the growth of carcinoma cells. Oncogene. 2008 Apr 3;27(15):2237–42.

237. Muhar M, Ebert A, Neumann T, Umkehrer C, Jude J, Wieshofer C, et al. SLAM-seq defines direct gene-regulatory functions of the BRD4-MYC axis. Science. 2018 May 18;360(6390):800–5.

238. Asangani IA, Dommeti VL, Wang X, Malik R, Cieslik M, Yang R, et al. Therapeutic targeting of BET bromodomain proteins in castration-resistant prostate cancer. Nature. 2014 Jun;510(7504):278–82.

239. Welti J, Sharp A, Yuan W, Dolling D, Nava Rodrigues D, Figueiredo I, et al. Targeting Bromodomain and Extra-Terminal (BET) Family Proteins in Castration-Resistant Prostate Cancer (CRPC). Clinical Cancer Research. 2018 Jul 1;24(13):3149–62.

240. Yokoyama Y, Zhu H, Lee JH, Kossenkov AV, Wu SY, Wickramasinghe JM, et al. BET Inhibitors Suppress ALDH Activity by Targeting *ALDH1A1* Super-Enhancer in Ovarian Cancer. Cancer Research. 2016 Nov 1;76(21):6320–30.

241. Barrows JK, Lin B, Quaas CE, Fullbright G, Wallace EN, Long DT. BRD4 promotes resection and homology-directed repair of DNA double-strand breaks. Nat Commun. 2022 May 31;13(1):3016.

242. Li X, Baek G, Ramanand SG, Sharp A, Gao Y, Yuan W, et al. BRD4 Promotes DNA Repair and Mediates the Formation of TMPRSS2-ERG Gene Rearrangements in Prostate Cancer. Cell Reports. 2018 Jan;22(3):796–808.

243. Ni M, Li J, Zhao H, Xu F, Cheng J, Yu M, et al. BRD4 inhibition sensitizes cervical cancer to radiotherapy by attenuating DNA repair. Oncogene. 2021 Apr 15;40(15):2711–24.

244. Dasari S, Bernard Tchounwou P. Cisplatin in cancer therapy: Molecular mechanisms of action. European Journal of Pharmacology. 2014 Oct;740:364–78.

245. Skowron MA, Oing C, Bremmer F, Ströbel P, Murray MJ, Coleman N, et al. The developmental origin of cancers defines basic principles of cisplatin resistance. Cancer Letters. 2021 Oct;519:199–210.

246. Ghosh S, Rao PB, Kumar PR, Manam S. Concurrent Chemoradiation with Weekly Cisplatin for the Treatment of Head and Neck Cancers: an Institutional Study on Acute Toxicity and Response to Treatment. Asian Pacific Journal of Cancer Prevention. 2015 Nov 4;16(16):7331–5.

247. Rose PG, Bundy BN, Watkins EB, Thigpen JT, Deppe G, Maiman MA, et al. Concurrent Cisplatin-Based Radiotherapy and Chemotherapy for Locally Advanced Cervical Cancer. N Engl J Med. 1999 Apr 15;340(15):1144–53.

248. Beckmann GK, Hoppe F, Pfreundner L, Flentje MP. Hyperfractionated accelerated radiotherapy in combination with weekly cisplatin for locally advanced head and neck cancer. Head Neck. 2005 Jan;27(1):36–43.

249. Caponigro F, Di Gennaro E, Ionna F, Longo F, Aversa C, Pavone E, et al. Phase II clinical study of valproic acid plus cisplatin and cetuximab in recurrent and/or metastatic squamous cell carcinoma of Head and Neck-V-CHANCE trial. BMC Cancer. 2016 Dec;16(1):918.

250. Pendleton KP, Grandis JR. Cisplatin-Based Chemotherapy Options for Recurrent and/or Metastatic Squamous Cell Cancer of the Head and Neck. Clinical Medicine Insights: Therapeutics. 2013 Jan;5:CMT.S10409.

251. Sanborn RE. Cisplatin Versus Carboplatin in NSCLC: Is There One “Best” Answer? Curr Treat Options in Oncol. 2008 Dec;9(4–6):326–42.

252. Li A, Wei ZJ, Ding H, Tang HS, Zhou HX, Yao X, et al. Docetaxel versus docetaxel plus cisplatin for non-small-cell lung cancer: a meta-analysis of randomized clinical trials. Oncotarget. 2017 Aug 22;8(34):57365–78.

253. Rao R. Induction Chemotherapy with Cisplatin and 5-Fluorouracil in Advanced Head and Neck Cancers: A Short Term Response Evaluation. JCDR [Internet]. 2015 [cited 2022 Nov 8]; Available from: http://jcdr.net/article_fulltext.asp?issn=0973-709x&year=2015&volume=9&issue=10&page=XC08&issn=0973-709x&id=6671

254. Kasiram MZ, Hapidin H, Abdullah H, Ahmad A, Sulong S. Combination Therapy of Cisplatin and other Agents for Osteosarcoma: A Review. CCTR. 2021 Jun 10;17(2):137–47.